MSc Program
Renewable Energy Systems

ACADEMY FOR
CONTINUING
EDUCATION

Techno-economic assessment of a power-to-gas facility at the biogas plant Bruck/Leitha

A Master's Thesis submitted for the degree of
“Master of Science”

supervised by
Ao.Univ.Prof. Dipl.-Ing. Dr.techn. Michael Harasek

Dipl.-Ing. Vartan Awetisjan

00835172

Vienna, 06.04.2022

ACADEMY FOR
CONTINUING
EDUCATION

Affidavit

I, **DIPL.-ING. VARTAN AWETISJAN**, hereby declare

1. that I am the sole author of the present Master's Thesis, "TECHNO-ECONOMIC ASSESSMENT OF A POWER-TO-GAS FACILITY AT THE BIOGAS PLANT BRUCK/LEITHA", 107 pages, bound, and that I have not used any source or tool other than those referenced or any other illicit aid or tool, and
2. that I have not prior to this date submitted the topic of this Master's Thesis or parts of it in any form for assessment as an examination paper, either in Austria or abroad.

Vienna, 06.04.2022

Signature

Abstract

A flexible, resilient, and renewable energy system, where all sectors are coupled via an integrated energy grid is the key to reach climate neutrality by 2040. The power-to-gas technology can be such a sector coupling technology by providing short- and long-term flexibility to the electricity grid by converting electricity into a gas, namely synthetic methane, which can be fed into the gas grid already today without any concern and can be seasonally stored in existing gas storage facilities. In order to produce synthetic methane with hydrogen from an electrolyser, a CO_2 source is required. A biogas upgrading plant, which already produces pure CO_2 as a by-product can be such a source. Therefore, this thesis will assess the technical and economic feasibility of a power-to-gas facility in combination with a biogas upgrading plant in order to produce synthetic biomethane, a renewable gas. This assessment was conducted as a case study for the biogas plant Bruck/Leitha. Based on a detailed literature and market review as well as real historic data from the biogas plant Bruck/Leitha and historic market prices for electricity and control reserve energy in Austria, the applicable electrolyser and methanation technologies, sizes and economic input data were gathered for the techno-economic assessment. The results showed, that even with a 45% investment grant and very low electricity prices (40-50 EUR/MWh), the long run generation costs (LRGC) of synthetic biomethane are not lower than 100 EUR/MWh and therefore, not economically feasible. It therefore makes sense, to use the ability of the alkaline or PEM electrolyser and the biological methanation reactor and provide positive or negative control reserve energy to the electricity grid by reducing or increasing the electrical consumption of the electrolyser. In this case, also a liquid CO_2 storage is necessary to compensate for fluctuations in the biogas production stream and increase the availability. When participating in the positive control reserve market, the power to gas plant becomes profitable. The profitability even increases with increasing electricity prices because the positive control reserve energy price correlates with the spot market price for electricity. Therefore, a 5 MW_{el} AEL power-to-gas unit with an output of 250 Nm^3/h of synthetic biomethane could generate profits of 375,000 EUR/a with 2020 prices and 1,800.000 EUR/a with 2021 prices when participating in the positive control reserve market. The total production of synthetic biomethane is then around 8 GWh/a with approx. 3000 full load hours.

Table of Contents

1. Introduction

One of the biggest challenges of the 21st century is dealing with the climate crisis and therefore changing our whole energy system from a fossil energy-based system to a sustainable and renewable energy system with net zero greenhouse gas emissions.

The Austrian federal government has legally defined in 2021 the goal of climate neutrality for Austria by 2040, preferably based on renewable domestic energy sources, by the renewable expansion act. This task considers the objectives of the European Green Deal and is based on the legally binding Paris Agreement concluded in 2015, with the goal of limiting the increase in average global temperature to well below 2°C compared to pre-industrial levels.

In addition to climate neutrality by 2040, the government also set up the goal of a 100% renewable electricity supply by 2030 within the renewable expansion act. In order to achieve the 2030 goal, volatile renewable electricity production capacity has to be increased tremendously. But electrical energy, which comes currently from approx. 75% renewable sources, has only a share of 15% of total energy demand of Austria, whereas fossil fuels have a share of approx. 66%. The substitution of the natural gas demand (approx. 90 TWh in 2019) is already a very challenging task by itself. Therefore, also the goal of reaching 5 TWh of domestic renewable gas production was set up in the renewable expansion act. (Statistik Austria, 2021)

In a future renewable energy system, where highly volatile electricity production from solar power and wind power requires a flexible electricity system with day-to-night short-time storage capacities and summer-to-winter seasonal storage capacities, sector coupling and a highly flexible and easy-to-store energy carrier is indispensable for security of supply.

This is where renewable gases such as green hydrogen and biomethane come into play. With highly flexible electrolysers, imbalances in the electricity grid due to volatile production can be compensated in the short term by producing hydrogen as well as the seasonal shift from summer to winter can be achieved with the produced hydrogen, which is then stored in large underground gas storage facilities, when a hydrogen infrastructure is becomes available.

In addition to that, biomethane as well as synthetic methane can substitute the natural gas easily and already today by using the existing infrastructure like the gas grid, gas storage facilities and the end user installations and therefore can reduce greenhouse gas emissions effectively already in the short term.

Unfortunately, out of 300 biogas plants in Austria producing approx. 2 TWh of biogas, only 13 plants upgrade the biogas to biomethane and fed approx. 150 GWh per year into the public gas grid. (AGGM Austrian Gas Grid Management AG, 2021) The remaining 280 plants produce electricity and heat with a gas engine with a rather low efficiency, especially when no waste heat can be utilized. Additionally, when upgrading the biogas to biomethane, the CO_2 must be removed from the biogas stream and is currently released into the environment without any further utilization.

This means, biogas plants already have good preconditions to not only produce the highly flexible energy carrier biomethane to substitute natural gas, but also provide flexibility to the electricity grid by producing synthetic methane with an electrolyser in combination with a CO_2 methanation. With this power-to-gas technology at a biogas plant, no additional hydrogen infrastructure such as pipelines or storage is required since the synthetic biomethane can be fed into the existing gas grid. Thus, flexibility in terms of electrical control reserve energy and an increase of renewable gas production could be achieved in the short term with a power-to-gas facility at a biogas plant.

This thesis therefore will address the question, how such a power-to-gas facility should look like from the technical point of view, which electrolysis and methanation technology fits best to a biogas plant and how it can be integrated in the biogas production and upgrading process. Furthermore, also the economics are addressed in detail in order to find out how and if such a power-to-gas facility can generate profits. Dimensioning the power-to-gas facility and the economic assessment was done using real historical data from the biogas plant Bruck/Leitha in Austria. Because of this, the results also give the biogas plant owner a first indication if an investment makes sense in terms of feasibility and profitability.

Based on a profound literature review, which is presented in chapter 2, on electrolysis and methanation technology the advantages and disadvantages for the power-to-gas application of alkaline, PEM and high temperature electrolysers as well as catalytic and biological methanation are illustrated. The input data for the economic evaluation such as available stack and reactor sizes, capital costs, operating costs, efficiencies, lifetime, energy demand were determined by market research about state-of-the art technology combined with literature data.

The techno-economic assessment was carried out by comparing several different electricity price scenarios as well as scenarios where the electrolyser offers control reserve energy. The sensitivity on capital costs was addressed by also comparing three capital costs cases representing the range found in the literature. The results of each scenario in terms of long-range generation costs of synthetic biomethane are presented in chapter 5.

2. Background information on technology

This chapter will give the reader an overview of state-of-the-art technology regarding biomethane production, power-to-gas technology such as water-electrolysis and CO_2-methanation. Furthermore, a brief overview will be given concerning electricity markets and control energy.

2.1. Biomethane technology

2.1.1. Biogas production

Biogas is formed in an anaerobic digestion process where organic matter is decomposed by bacteria in four biochemical processes:

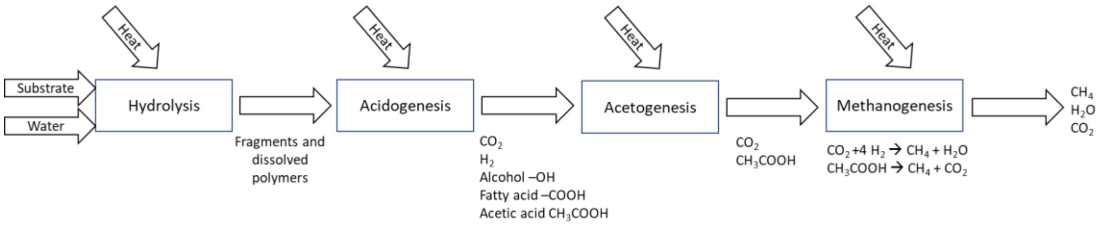

Figure 1: Process of Biogas production (Watter, 2019, p. 233).

During **hydrolysis**, the biopolymers are broken down into monomeric fragments or other soluble degradation products. Fats are broken down into fatty acids, carbohydrates (e.g., polysaccharides) into mono- or oligosaccharides and proteins into peptides and amino acids. These reactions are catalysed by anaerobic microorganisms, which hydrolyse the reactants by means of excreted exoenzymes. This step is due to the complexity of the starting material speed determining (Watter, 2019, p. 233).

The **acidogenesis** takes place simultaneously with hydrolysis. During this phase the monomeric fragments are converted, on the one hand, into lower fatty-/carboxylic acids such as butyric acid, propionic acid and acetic acid. On the other hand, into lower alcohols such as ethanol. At this conversion step, the anaerobic microorganisms gain energy for the first time and already up to 20% of the total acetic acid is formed (Watter, 2019, p. 233).

The **Acetogenesis** is the third stage of the anaerobic degradation during fermentation. In this process, the lower fatty-/carboxylic acids and lower alcohols formed during hydrolysis and acidogenesis are primarily converted by acetogenic microorganisms to acetic acid or its dissolved salt, the so-called acetate. This stage of anaerobic degradation can be regarded as "specific organic acid formation" (Watter, 2019, p. 234).

In the last phase, the so-called **methanogenesis** - the acetic acid is converted into methane by acetoclastic methane forming bacteria. About 30% of the methane is formed from hydrogen and carbon dioxide. What remains is a mixture of organic material that is difficult to degrade, for example lignin and inorganic substances such as sand or other mineral substances, the so-called digestate. This digestate be used as fertilizer since it still contains all trace elements and additionally almost all the nitrogen of the substrate in a bioavailable form (Watter, 2019, p. 234).

Biogas can be produced from several different kinds of biomass feedstocks such as:

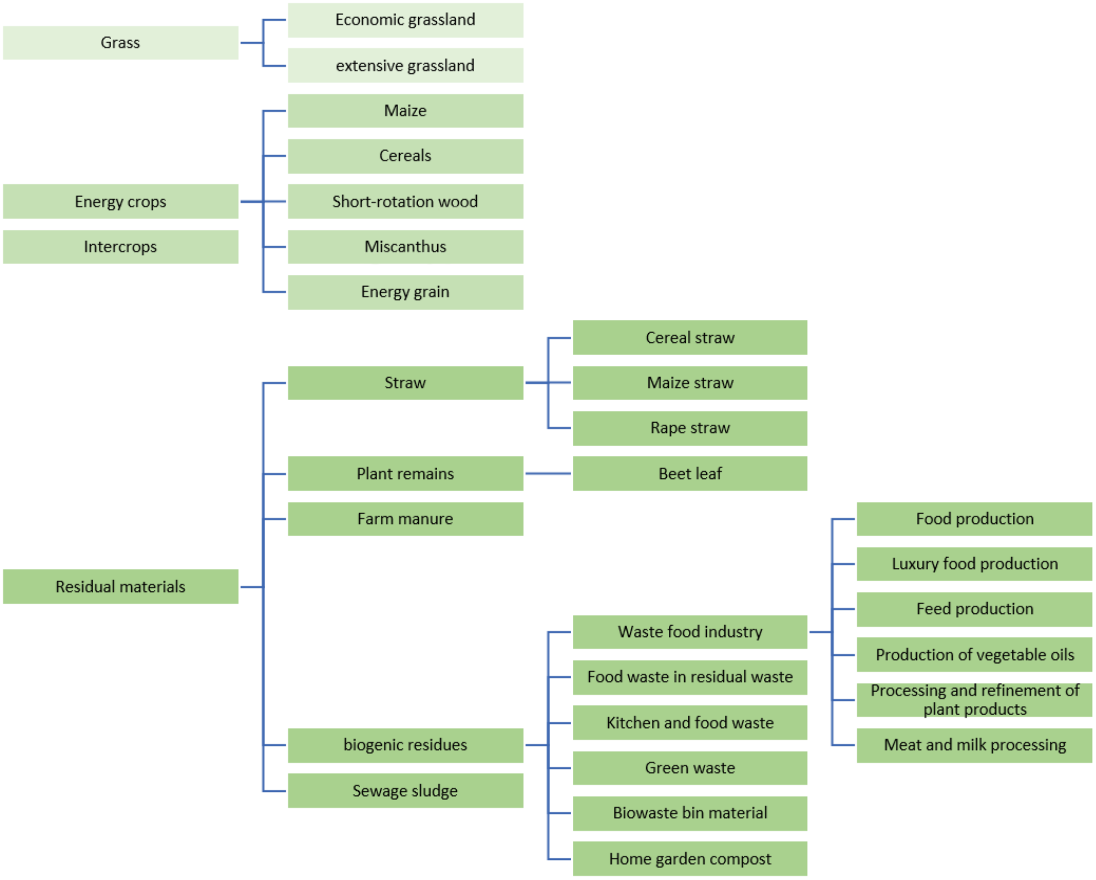

Figure 2: Biomass feedstocks for biogas production (Kranzl & Haas, 2008, p. 219) (Lindorfer, et al., 2017, p. 3).

Depending on the feedstock, biogas can consist of following molecules and concentrations:

Table 1: General composition of biogas (Koonaphapdeelert, et al., 2020, p. 2).

Biogas Composition	Concentration levels
Methane	50 – 80% vol.
Carbon dioxide	20 – 50% vol.
Ammonia	0 – 300 ppm
Hydrogen sulphide	50 – 5000 ppm
Nitrogen	1 – 4% vol.
Oxygen	<1% vol.
Moisture (H_2O)	saturated 2 – 5% by mass

2.1.2. Biogas Upgrading

In order to inject the produced biogas into the public gas grid in Austria, requirements according to the technical regulation ÖVGW G B210 (Table 2) have to be fulfilled. Therefore, it is necessary to clean, dry and upgrade the biogas to biomethane, where the levels of carbon dioxide, hydrogen sulphide, ammonia etc. are reduced and thus increasing the quality.

Table 2: Requirements on gas quality in Austria for local grid injection at Standard conditions 25/0 (ÖVGW, 2021).

	Min	Max.	Unit
Sulphur	-	21	mg/m³
Hydrogen sulphide	-	5	mg/m³
Mercaptan sulphur	-	6	mg/m³
Oxygen	-	0.001% or 1%*	mol/mol
Carbon dioxide	-	2,5% or 4%*	mol/mol
Carbon monoxide	-	0,1%	mol/mol
Ammonia	-	10	mg/m³
Amine		10	mg/m³
Nitrogen	-	5%	mol/mol
Methane number	-	85	
Wobbe-Index	13.25	15.81	kWh/m³
Calorific value	9.37	13.23	kWh/m³
Relative density	0.555 or 0.5**	0.7	-
Hydrogen	-	10%	mol/mol

*) However, where it can be proven that the gas does not flow to facilities that are sensitive to higher concentrations, such as underground storage facilities, a higher limit may be applied.

**) If it can be ensured that the K-number calculation (e.g., according to ÖNORM EN ISO 12213) complies with the legal requirements, the limit value of 0.5 can be applied.

Hydrogen sulphide can be removed by several methods listed in Table 3.

Table 3: Hydrogen sulphide removal methods (Koonaphapdeelert, et al., 2020, p. 18).

Method	**Removal efficiency**	**Capital cost**	**Operating cost**	**Complexity**
Biological removal	Moderate	Moderate	Low	Moderate
Iron chloride dosing	Moderate	Low	Moderate	Low
Water scrubbing	High	High	Moderate	High
Activated carbon	High	High	Moderate	Moderate
Iron sponge method	High	Moderate	Moderate	Moderate
NaOH scrubbing	High	Moderate	High	Moderate

Water vapor or moisture can be reduced by refrigeration, thus cooling the biogas below its dew point temperature in order to condense the moisture. Usually followed by removing liquid water in a knock-out vessel before reheating the biogas to ensure no condensation inside the upgrading equipment (Koonaphapdeelert, et al., 2020, p. 21).

The ammonia content can be removed by condensation drying using the effect of dissolving. Also, water absorption can remove both moisture and ammonia. Another method could be the use of a gas wash dryer in cases with high ammonia concentrations (Koonaphapdeelert, et al., 2020, p. 21).

In order to reduce the CO_2 content, several methods can be applied:

Table 4: Biogas pre-treatment methods (Koonaphapdeelert, et al., 2020, p. 21).

Method	**Containments**		
	Removed	**Partially removed**	**Not removed**
Water scrubbing	CO_2	VOC, H_2S, NH_3	O_2, N_2, H_2, H_2O
Amine scrubber	CO_2	VOC, H_2S, NH_3	O_2, N_2, H_2, H_2O
Membrane	CO_2, O_2, H_2S (low)	H_2S, H_2O, H_2	VOC, NH_3, N_2
Pressure Swing Absorption	CO_2	N_2, H_2O	VOC, NH_3, H_2
Other physical scrubber	CO_2	VOC, H_2S, NH_3	O_2, N_2, H_2, H_2O
Cryogenics	CO_2	VOC, H_2S, NH_3	O_2, N_2, H_2, H_2O

In **amine or carbonate scrubbing** process, the gases are purified by a scrubber. There, the CO_2 is separated by absorption by finely dispersed amine droplets. In a second step, the amines or the hydrogen carbonates are thermally expelled into a stripper so that the CO_2 is again present in concentrated form. The scrubbing substance can then be reused. In the amine scrubber, CO_2 is absorbed by the amine droplets at 27°C, and expelled at 150°C. In the carbonate scrubber, absorption occurs at about 40°C and desorption at 105°C. The carbon dioxide separation rate is about 90%. The high temperatures required for desorption lead to a reduction in efficiency of the whole system of about 10% (Watter, 2019, p. 240).

In **pressure swing adsorption**, the biogas is compressed to 4 to 7 bar. Water, carbon dioxide and hydrogen sulphide accumulate on activated carbon, zeolites or molecular sieves. The stable, more inert methane molecule passes through the adsorber (Watter, 2019, p. 240).

In **pressurized water scrubbing**, the easily soluble CO_2 dissolves in the water as the pressure increases. Gases generally tend to dissolve in liquids under pressure (absorption). This process usually works with a pressure of 5 to 20 bar. After the scrubber, dehumidification by cooling and falling below the dew point temperature or alternative drying processes is necessary (Watter, 2019, p. 241).

The **Membrane technology** takes advantage of the different sizes of gas molecules. CO_2 molecules are smaller than methane molecules. Therefore, the CO_2 can penetrate the micropores of the polymer membrane. Methane collects on the high-pressure side, while the unwanted components of the biogas such as CO_2, hydrogen, oxygen, or low contents of H_2S pass through the membrane. This method usually works with pressures of about 5 – 16 bar (Watter, 2019, p. 242).

2.2. Power-to-Gas Technology

Power-to-Gas refers to the conversion of electrical energy into chemical energy. Electrical energy, preferably produced by renewable energy sources such as wind power, solar power or hydro power for example can be converted into hydrogen by electrolysis. This green hydrogen, when produced from renewable energy sources, can be stored in tanks, injected into the gas grid up to several percentage or used directly in industrial process. Additionally, this green hydrogen can further be converted into renewable synthetic methane in the CO_2 Methanation process. A source of CO_2 could be the pure off-gas stream of biogas plants after upgrading.

This renewable synthetic methane can easily substitute natural gas by injecting it into the public gas grid. When injected into the gas grid, the renewable synthetic methane can be used in all applications connected to the grid, such as industrial process, process heat, domestic heat, electricity production and it can be stored efficiently over a long-time (seasonally) in underground gas storage facilities. Therefore, with the power-to-gas output such as hydrogen or synthetic methane more volatile renewable electrical energy such as wind or solar can be used due to the ability to store in chemical energy in large quantities over a long period and thus contribute to the seasonal shift of renewable energy.

Figure 3 shows the complexity of the power-to-gas process.

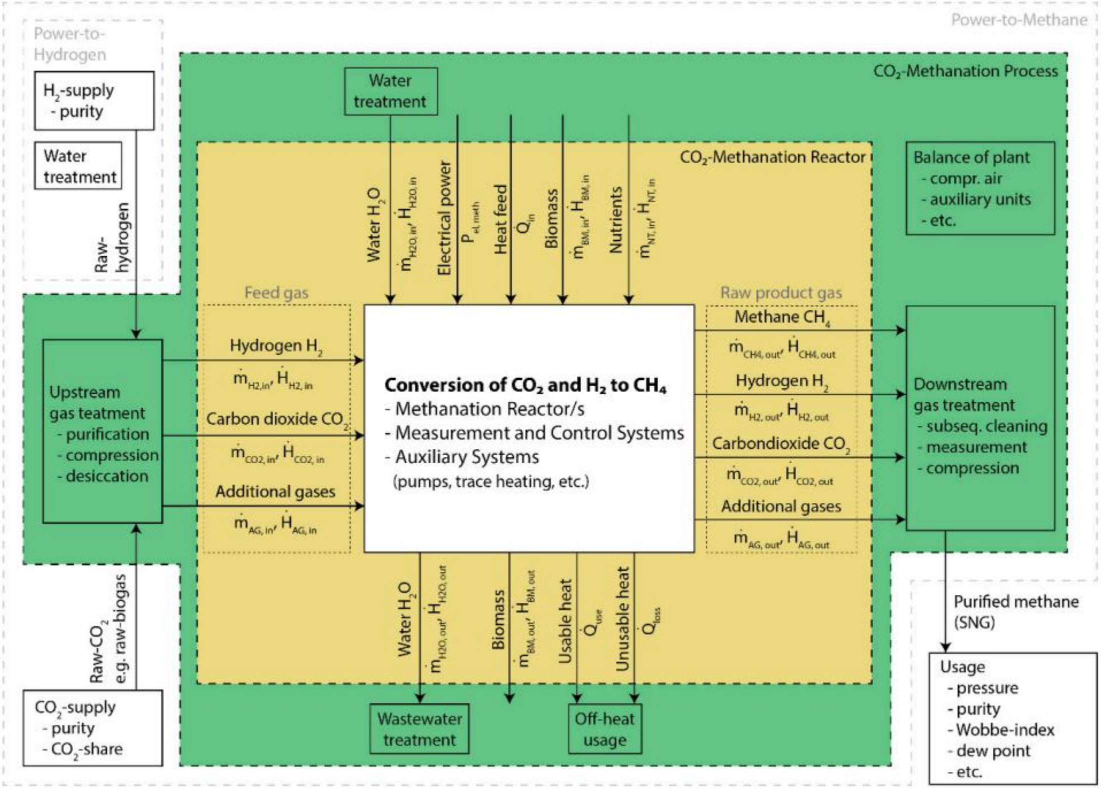

Figure 3: Power-to-gas process steps. (Thema, et al., 2019, p. 5)

2.2.1. Electrolysis

Electrolysis refers to the process of electrochemical decomposition of a substance by the application of an electric current. The decomposition is achieved by a redox reaction, which is forced by the applied current. In water electrolysis, this principle is applied to the decomposition of water (H_2O). During the oxidation at the anode, elemental oxygen (O_2) is formed. The reduction at the cathode leads to the formation of elemental hydrogen (H_2O) according to equation 1 (Tjarks, 2017, p. 5).

$$H_2O \leftrightarrow H_2 + \frac{1}{2}O_2 \qquad \Delta H_R = +285{,}83 \left[\frac{kJ}{mol_{H2}}\right] \qquad Equation\ 1$$

ΔH_R Reaction enthalpy

The reaction chambers of the anode and cathode must be separated spatially as well as electrically in order to be able to carry out the redox reaction in a controlled manner and movement of ions between the anode and cathode spaces must be possible. The movement of ions is achieved by an electrolyte, which has insulating properties for electrons. The electrolysis of water can be carried out with three ionic charge carriers: hydroxide ions, oxide ions and single charged protons. The cations move from the positively charged electrode to the negatively charged one, while the anions move the opposite way (Tjarks, 2017, p. 5).

There are basically three kinds of electrolyzes based on the type of ion transport: (a) alkaline electrolyzes (AEL), (b) Polymer-electrolyte membrane electrolyzes (PEM) and (c) High temperature electrolyzes (HTEL) as shown in Figure 4.

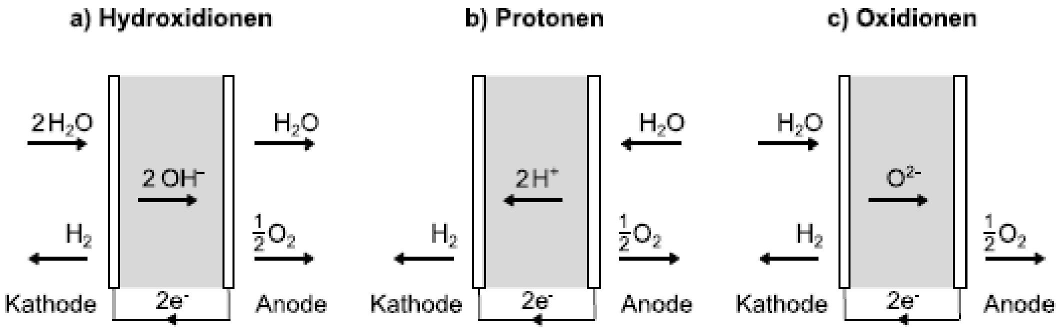

Figure 4: Ion carries in the AEL (a), PEMEL (b) and HTEL (c) (Tjarks, 2017, p. 6).

Classical alkaline electrolysis uses hydroxide ions as charge carriers. An alkaline liquid is usually used as the electrolyte. Polymer-electrolyte membrane electrolysis is based on the charge transport of protons. The electrolyte consists of an ion-conducting polymer membrane. In high-temperature electrolysis oxide ions are transported from the cathode to the anode. For the electrolyte, yttrium-stabilized zirconium oxide is used (Tjarks, 2017, p. 6).

The energy input of the endothermic reaction required for water splitting is shown in equation 1 and corresponds to the calorific value of hydrogen. The reaction enthalpy ΔH_R is given by the Gibbs-Helmholtz equation and consists of the free reaction enthalpy ΔG_R (Gibbs potential) and the product of temperature T and entropy ΔS_R (Graf, et al., 2021, p. 69).

$$\Delta H_R = \Delta G_R + T\Delta S_R \qquad \textit{Equation 2}$$

The minimum energy required for water electrolysis that must be supplied by electrical energy is defined by the Gibbs potential. In combination with the Faraday constant F and the number of transferred electrons z (equivalent number), the minimum required cell voltage (also known as reversible cell voltage V_{rev}) can be calculated according to equation 3 (Graf, et al., 2021, p. 69).

$$V_{rev}^0 = \frac{\Delta G_R^0}{z * F} = \frac{237{,}2\ [kJ * mol^{-1}]}{2 * 96485\ [C * mol^{-1}]} = 1{,}23\ [V] \qquad \textit{Equation 3}$$

V_{rev}^0	Reversible cell voltage at standard conditions
ΔG_R^0	Gibbs potential at standard conditions

The other fraction determined by temperature and entropy can also be supplied as heat energy. In case of low temperature electrolyzes such as alkaline and PEM electrolyzes, no or hardly any heat can be absorbed from the environment and therefore the energy has to be supplied by electrical energy as well. The result is the thermoneutral voltage V_{th} which can be calculated according to equation 4. (Graf, et al., 2021, p. 70)

$$V_{th}^0 = \frac{\Delta H_R^0}{z * F} = \frac{285{,}8\ [kJ * mol^{-1}]}{2 * 96485\ [C * mol^{-1}]} = 1{,}48\ [V] \qquad \textit{Equation 4}$$

V_{th}^0	Thermoneutral voltage at standard conditions
ΔH_R^0	Reaction enthalpy at standard conditions

The reversible cell voltage and the thermoneutral voltage shown in equation 3 and 4 vary with changing process temperature. With increasing temperature, the free reaction enthalpy decreases, and the entropy part increases. Therefore, the reversible cell voltage decreases as well, and the demand of electrical energy can be reduced. At temperatures of 800°C, the required electrical energy is reduced by 25% for example. This thermodynamic advantage is used by the high temperature electrolyzes, especially when already high temperature (waste) heat is available. (Graf, et al., 2021, p. 71)

Furthermore, the reversible decomposition voltage (V_{rev}) depends on the pressure, as can be derived from the Nernst-equation (equation 5). With increasing pressure, the reversible cell voltage and thus the required energy. This is because the gas bubbles formed at the electrodes must apply more force to detach from the electrodes at higher pressures. However, this has only a minimal effect on the reversible decomposition voltage e.g. at 298 K the reversible cell voltage increases from 1.23 V at 1 bar to approx. 1.29 V at 30 bar. (Graf, et al., 2021, p. 71)

$$V_{rev} = V_{rev}^{0} \frac{\mathrm{R} * \mathrm{T}}{z * F} * \ln\left(\frac{p(H_2) * p(O_2)^{\frac{1}{2}}}{p(H_2O)}\right) \qquad \textit{Equation 5}$$

R Gas constant

In the real operation, the reversible state cannot be achieved and losses cannot be avoided. In order to reach high hydrogen production rates in an electrolytic cell, the aim is rather to impose as large currents as possible. Due to the unavoidable losses the real cell voltage is always higher than the reversible cell voltage when an external current flow is imposed, and the efficiency is reduced. (Graf, et al., 2021, p. 72)

Several following factors influencing the losses in an electrolytic cell:

Ohmic losses R_A: The electric flows are opposed by resistances in an electrolytic cell. which are caused by the ionic resistance of the electrolyte, the internal electrical resistances of the electrodes, current distributors and bipolar plates, as well as by the contact resistances at the interfaces of the individual cell components. The ohmic losses increase in proportion to the current. (Graf, et al., 2021, p. 72)

Kinetic losses η_{Anode} & $\eta_{Cathode}$: These occur at both electrodes, due to the velocity-limited transfer of electrons at the interface of electrode and electrolyte. These losses generate an overpotential at the electrode, which counteracts the direction of the reaction. Since at the cathode only two electrons must be transferred for hydrogen formation, whereas four electrons must be transferred for oxygen formation at the anode, the overpotential on the hydrogen side (cathode) is significantly lower than those on the oxygen side (anode). (Graf, et al., 2021, p. 72)

Mass transportation limitation losses η_{MTL}: These losses occur due to restrictions in the supply or removal of gases and liquids to the electrode. The supply shortage with reactants reduces the mass transfer at the electrode and if the cell is operated with constant cell voltage, the current decreases as well. However, when the cell is operated with a constant current the overpotential must be increased in order to maintain the mass transfer. The larger overpotential increases the cell voltage in total. Mass transport limitations occur independently at the cathode and the anode. (Graf, et al., 2021, p. 73)

A well-known example is the so-called bubble overpotential at gas electrodes in liquid electrolytes, as they are also used in water electrolysis. Due to increased gas generation, the gas bubbles displace the electrolyte so that the electrode no longer has ionic contact. This reduces the effective surface area at the electrode and results in higher local currents. (Graf, et al., 2021, p. 73)

All these losses result in a higher energy demand for hydrogen production and the resulting cell voltage V_{Cell} can be calculated with equation 6. The ohmic losses ΣR_A as well as the overpotential (kinetic losses $\eta_{An} + \eta_{Ca}$) release joule heat, which is partly used to cover the heat demand $T\Delta S_R$ from equation 2. (Graf, et al., 2021, p. 73)

$$V_{Cell} = V_{rev} + \eta_{An} + \eta_{Ca} + i * \Sigma R_A + \eta_{MTL} \qquad \textit{Equation 6}$$

i Current

The ideal electrical efficiency ε_{ideal} is defined by the ideal thermodynamic efficiency of a galvanic cell according to equation 7. This ideal electrical efficiency defines the maximum transformation efficiency of an electrolyser cell if it works reversible and without losses. At standard conditions, ε_{ideal} of up to 83% can be reached and 17% of the supplied electrical energy is used to account for the reversible heat loss $T\Delta S_R$ to the surrounding, so the cell does not cool down (Graf, et al., 2021, p. 74).

$$\varepsilon_{ideal} = \frac{\Delta G_R}{\Delta H_R} \qquad \textit{Equation 7}$$

The real electrical efficiency of the cell is the sum of the voltage efficiency (which accounts for the ohmic and overpotential losses) and the faraday efficiency (which accounts for leakage currents, short circuits, cross reactions, permeability processes or recombination of hydrogen with oxygen). Equation 8 shows that, the higher the cell voltage, the lower the cell efficiency ε_V. (Graf, et al., 2021, p. 76)

$$\varepsilon_V = \frac{V_{th}^0}{V_{cell}} \qquad \textit{Equation 8}$$

When looking at the system electrical efficiency ε_{HHV} with regards to the higher heating value *HHV* in equation 9, also the power for auxiliary components $\Sigma P_{BoP,i}$ such as water treatment, compression, conditioning (cleaning and drying) as well as the efficiency of the AC/DC rectifier ε_{RF} must be considered. In case of a high temperature electrolysis, the term $\Sigma \dot{Q}_{th,i}$ accounts for the supplied high temperature heat as well as all other peripheral heat supplies (Graf, et al., 2021, p. 77).

$$\varepsilon_{HHV} = \frac{\dot{m}_{H2} * HHV}{\frac{P_{DC}}{\varepsilon_{RF}} + \Sigma P_{BoP,i} + \Sigma \dot{Q}_{th,i}} \qquad \textit{Equation 9}$$

P_{DC}	Electrical power (direct current)
$\dot{m}_{H2}$	Mass flow of hydrogen

2.2.2. Alkaline electrolysis

The alkaline technology is the oldest electrolysis with industrial applications dating back 120 years ago and is still dominating today's market.

The alkaline electrolysis consists of the two half-cells, which are separated by a diaphragm. The diaphragm is only permeable to hydroxide ions (OH-), but not to the gases, although mixing of the two product gases can never be completely eliminated. The two electrodes are made of perforated metal sheets, which usually have a porous structure on the surface or consist of woven nickel meshes which are coated with an additional catalyst (ruthenium dioxide) to increase the electrochemical activity. The electrodes are positioned as close as possible to the diaphragm to minimize ionic resistance in the cell. Electrical contact is made between the electrodes and the end plates in a single cell or the bipolar separator plates in a cell stack via the pre-sheets.

The diaphragm and electrodes are embedded in a cell frame which prevents leakage of the alkaline electrolyte (Graf, et al., 2021, p. 78).

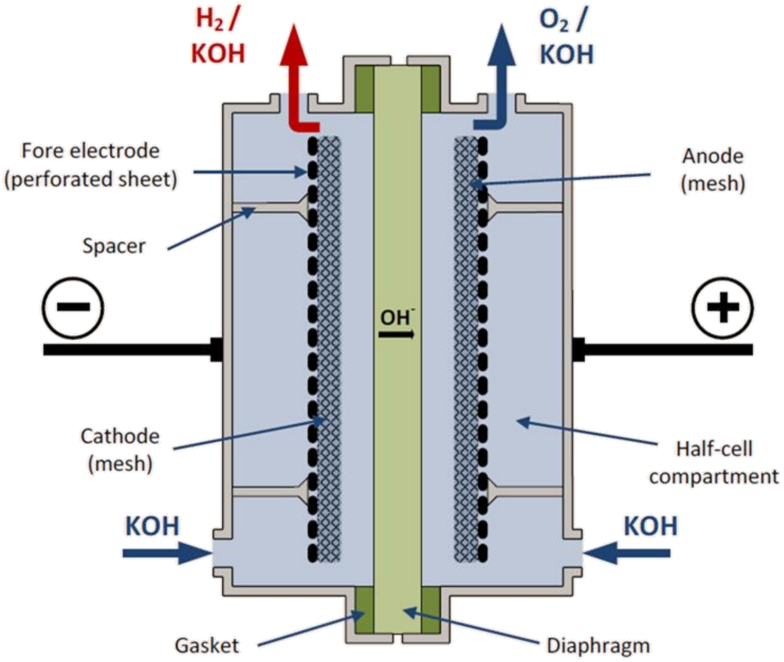

Figure 5: Alkaline electrolysis cell (Graf, et al., 2021, p. 79).

The alkaline electrolyte, usually 20-40% concentrated potassium hydroxide solution, flows through the two half cells. A direct current is applied to the two electrodes. In the gas-water separators, the gases produced are separated from the lye solution and transported for further processing.

Operational conditions

Alkaline electrolytic cells generally operate at an operating temperature of 70°C to max. 90 °C with a current density j of 200 - 400 mA/cm^2 or even up to 600 mA/cm^2 with advanced electrodes (Graf, et al., 2021, p. 81).

According to Faraday’s law (equation 10), the current density and the cell size, determine the hydrogen production capacity per cell.

$$m_{H2} = \frac{j * A * t}{z * F} * M_{H2} \qquad \textit{Equation 10}$$

m_{H2}	Mass of hydrogen
M_{H2}	Molar mass of hydrogen
A	Active cell area (geometric surface of the electrode)
t	Time

In order to obtain larger production capacities, several cells are therefore connected to form a cell stack, typically of filter press design. The individual electrolysis cells of a stack are clamped between two end plates and pressed together with threaded rods. The active cell area (geometric surface of the electrode) of alkaline electrolysers is usually between 0.5 and 3.0 m². and are therefore significantly larger than the cells of PEM or HT electrolysis. (Graf, et al., 2021, p. 81)

Alkaline electrolysers usually operate under atmospheric conditions. This mean, that in operation, no pressure is built up in the cell stack and the generated gases only have to overcome the hydrostatic pressure in the system. But there are also AEL Systems that have an operating pressure of 15 bar or 30-35 bar on the market. Some Chinese manufacturers offer already systems with up to 50 bar operating pressure. (Graf, et al., 2021, p. 82).

The choice of the ideal operating pressure depends on several factors, such as technical effort versus investment costs and especially the use of hydrogen. On the one hand, a higher operating pressure causes smaller gas bubbles and therefore the cell thickness can be reduced and/or the cell size can be increased. In total the system can be more compact (e.g., smaller gas separators) and the produced gases are under pressure, which helps with the mechanical compression afterwards or even eliminates it. On the other hand, the pressure resilient construction and lower gas quality increases investment costs. Also, the operational dynamics will be affected negatively, and the on-off procedure will be more complex. (Graf, et al., 2021, p. 83)

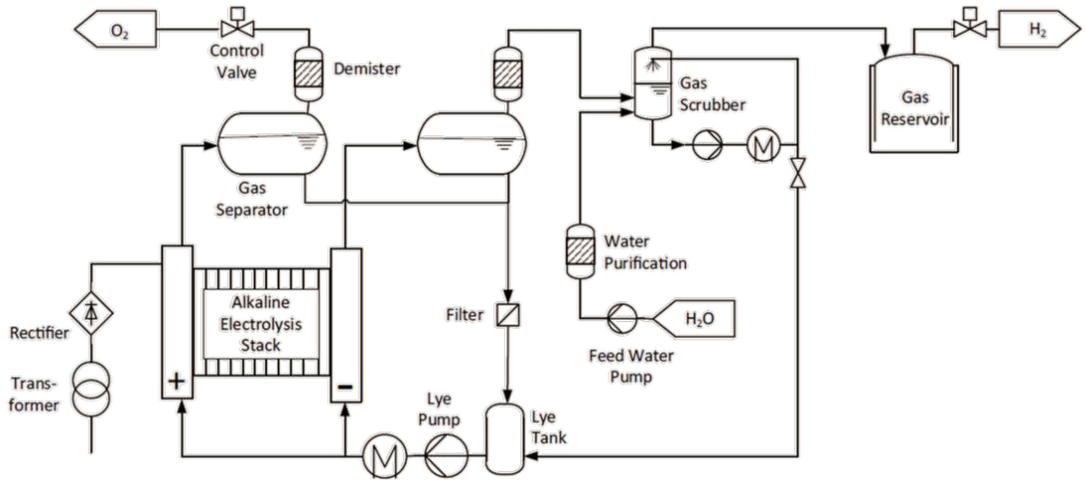

Figure 6: Schematic setup of an alkaline electrolyser without gas cleaning (Graf, et al., 2021, p. 84).

Figure 6 shows the AEL system. Hydrogen and Oxygen are produced in the electrolysis stack by the applied current and flow with the lye into the gas separator, where hydrogen, oxygen and lye are separated by their density difference at deflector plates. Afterwards, in conventional alkaline electrolysis, the lye streams from the oxygen and hydrogen fed back into the electrolyser via a pump and cooler. The merging of the two caustic circuits leads to impurities due to the gases dissolved in the caustic. Particularly in part-load operation the gas quality decreases, due to the increase of the ratio of gas dissolved in the recycled electrolyte to the gas produced in the cell stack. An additional KOH tank is used to maintain the lye concentration. It is also possible to have systems, where the natural convection by the produced gases replaces the lye circulation by the lye pump, which decreases the energy demand. However, this natural convection impairs the system dynamic, especially for starting the process.

(Graf, et al., 2021, p. 83)

After the gas separator, a demister filters small droplets off the hydrogen stream and a gas scrubber removes the leftovers of the lye with the aid of water. Additionally, a water treatment and a water tank for uninterruptible water supply, a gas chiller and dryer to increase gas quality and a compressor and a recirculation cooling unit to gather the heat can be installed. (Graf, et al., 2021, p. 84)

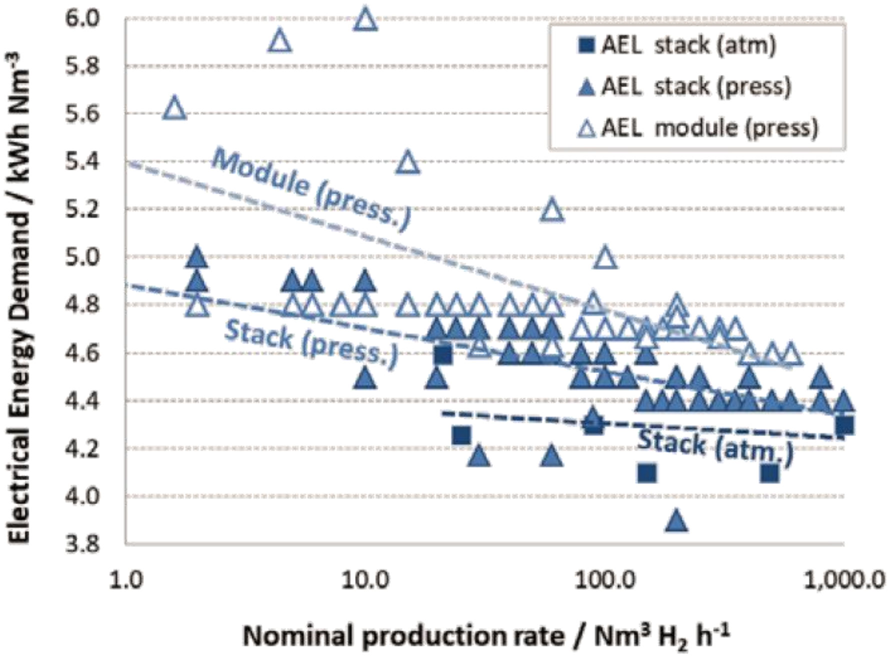

Figure 7: Electrical energy demand of AEL stated by manufacturers (2010-2020). (Graf, et al., 2021, p. 85)

Figure 7 shows the electrical energy demand versus nominal hydrogen production rate according to the manufacturers. It has to be noted, that the system boundaries are not often clear and therefore comparison is difficult. In general, atmospheric AEL reach a specific electrical energy demand of 4,1-4,5 kWh/Nm³ (HHV) which equals to 85% efficiency. An additional hydrogen compression to 30 bar increases the demand by 0,2 kWh/Nm³. Large pressurized AEL show a specific electrical energy demand of 4,5-5 kWh/Nm³ (HHV) due to the electrochemical compression. The larger the electrolyser, the smaller the difference between atmospheric and pressurized stacks. (Graf, et al., 2021, p. 85)

Most of the manufacturer indicate a minimum partial load of 20%. Continuous operation in partial load reduces the gas quality due to the dissolved gaseous impurities in the recirculated lye feed. This occurs especially during intermittent operation and increases with increasing operating pressure. This can effectively be minimized by a complete separation of the lye streams of the oxygen and the hydrogen side and therefore minimum partial load of 5% could be achieved. (Graf, et al., 2021, p. 86)

In general, AEL cells show a very high dynamic during load changes (within seconds) if the cells have reached the operating temperature. Therefore, AEL are also possible to deliver primary and secondary control reserve energy. (Graf, et al., 2021, p. 86)

In general, alkaline electrolysis systems are technically mature and therefore also very reliable. The most critical component of an alkaline electrolysis system is the cell stack. AEL pressure stacks with plastic diaphragms reach more than 50,000 h of operation. As a rule of thumb, a general overhaul every 7-12 years is necessary, where the electrodes are replaced or reactivated, and the diaphragms are exchanged. Most of the components such as the bipolar plates can be reused. Conventional alkaline electrolysers of the Lurgi or Demag type have been in operation for over 20 years in some cases without opening of the module. Factors, that influence the lifetime negatively are a high lye concentration, high operating temperature, fast heat up and cooling down when starting and turning off the system and often on-off operations. (Graf, et al., 2021, p. 87)

2.2.3. PEM electrolysis

PEMEL were first developed for military and space travel purposes in the 1960s and 1970s and the commercial breakthrough happened in the 2000s. A PEM electrolytic cell consists of a membrane electrode assembly (MEA) as shown in Figure 8.

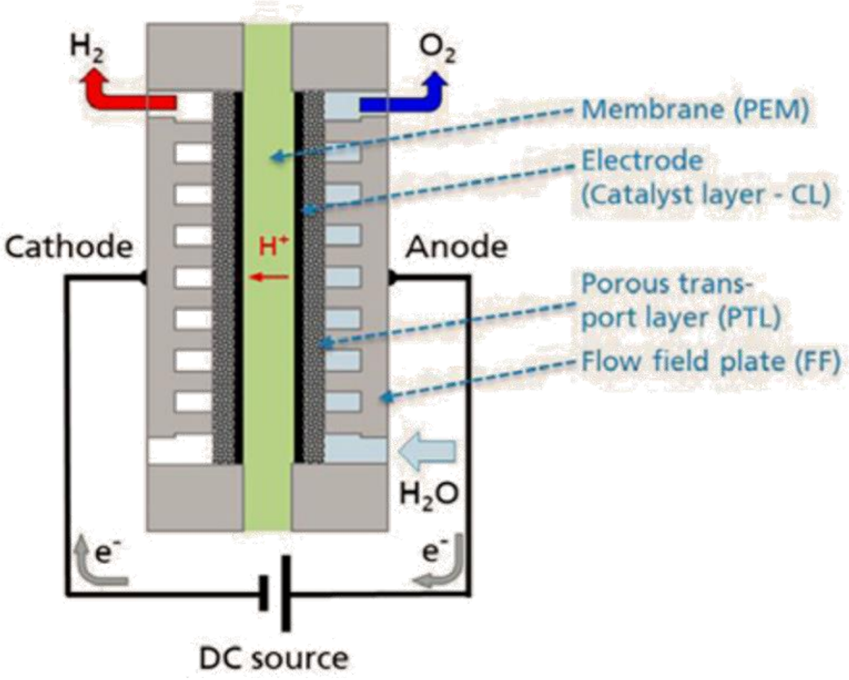

Figure 8: Schematic assembly of a PEM cell (Graf, et al., 2021, p. 88).

The two half-cells which are separated by the proton-conducting membrane with acidic properties, which acts as a solid electrolyte in the cell. The membrane is covered with a catalyst layer which acts as electrodes. Oxygen is produced at the anode and hydrogen is produced at the cathode. Porous transport layers are pressed against the electrodes which deliver and dissipate the current. The porous transport layers enable the supply of water to the anode and that oxygen and hydrogen can dissipate from the electrodes. A flow field plate is connected to the transport layer for distributing the water over the whole cell area and dissipating the product gases evenly. The membrane usually consists of perfluorinated sulfonic acid (PFSA) membranes, such as Nafion® from Chermours (formerly DuPont) or fumapem® from FuMA-Tech with a thickness of 50-300 µm. These membranes offer very high proton conductivity, low gas transmissibility and ideal mechanical and chemical stability, however zero permeation of hydrogen and oxygen cannot be achieved in real operation, especially when operating the cell with different pressures. Typical hydrogen purity qualities at the cell outlet are 2.8 to 4.0, based on the dry hydrogen. (Graf, et al., 2021, p. 88)

Due to the acidic properties of the membrane, the electrodes must be noble metal materials. On the hydrogen side, platinum is used as a catalyst and on the oxygen side iridium is preferred but also ruthenium and their oxides are used. The layers of these catalysts are only few microns thick. Also, the porous transport layers and the flow field plates must be made from a corrosion resistant material such as titanium which is quite cost intensive. (Graf, et al., 2021, p. 90)

Operational conditions

The PEM-cells usually operate between 55 to 70°C with a pressure of approx. 30 to 45 bar. The limitation regarding temperature is the PFSA-membrane with about 80°C. PEM-cells also can have high current densities of 1.5 to 3.0 A/cm² at cell potentials of 1.7-2.1 V. Due to the use of noble metals as electrodes, the kinetic overpotential losses are low and the current density mostly depends on the ionic resistance and thus on the thickness of the membrane. (Graf, et al., 2021, p. 91)

A PEMEL stack usually consists of 50 to 200 cells per stack and is built in a filter press design. Typical cell areas are nowadays 300 – 1500 cm² with already prototypes up to 5000 cm² cell area. Since cell thickness is around 2 – 5 mm, PEM stacks are much more compact with regards to cell number, area and volume compared to AEL stacks. The electrical power of one PEM stack ranges from 100 kW up to 1.5 MW currently. (Graf, et al., 2021, p. 93)

The next generation of PEMEL aims to reach 3 MW. By combining several stacks to modules or arrays, a scale-up to 100 MW or more can be reached. (Graf, et al., 2021, p. 97)

Figure 9 shows the typical system components of a PEMEL. There two design approaches, one is the equal-pressure-system, where both sides of the stack operating with the same pressure and the other is the difference-pressure system, where the hydrogen side has a different (usually higher) pressure than the oxygen side. The difference-pressure system requires a more complicated and robust membrane design to withstand the pressure differential of 30 or more bar. This saves costs and minimizes oxygen permeation compared to an equal-pressure-system, where both sides operate at 30 bar for example. (Graf, et al., 2021, p. 94)

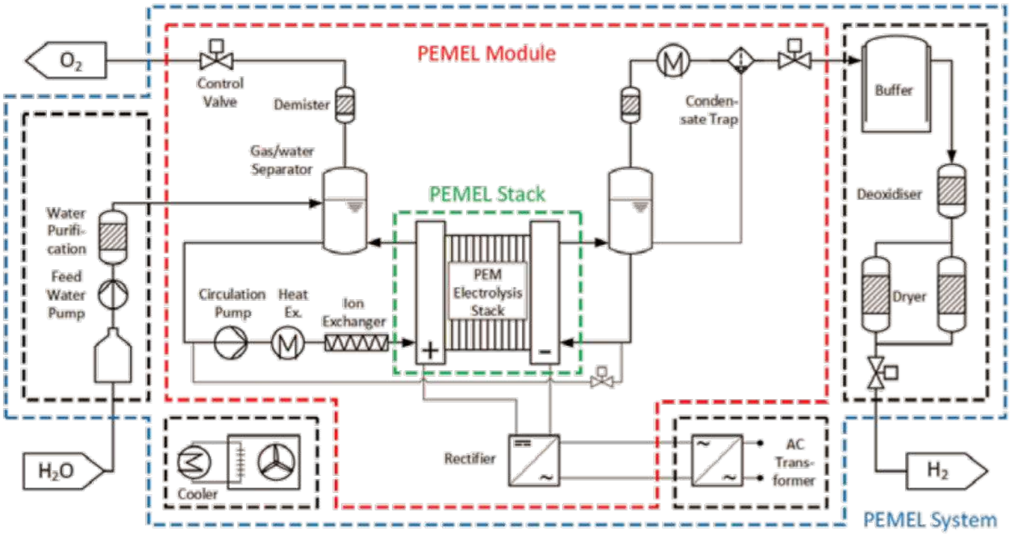

Figure 9: Schematic setup of PEM electrolyser system with gas cleaning and water treatment (Graf, et al., 2021, p. 95).

The system is supplied with feed water via a fresh water supply, which must be purified to the necessary water quality. The water pressure is increased to the pressure of the anode side by a feed water pump and fed to the process. For cooling the anode circuit, external coolers are usually used, which dissipate the process heat to the environment. Lower temperatures are required for cooling the gas streams in order to condense out as much water as possible from the gas streams. In order to be able to use the hydrogen for subsequent applications or for storage, it must be dried, and entrained oxygen must be removed. Oxygen removal is performed by a DeOxo reactor, usually based on a palladium catalyst. For fine drying, a pressure swing or preferably temperature swing adsorption is used. To enable a continuous volume flow in the gas purification, a buffer tank may be connected upstream of this. (Graf, et al., 2021, p. 96)

The specific electrical energy consumption of PEM electrolysis systems decreases with increasing production rate, although the energy consumption at the stack level remains almost constant. Specific energy consumption for small systems up to 50 kW_{el} is typically between 6 and 7 kWh/Nm^3, for medium systems up to 500 kW_{el} below 6 kWh/Nm^3 and for large systems > 1 MW_{el} around 5 kWh/Nm^3, which is like alkaline electrolysers. (Graf, et al., 2021, p. 97)

Similar to AEL, the lower operational limit is around 5% of the nominal load due to gas quality requirements as well as electrical demand of the auxiliary equipment. The biggest advantage comparted to AEL systems is the separate electrolyte circulation, which reduces dissolved oxygen on the hydrogen side and vice versa. However, diffusion over the membrane cannot be prevented completely, which is a function of partial pressure difference and temperature. Hydrogen quality reaches under normal operating conditions values of 2.8 to 4.0. Another advantage of the PEM-cell is the high overload capacity, up to 50% of the nominal current density. The limiting factor of the system when it comes to overload operations is mostly the rectifier and therefore a larger and thus more expensive rectifier is mostly used if overload operation is wanted. During overload operation, the generated heat is increasing rapidly and the limit of the thermal management in order to stay below critical cell temperature is reached. Usually overload operation is limited to several minutes up to one hour. (Graf, et al., 2021, p. 98)

The fast dynamic operation is another advantage. The electrolytic cell shows no lag in dynamic operation, however the auxiliary equipment such as water pump, liquid-gas separators show a larger lag. Due to the smaller thermal capacities compared to the AEL, the intermittent operation is quicker as long as cooling the cell is designed properly and also the start-up temperature is reached faster. During stand-by, start-up and shutdown, negative effects, also known from the AEL system, occur in the stack and system. Diffusion processes across the membrane increase the gas impurities. In particular, the permeation of hydrogen at higher pressure and the parallel recombination to water, which occurs at the electrodes or at the recombination layer are relevant issues. The recombination leads to a pressure decrease in the two half-cells and can cause mechanical stress, especially at the membrane. After shutdown or in stand-by, the entire system cools down; during start-up, heating occurs again; this thermal cycling has a negative effect on the lifetime of various components such as seals. Start-up from a cold state causes higher cell voltages due to the poorer kinetics and thus the current must be ramped up; however, PEM electrolysis has advantages over alkaline electrolysis in that matter. (Graf, et al., 2021, p. 99)

With regards to lifetime, the most critical component is the membrane. Mechanical stresses due to on-off processes and differential pressure and thinning of the material due to radical attacks case the decrease in gas quality and in the end failure of the membrane due to cracks. Furthermore, the purity of the feed water is essential since impurities (metal ions) remain as residues on the electrode or penetrate the membrane, therefore lowering the ionic conductivity, promote radical attack and cause electrical short circuits. Other degradation effects are titanium embrittlement, corrosion of the catalyst as well as aging of the seals. All of this can be minimized with the right design for the specific operational conditions. The technical lifetime for the PEMEL as for the AEL is defined by the maximum average cell voltage which is determined by the maximum tolerable power consumption of the stack, where cooling is still possible. Usually, a 10% increase of power consumption is tolerated until the efficiency is too low to operate economically. This means, the stack must be replaced or overhauled since it is out of specification, but it does not mean it is broken or not working anymore as it would be in the case of cracks. (Graf, et al., 2021, p. 100)

Early military PEMEL reached operating hours of up to 100,000 h and mature PEM designs reach lifetimes of 10 to 15 years. The stacks itself reach under commercial operation over 50.000 h. Although, new developments on the market have a lower lifetime. (Graf, et al., 2021, p. 99)

2.2.4. High Temperature electrolysis

The high temperature electrolysis (HTEL) which operates at 600 – 1000°C is based on a solid oxide electrolyte and therefore also called solid oxide electrolysis (SOEL). First developments date back to the 1970s and research in the last decades was concentrated on the solid oxide fuel cell, which also helped the SOEL. In the past years also the SOEL research and development intensified since the technology ready level is still lower compared to AEL and PEMEL. (Graf, et al., 2021, p. 101)

In order to withstand those high temperatures, ceramics have to be used as cell materials. Due to the brittle mechanical characteristics of these ceramics, the cell areas are rather small compared to the AEL or PEMEL. Also, the number of cells which can be combined to a stack is limited to 10 – 60. Therefore, more stacks (up to 24 stacks) are numbered up to a module to achieve higher water production rates. (Graf, et al., 2021, p. 104)

A simplified system of a possible SOEL arrangement including auxiliary equipment and high temperature heat integration (process steam) is shown in Figure 10.

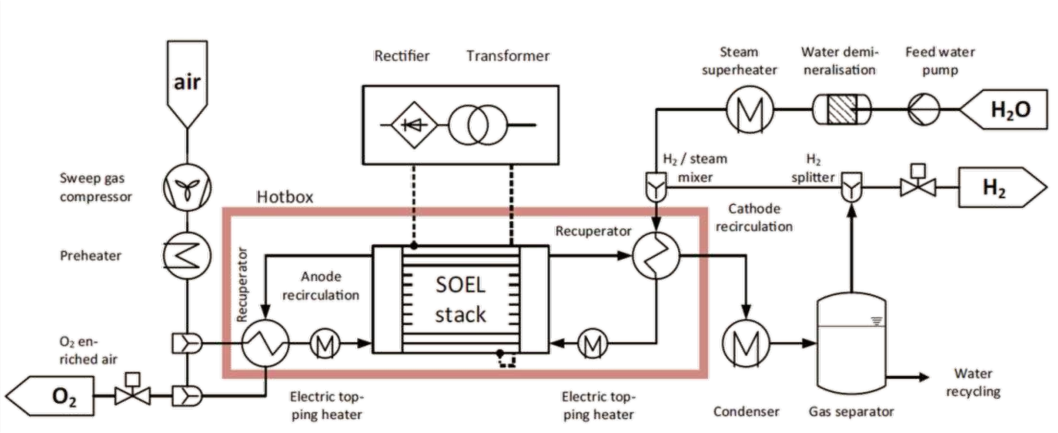

Figure 10: Schematic layout of SOEL system without gas treatment and compression (Graf, et al., 2021, p. 106).

The heavily insulated hotbox includes the module as well as a heat exchanger (recuperator) to re-use the high temperature heat of the outlet to heat up the inlet gas-water mixture stream. In a first step, the water is demineralized and evaporated and superheated using onsite available the process steam (around 200°C) in the steam superheater. The superheated steam is fed via a hydrogen/steam mixer into the cathode recirculation (water steam and hydrogen mixture with 10% H_2) and then heated to almost stack temperature in a recuperator which reduced the reoxidation of the electrode. Optional additional electrical heater at the entrance of the electrode enables a faster preheating and therefore more flexible operations. The feed steam will be decomposed electrochemically up to max. 80% to reduce undersupply of the electrodes and thus damage. The exit steam is cooled down in the recuperator, water is recondensed in the gas separator and then sent to the water recycling. The hydrogen is also removed and sent to gas conditioning. At the anode, also a sweep gas (during start up, air is used and during continuous operation also pure oxygen can be used) is circulated to remove the produced oxygen easier and to enable an efficient thermal management. (Graf, et al., 2021, p. 106)

Operational conditions

Until now, only few systems are operating under real conditions, with the biggest SOEL system the HyLink200 by Sunfire with 730 kW_{el} and 200 Nm^3/h hydrogen production rate in Salzgitter, Germany. (Graf, et al., 2021, p. 106)

In the laboratory, the electrical energy demand was around 3.0 – 3.3 kWh/Nm³ hydrogen with temperatures of 800°C. In the smaller field test systems with additional electrical heating, the electrical energy demand increases to 4.1 kWh/Nm³. In case of the use of onsite high temperature process heat, the electrical energy demand is expected to be around 3.7 kWh/Nm³. (Graf, et al., 2021, p. 107)

A SOEL cell can operate in either an endothermic, autothermic or exothermic mode. The joule heat created in the cell due to losses depends on the current density. At low current densities, the cell is endothermic and thus needs external heat and at high current densities, the additional heat must be removed. The ideal operating point of a SOEL-cell is autothermic, where the joule heat is equal to the heat required for water splitting at operating temperature. This enables a homogenous temperature and a very low temperature gradient between feed and exit stream, which reduces thermal-induced mechanical tension on the ceramics and thus increases the lifetime. Also, low part load operation is no problem for a SOEL cell if the thermal management is properly designed. Also, quick load changes can be achieved by the SOEL cell, however this quick load changes cause temperature differences and therefore the already mentioned tensions can cause cracks in the ceramics and lifetime is reduced. The temperature differences also occur during on and off phases and therefore it is a rather slow process compared to AEL and PEMEL. To increase the start up speed, a hot standby can prevent a fast cold start. Usually, SOEL systems operate under atmospheric conditions because a pressurized system which must withstand such high temperatures would not be economic. (Graf, et al., 2021, p. 108)

Due to the lower technology readiness level compared to AEL and PEMEL, long-time operating tests are rare. In general, the lifetime is lower than those of AEL and PEMEL, especially in dynamic operation. (Graf, et al., 2021, p. 109)

2.3. CO_2 Methanation

The conversion of carbon oxides (CO, CO_2) by means of hydrogen to methane has been known by Sabatier and Senderens (1902) since the beginning of the 20th century.

It must be distinguished between the catalytic methanation and the biological methanation. These two types of methanation principles are further discussed and compared in this chapter.

The gas hourly space velocity – GHSV [1/h] of a methanation reactor is the relation between the total feed gas volume stream into the reactor to the corresponding reactor volume Normally the GHSV is given for standard conditions. The GHSV defines under given yield the required reactor volume for a given reactant stream. It has to be noted, that the reactor volume is sometimes defined as the catalyst volume or as the actual geometric volume of the reactor, which can differ quite a lot. (Graf, et al., 2021, p. 163)

2.3.1. Catalytic Methanation

The direct catalytic methanation of CO_2 is described by two steps. The first step is the reverse water gas shift reaction (equation 12), where CO is formed, which then reacts in the CO methanation with H_2 to CH_4 (equation 11). Since the actual reaction mechanisms in place are not yet identified totally and research is still going on, the CO_2 methanation can by described by equation 13. It is a strong exothermic hydration of carbon oxides with the aid of a catalyst. (Graf, et al., 2021, p. 161)

$$CO + 3H_2 \leftrightarrow CH_4 + H_2O \qquad \Delta H_R = -206.4 \left[\frac{kJ}{mol}\right] \qquad Equation\ 11$$

$$CO_2 + H_2 \leftrightarrow CO + H_2O \qquad \Delta H_R = 41.5 \left[\frac{kJ}{mol}\right] \qquad Equation\ 12$$

$$CO_2 + 4H_2 \leftrightarrow CH_4 + 2H_2O \qquad \Delta H_R = -164.9 \left[\frac{kJ}{mol}\right] \qquad Equation\ 13$$

The use of a catalyst reduces the activation energy of a chemical reaction and therefore the reaction speed and the GHSV will increase. For the catalytic methanation a metal catalyst is used on a carrier made from SiO_2, Al_2O_3, ZrO_2 or other oxides. The aim of the carrier is to increase the surface area of the active catalyst. (Graf, et al., 2021, p. 165)

Due to costs and activity as well as selectivity reasons, nickel-based catalysts are normally used for the CO_2 Methanation, since they also promote not only the CO hydration but also the reverse water gas shift reaction. The activity of these nickel catalysts can be affected by several deactivation processes: (Schmidt, et al., 2018, p. 12)

Mechanical damage due to blocking of pores or catalyst surface (due to particles in the gas stream are scoot formation) as well as mechanical abrasion due to erosion especially in fluidized bed and slurry reactors.

Chemical processes which poison (e.g. sulphur compounds) the catalyst by adsorption and blocking as well as reactions which production inactive and volatile components.

Thermal deactivation due to very high temperatures caused by sintering of the catalyst and/or the carrier material and thus reducing the catalyst surface.

In literature four different reactor concepts for the catalytic methanation are discussed. The main aim the reactor design is to have a sufficient temperature control (dissipate large amount of specific heat) in the main reactor zone as well as to reach a maximum methane yield. In general, there are two-phase reactor systems, where the reaction gases flow directly around a solid catalyst and three-phase reactor systems, where an additional liquid phase is present to dissipate the heat out of the reactor. (Graf, et al., 2021, p. 169)

Fixed bed reactors

Fixed bed reactors are widely used in the chemical industry. The reaction takes place on the surface of a porous catalyst particles, which are introduced into the reaction chamber as a filling bed. In general, a distinction is made between adiabatically and isothermal operated reactor systems. In the simplest case, adiabatic fixed-bed reactors consist of a cylindrical shell in which the catalyst rests loosely on a grid screen and is flown through axially. For selective reactions limited by thermodynamic equilibrium, multistage reactor systems with intercooling are usually used to ensure high product yields. Various technologies, such as vapor recirculation, vapor moderation or kinetic limiting of the conversion, are known for thermal control measures of the process. In general, fixed-bed reactors have different temperature levels to optimize both residence time and conversion rates. (Schmidt, et al., 2018, p. 13)

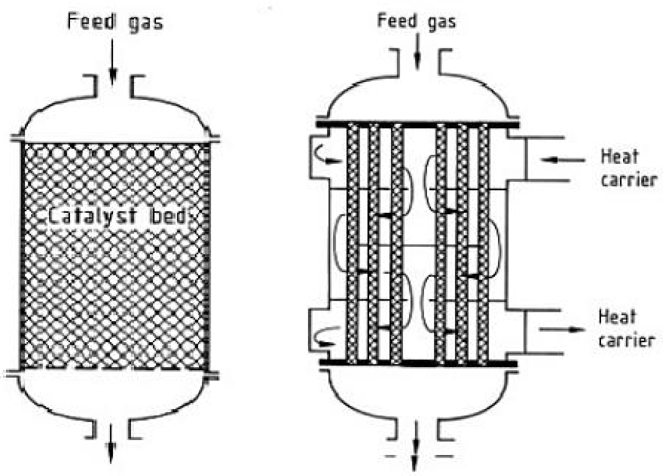

Figure 11: Fixed bed reactor types: (left) adiabatic and (right) quasi isothermal (Schmidt, et al., 2018, p. 14)

In general, the process engineering effort is usually quite high since several reactors are required and/or recirculation streams must be operated. These concepts are therefore for plants with a large methane production capacity of 100 MW or more, which are also not aimed at dynamic operation. (Graf, et al., 2021, p. 170)

Wall-cooled isothermal reactor types allow the thermal process control to be adapted to the requirements for a maximum degree of conversion. This enables almost complete conversion in a single reactor stage. By introducing a heat transfer surface into the fixed-bed fill, the heat generated, can be dissipated during process and therefore temperature peaks can be minimized. The fixed-bed shell-and-tube reactor represents the oldest and still predominant representative of the reactor classification. The catalyst bed is in the individual tubes of the tube bundle, while the heat transfer medium (e.g., pressurized water, thermal oil, or molten salt) circulates around the tube bundle through an external heat exchanger. (Schmidt, et al., 2018, p. 13)

Such a molten salt wall-cooled isothermal reactor type is used in the 3.2 MW methanation plant in Werlte, Germany. (Graf, et al., 2021, p. 170)

Typical fixed bed reactors should operate in a load window between 40% minimum load and up to 100% maximum load. Overload operation is problematic due to temperature control issues and usual load change dynamics are with +/- 1% per minute quite slow compared to electrolysis. Rapid load changes cause high temperature gradients and dangerous hotspots on the catalyst surface which can lead to deactivation. Measures for thermal management could be gas recirculation with intercooling. (Graf, et al., 2021, p. 176)

Fluidized bed reactors

Compared to fixed bed reactors, a better transfer of the generated heat is achieved by a fluidized bed reactor, where the reactant gas stream is brought into the reactor at the bottom and the fine catalyst particles are therefore fluidized and develop the fluidized bed. (Graf, et al., 2021, p. 171)

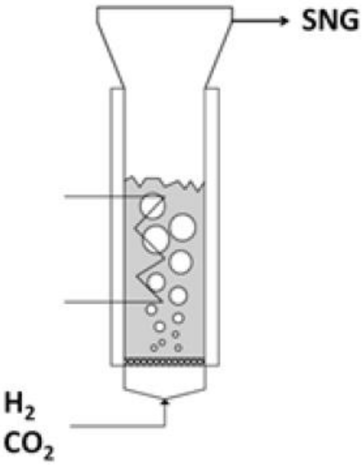

Figure 12: Fluidized bed reactor type. (Schmidt, et al., 2018, p. 15)

The intensive agitation and uniform distribution of the catalyst enables high heat transfer rates and homogeneous reaction conditions throughout the entire reaction chamber. A heat exchanger in the fluidized bed enables heat dissipation and thus creating almost isothermal conditions in the reactor. (Schmidt, et al., 2018, p. 14)

The good heat dissipation also ensures increased tolerance of the reactor to impurities in the reactant gas stream, especially from upstream gasification processes of solid biomass for example. If suitable catalysts are selected, unsaturated hydrocarbons can be hydrogenated in situ as well. Therefore, a fluidized-bed reactor type can be used for methanation of a synthesis gas from wood gasification. An example would be the 1 MW plant by REPOTEC in Güssing, Austria. (Graf, et al., 2021, p. 171)

The disadvantage of fluidized bed systems is that the high mechanical stress on the moving catalyst particles can lead to abrasion and discharge of the catalyst from the reactor as well as corrosion of reactor internals. Another disadvantage is the limited flexibility in dynamic load operation, since the fluidized bed needs a certain minimum gas stream for creating the fluidized bed as well as a maximum stream, so no solids are brought out of the reactor. (Graf, et al., 2021, p. 172)

Structured reactors

Structured reactor types are basically special isothermal fixed bed reactors which are liquid cooled from the outside. The reactant gases are flowing through over the catalyst surface which is coated on a carrier material with very high thermal conductivity.

The advantage of these structured reactors is that the improved heat conduction allows larger diameters of the individual reaction tubes, which drastically reduces their number and thus also their cost. Furthermore, the improved heat transfer ensures that these systems have a significantly increased tolerance to dynamic load changes and the associated temperature changes, which makes them particularly suitable for power-to-gas applications. Usually, these reactors have a honeycomb structure made out of metal or ceramics on which the catalyst is coated. (Graf, et al., 2021, p. 172)

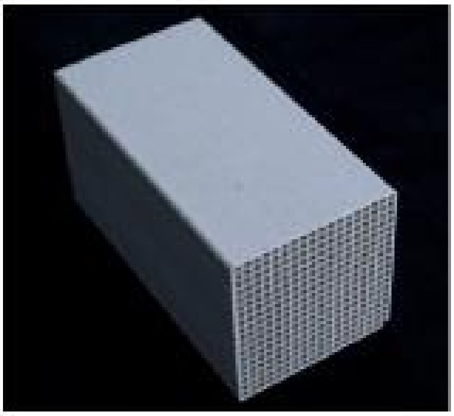

Figure 13: Honeycomb structure of a structured reactor type developed by Montanuniversity Leoben. (Biegger, et al., 2016, p. 9)

The Montanuniversity Leoben together with Christof Project GmbH developed a methanation process based ceramic honeycomb catalyst carrier made from Cordierite which offers high resistance to temperature changes as well as a high heat storage capacity. The honeycombs are placed in two or more chambers which offers modulation of the gas stream, and thus 20%-part load operation can be achieved. Cyclic switching of the chambers keeps their reaction temperature constant. This offers high dynamic operations, efficient stand-by mode as well as easy scale up. (Biegger, et al., 2016, p. 7)

Three-phase-reactors

Three-phase bubble column reactors (suspension reactors) are basically a special form of fluidized bed reactor in which an additional liquid phase is present in addition to the solid catalyst and the gaseous reactants. The solid catalyst forms a suspension with the stable liquid phase under reaction conditions. The main advantage of the liquid phase, which has a very high heat capacity and conductivity, is the improved heat transfer properties in the reactor system. to the cooled reactor walls, inbuilt cooling register or external heat exchanger. (Graf, et al., 2021, p. 173)

Due to the high degree of mixing in the reactor, it can be operated quasi isothermally and temperature hot spots in the reactor can thus be avoided, which would lead to catalyst deactivation and limit the conversion via thermodynamic equilibrium. In contrast to the two-phase fluidized bed with a limited operating window, three-phase reactors can be operated efficiently in a significantly wider load range. In extreme cases, e.g., when a pumped liquid circulator is used, the minimum load to operate the reactor can theoretically be reduced to zero. Together with the high heat capacity of the reactor material, operation with dynamic load changes, temporary standstill or intermittent operation under overload is therefore possible. (Graf, et al., 2021, p. 174)

Currently, the only implementation of a bubble column reactor for methanation is the three-phase methanation plant at KIT's Energy Lab 2.0 in Karlsruhe. The plant delivers 100 kW of methane output and was commissioned in 2019. Initial tests show a highly dynamic operating behaviour of the reactor with respect to load changes in the reactant gas and therefore large load changes can be implemented within seconds. (Graf, et al., 2021, p. 175)

2.3.2. Biological Methanation

The biological methanation is the enzymatic production of methane from hydrogen and carbon monoxide by microorganisms called Archaea as a catalyst according to equation 14. Since the usual operating temperature is around 30-70°C, the water is liquid, and the enthalpy of reaction is therefore lower than for the catalytic methanation. (Graf, et al., 2014, p. 8)

$$CO_2 + 4H_2 \leftrightarrow CH_4 + 2H_2O \qquad \Delta H_R = -253\left[\frac{kJ}{mol}\right] \qquad Equation\ 14$$

Compared to the catalytic methanation, H_2S as well as NH_3 are not harmful to the biological process, in fact they are in limited concentrations (up to 6,3-7,5 mmol/l) beneficial for the metabolism of the microorganisms. (Graf, et al., 2021, p. 177)

The optimum pH-value for methane production from hydrogen should be between 6.9 to 7.8. (Graf, et al., 2014, p. 9)

Microorganisms are very resilient to pressure and can produce methane in an environment with constant pH of up to 400 bar. From the process engineering point of view, pressures up to 20 bar are more realistic though. (Graf, et al., 2014, p. 12) In general, a higher pressure fosters methane production due to a higher nutrition supply and there a higher concentration of microorganisms in the reactor. (Graf, et al., 2014, p. 15)

Since water is present in the liquid state, the gaseous hydrogen must be dissolved in the liquid phase. The limiting factor therefore is the bad solubility of hydrogen in water which limits the hydrogen transport to the microorganisms, which are present in the liquid phase, and the maximum possible equilibrium concentration cannot be reached. A high hydrogen transport can be reached with large exchange areas as well as a low transport resistance. (Graf, et al., 2014, p. 14)

In general, the gas hourly space velocity GHSV is much lower than for the catalytic methanation, therefore the reactors for biological methanation are much larger in order to reach the same performance. Biological methanation can take place in the common fermenter of a biogas plant, (in-situ) or in a separate reactor (ex-situ) after fermentation. (Graf, et al., 2021, p. 178)

In-situ biological methanation

In the in-situ methanation, the hydrogen is brought into the fermenter of the biogas plant and methanation of CO_2 happens in parallel to the anaerobic digestion of biomass. The big advantage is, that existing biogas plants can be used, and no separate reactor is needed, in case the fermenter is quite hydrogen tight. The disadvantage can be a negative influence on the anaerobic digestion due to higher hydrogen concentration in the liquid phase which can hinder certain processes (e.g. degradation of propionic acid) thermodynamically and can cause acidification. In the worst case it can stop biological growth and elution of microorganisms. (Graf, et al., 2021, p. 178)

The biggest challenge of the in-situ methanation is the increase of hydrogen concentration in the liquid phase, so that most of the hydrogen will be processed to methane. A simulation (of an in-situ methanation in a fermenter, assuming a mixture of stirring tank and bubble column reactor, shows that a certain liquid column height (>15 m) is necessary to increase the hydrogen conversion. (Graf, et al., 2021, p. 178)

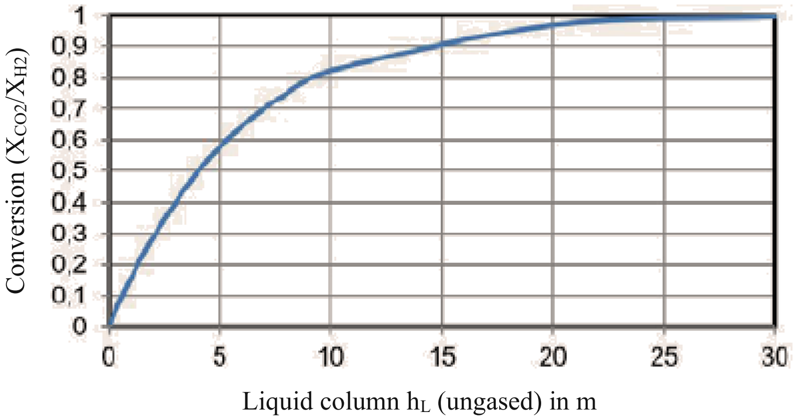

Figure 14: Variation of the liquid height h_L in a bubble column reactor (p = 1 bar, T = 37 °C, uGas = 0.01 m/s, $(H2/CO2)_{input}$ = 4 (Graf, et al., 2021, p. 179)

Ex-situ biological methanation

The ex-situ biological methanation takes place in a separate reactor, where either the untreated biogas or the pure CO_2 after upgrading can be brought in the reactor with H_2. When using the raw biogas for methanation, H_2O, O_2 and H_2S and small parts of leftover CO_2 must be removed in a gas treatment process afterwards. If there is a full conversion of CO_2 in the reactor, a removal can be spared. The advantage of using the CO_2 stream compared to the whole biogas stream is that the reactors can be build smaller and an integration to an existing biogas upgrading plant is easy. (Graf, et al., 2021, p. 179)

In general, ex-situ biological methanation has the advantage that the operating conditions in the reactor (pH, temperature and pressure) can be optimized with respect to hydrogenotrophic methanogenesis. This includes the use of special pure cultures or cultures adapted to changing conditions during operation. This would not be possible with conventional fermentation, since non-sterile microorganisms are continuously introduced through the biomass and the complex degradation steps from biomass to biogas require a large number of different microorganisms. (Graf, et al., 2021, p. 180)

Reactor concepts

There are different reactor types which all have the aim to transport the reactants to the microorganisms in the liquid phase the best way possible. The gas-to-liquid mass transport of hydrogen across the phase boundary depends on the volumetric mass transfer coefficient, the specific surface area, and the concentration gradient between the phases. These limitations can be improved in different reactors by different measures: (Thema, et al., 2019, p. 10)

- Stirring or higher flow velocities in the liquid phase
- Using a packing material inside the reactor or adapting hydrodynamics to create smaller bubbles or droplets
- Increasing the operating pressure

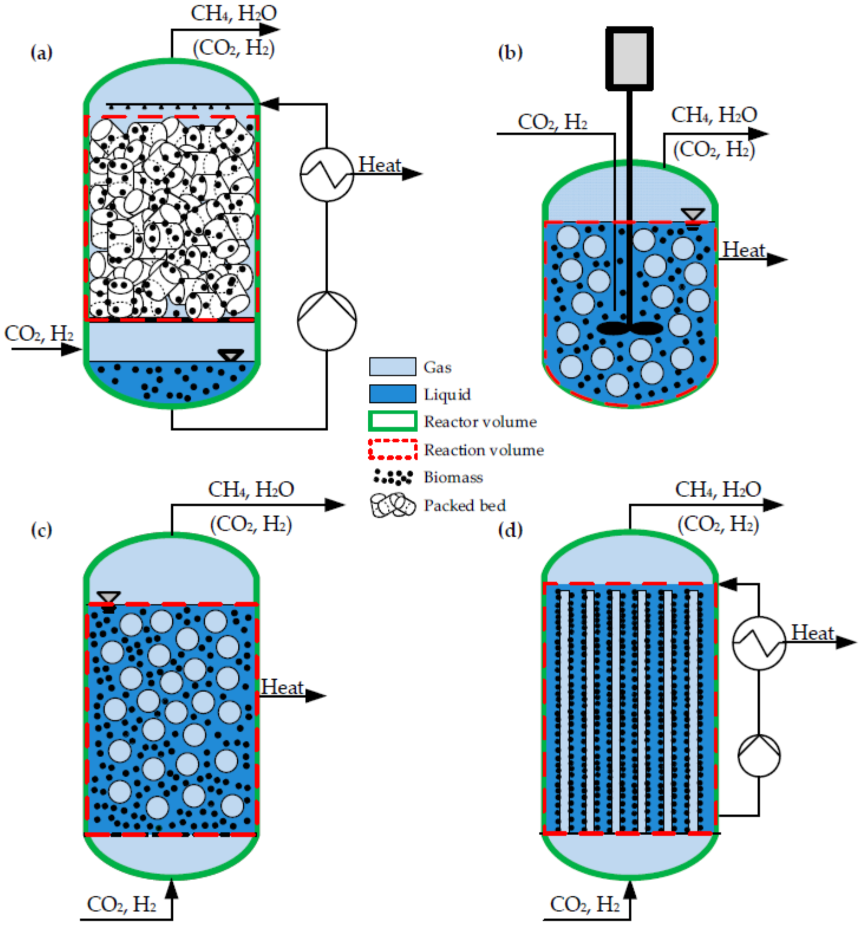

Figure 15: Reactor types of ex-situ biological methanation (a) trickle-bed reactor TBR, (b) continuous stirred tank reactor CSTR, (c) bubble column reactor BCR and (c) membrane reactor MR. (Thema, et al., 2019, p. 11)

In order to quantify and compare the performance of the reactors with each other the GHSV and the methane formation rate *MFR* as a kind of reactor utilisation are one of the most important indicators. (Graf, et al., 2021, p. 180)

$$MFR = \frac{\dot{V}_{CH4,out} - \dot{V}_{CH4,in}}{V_r} \qquad \text{Equation 15}$$

$\dot{V}_{CH4,out}$	Volumetric output flow of methane
$\dot{V}_{CH4,in}$	Volumetric input flow of methane
V_r	Reactor volume

In continuous stirred tank reactor (CSTR) the mixer divides the bubbles to increase the surface area. This improves the mass transfer of hydrogen into the liquid phase with increasing rotational speed (usually 300 – 1200 rpm). This also increases the power consumption of the process which is proportional to f^3d^5 (frequency *f* and diameter *d*) and can result in up to 16% of the total energy input. Therefore, the geometry of the mixer is of special importance and a higher pressure increases the mass transfer rates. When the reactor pressure is increased, the hydrogen partial pressure increases and thus the concentration of hydrogen at the phase interface also increases. This results in a larger concentration gradient in the liquid film and thus a faster mass transport of hydrogen into the liquid phase. (Graf, et al., 2021, p. 181), (Graf, et al., 2014, p. 15)

A major disadvantage of the CSTR is the strong back-mixing of the gas and liquid phases. As a result, the composition of the gas phase in the entire reactor corresponds to the product gas composition at the reactor outlet. In order to achieve a low hydrogen concentration in the product gas, high hydrogen conversion is needed. This results in a low hydrogen concentration in the gas phase and therefore in a low concentration gradient. (Graf, et al., 2021, p. 181)

To increase the concentration gradient and therefore increase the mass transfer from the gas into the liquid phase reactors where back mixing is almost not existing such as counter current trickle bed reactors (TBR) and bubble column reactors (BCR) are used. In these reactors, the hydrogen and carbon dioxide enter the reactor at a stoichiometric relationship of 4 H_2/CO_2, and the concentration of hydrogen in the gas phase decreases within the reactor due to the biological methanation to the product gas concentration level. This allows a higher average concentration gradient and thus a higher mass transfer. At the same time, these reactors can be designed as pressure reactors, so that the methane content in the product gas is increased and the methane formation rate (MFR) is increased while the GHSV remains constant. (Graf, et al., 2021, p. 181)

Furthermore, the energy demand of the TBR is lower than for BCR and CSTR, since no additional energy except pumping the gas to the top of the column has to be used in order to disperse the liquid into droplets. (Thema, et al., 2019, p. 10)

A rather new and still in academic research is the membrane reactor, where the microorganisms are immobilized in a biofilm on the outside of the cylindrical membranes. This separates the liquid and the gas phase. (Thema, et al., 2019, p. 10)

Operational conditions

Regarding flexible load operations, the microorganisms react quite well on load changes and start-up after stand-by is possible within several minutes. A minimum load for stirred systems is required, which is defined by the energy consumption of the mixer and the heating. Since the reactors operate around 40-70°C, heat recovery is limited to the temperature level. (Graf, et al., 2021, p. 183)

2.3.3. Post-gas treatment

After both biological and catalytic methanation, a product gas treatment process is necessary to reach gas grid specifications according to Table 2. A drying process reduces the water content to meet the dew point limitations. Furthermore, trace elements such as H_2S and NH_3 as well as not fully converted CO_2 and H_2 may have to be filtered out of the product gas stream using the same processes and techniques as for biogas upgrading as presented in chapter 2.1.2 and therefore, synergies concerning the gas treatment can be used. (Thema, et al., 2019, p. 7)

3. Methodical Approach

In this chapter, the methodical approach of the techno-economic assessment a multi-energy facility at the biogas plant Bruck/Leitha was carried out.

3.1. *Market research*

For a complete techno-economic assessment of a power-to-gas plant several following technical and economic parameters of an electrolysis system and the methanation system are required to determine the economic feasibility.

- Capital costs
- Operating costs
- Lifetime
- Efficiency
- Power demand
- Heat demand and output
- Water demand

These parameters were gathered conducting a meticulous market research of state-of-the art technology manufactures of electrolysers and methanation plants in Central Europe combined and backed-up with data from the literature. Furthermore, data on electricity prices were gathered from historical market data in Austria and the source of the grid connection fees was the local distribution system operator.

Based on this research three scenarios (low, mid and high) with different assumptions for costs, efficiencies and electricity prices were set up in order to reflect the uncertainties of the gather data and provide a wider range of outcomes with different input data.

3.2. *Real data from the biogas plant*

In order to develop a concept and determine the right size of the power-to-gas plant to the given biogas plant in Bruck/Leitha, the following real historical data of one year was gathered during two sessions at the plant:

- Product gas (biomethane stream)
- Off gas (CO_2) Stream

- Power demand of several applications
- Heat demand and temperature levels of several applications

3.3. Dimensioning and calculation of long run generation costs (LRGC) of the Power-to-Gas plant

Based on the gathered techno-economic data of electrolysers, methanation plants and the historic data of the biogas plant, several options of different plant sizes were selected and the long run costs of synthetic biomethane generation for each plant size was calculated for each low, mid and high price scenario and also for different electrolyzes technology. In the calculation, the available CO_2 stream of biogas upgrading over one year of production, a CO_2 storage for buffering and the possible waste heat integration different temperature levels of the power-to-gas plant on were taken into account. Since the electricity price for electrolysis has a major influence on the long run generation costs (LRGC), different electricity price models (spot market model, future model, fixed price model) were considered as well as the positive and negative balance energy market, since the electrolysis can deliver primary, secondary and tertiary balance energy. The calculated long range generation costs of synthetic biomethane of each scenario and variant are compared to each other and the best plant size, technology and electricity price model are presented in chapter 4.

4. Research Problem and Input Data

The integration of the different energy sectors gas, power and heat will play a key role in achieving a resilient and carbon neutral energy system. In order to realise this so-called sector coupling, locations where energy is not only produced, but also converted or even stored in an efficient way are necessary to meet the future demands and provide flexibility by reducing the loads on the individual grids. The most promising technology to couple the electricity and the gas sector is the power-to-gas technology, where electricity is used to split water into hydrogen and oxygen. Since there are no pure hydrogen grids yet, and local hydrogen storage and transportation in trailers is rather expensive and requires a certain amount of energy power-to-gas is not done yet on a large scale. Also, the injection of hydrogen into the existing grid is limited to maximum 10% vol. in Austria and in summer due to low gas consumption the gas flow is also on a low level and blending is rather limited. Therefore, it makes sense to add another step and convert the hydrogen to synthetic methane with CO_2 in the methanation process. This synthetic methane fulfils the technical requirements for grid injection and can therefore be injected everywhere into the public gas grid without problems. One of the best CO_2 sources are biogas upgrading plants which produce apart from biomethane also pure biogenic CO_2 from anaerobic digestion of wet biomass, which is so far primarily vented into the air. Therefore, the CO_2 is not only renewable but also already present in a highly concentrated (99%) stream. This makes biogas upgrading plants an ideal location for a power-to-methane plant, since the gas grid connection is already in place, when biomethane is produced.

Therefore, this work will focus on how such a power-to-gas facility could look like from a technical point of view to produce synthetic biomethane in combination with a biogas upgrading plant. In specific the right size of power-to-gas plant will be determined by the existing CO_2 output of the biogas plant in Bruck/Leitha. In order to answer the question which specific electrolysis and methanation technology in combination with the right operational strategy fits to the biogas plant will be answered by comparing the long run generation costs of synthetic biomethane. This assessment will also deeply focus on the most important influencing factors concerning the production costs of synthetic biomethane and how such a power-to-methane plant could be integrated in the existing process of the biogas plant Bruck/Leitha. Therefore, special focus will be put on heat integration of the power-to-methane plant.

4.1. Biogas plant Bruck/Leitha

The biogas plant in Bruck/Leitha is one of the biggest biogas plants in Austria with a capacity of recycling 34.000 t of organic waste material (wet biomass) from food industry, kitchen- and canteen waste as well as agricultural residual waste. The plant went into operation in 2004 and produced green electricity in two cogeneration plants (2 x 836 kW_{el}) and heat, which was fed into the local district heating grid for 10 years. In 2014, a biogas upgrading technology, a membrane system, was implemented and up to 1000 Nm^3/h of raw biogas can be upgraded to biomethane. The cogeneration plants were not in operation anymore and up to 500 m^3/h of biomethane was fed into the gas grid. (Mauthner, 2021)

The feedstock is consisting of approximately 30% vegetable residues from harvest and treatment, 30% packed and/or animal material which need thermal treatment (disinfection at more than 70°C) and 30% materials, which neither need thermal treatment nor belong to the first group. (Biogas Bruck/Leitha GmbH & Co KG, 2021)

The biogas plant has four 300 m^3 storage tanks for liquid materials and surface water, two 300 m^3 mixing tanks, three 3,000 m^3 main fermenters and two 5,000 m^3 post digesters. Furthermore, the plant has also one depackaging line, two disinfection facilities and a 30 m^3 heat storage tank. The upgrading unit consists of a chemical scrubber, a membrane upgrading system and a gas injection facility, where gas is measured, quality checked and fed into the local distribution grid at approximately 3 bar. In case, the biomethane production exceeds the local demand in the local level 3 grid, two high pressure compressors can compress the gas up to 60 bar to transport it on the level 2 grid and therefore a continuous operation of 365 days per year can be assured. Furthermore, the biogas plant is supplied by heat (around 90°C) from the district heating grid Bruck an der Leitha. (Biogas Bruck/Leitha GmbH & Co KG, 2021)

Due to the fact, that the plant recycles food and fodder residuals and uses the most modern technologies for waste conditioning, a high efficiency regarding material recycling can be achieved. The by-products of the formation process, an authorized fertiliser “Terra Juva”, can be used on agricultural areas, which closes the nutrient cycle and leads to a circular economy as well as enhances the sustainable productivity of the fields. Therefore, producing biomethane from organic residuals is the most ecological way of producing renewable gas locally in Austria and therefore reduce not only carbon emissions but also decrease the import dependency by substituting natural gas. (Biogas Bruck/Leitha GmbH & Co KG, 2021)

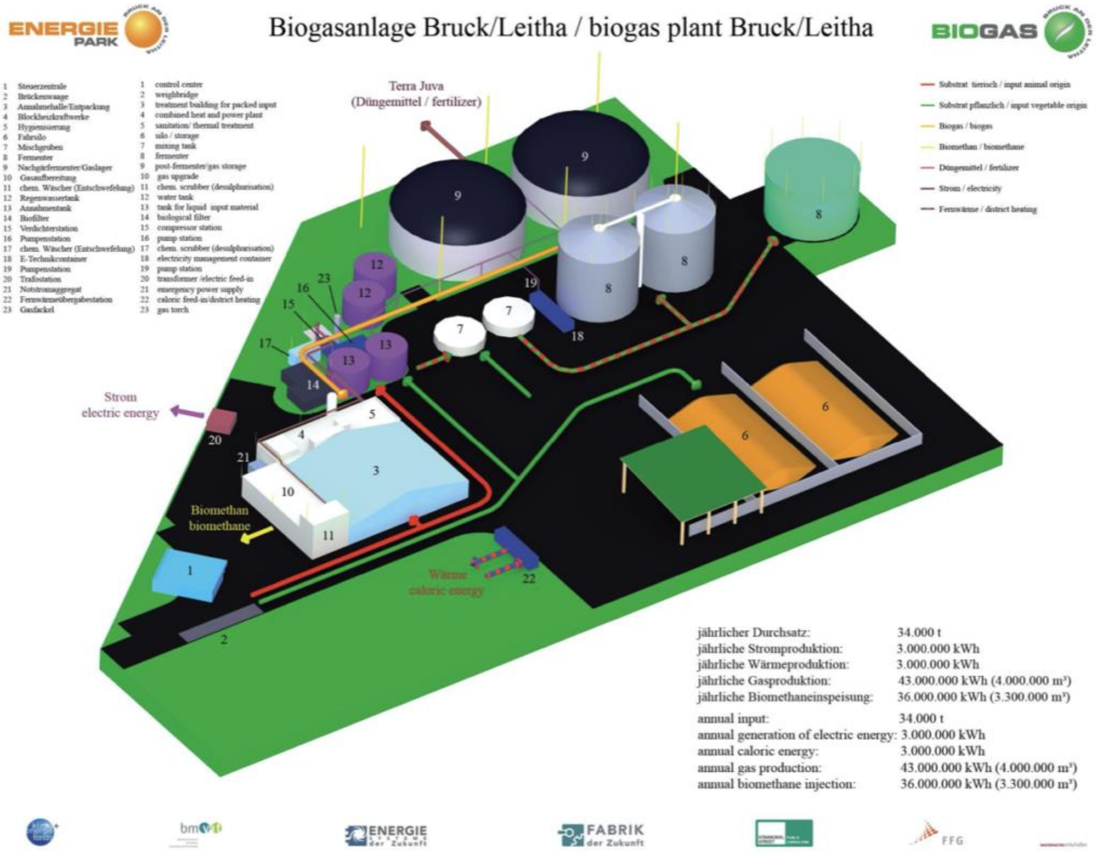

Figure 16: Scheme of the biogas plan Bruck/Leitha. (Energiepark Bruck an der Leitha, 2022)

Operational data

The hourly operational data over the year 2020 of biomethane production volumes, off gas (CO_2) quantities and heat demand are gathered from flow measurements of biomethane grid injection, off gas stream calculated via a quality measurement and heat supplied by the district heating grid. Figure 17 and Figure 18 shows that the biogas plant produces 250 to 500 Nm³/h biomethane and 100 to 250 Nm³/h pure (99%) CO_2 with a relationship of approximately 2:1 biomethane/CO_2. The variation of the output depends mainly on the amount of available feedstock, which varies over the year, but also operational influences (e.g., mechanical or biological constraints) may lead to a reduction of output. Because of this varying production profile, a CO_2 storage tank can be helpful to ensure a certain supply of CO_2 for the methanation process.

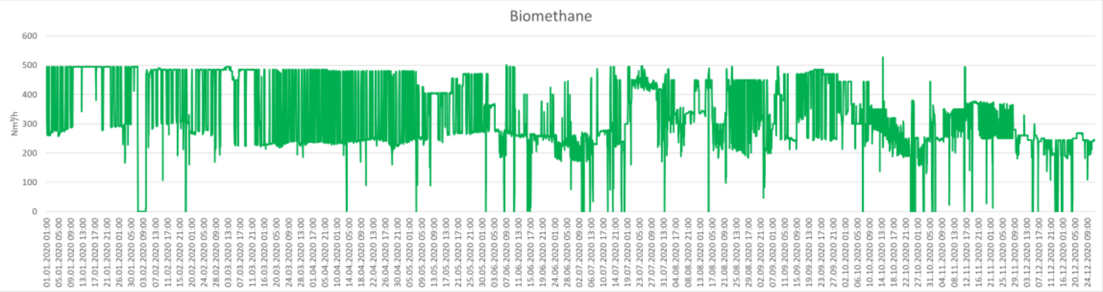

Figure 17: Hourly biomethane production of 2020. Own figure based on (Mauthner, 2021)

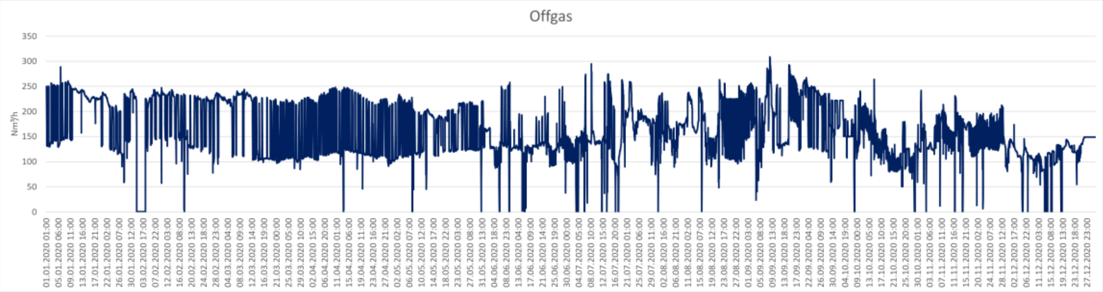

Figure 18: Hourly off gas production of 2020. Own figure based on (Mauthner, 2021)

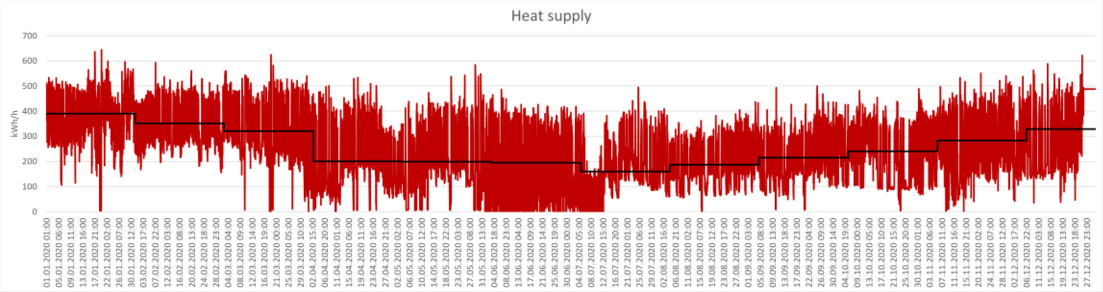

Figure 19: Hourly heat supply by district heating grid and monthly average (black line) of 2020. Own figure based on (Mauthner, 2021)

Figure 19 shows the hourly heat supply by the district heating grid in red, which is fed into the heat storage tank via a heat exchanger. The black line shows the average monthly heat demand. The two main heat sinks at the biogas plant are fermenter heating at around 40°C, which is only necessary in winter and constant disinfection of feedstock at more than 70°C. This indicates that constant disinfection requires about 200 kW of heat continuous over the whole year and fermenter heating requires up to 200 kW of heat, depending on the outside temperature.

4.2. Electrolyser market research

For this assessment alkaline and PEM-electrolysers were considered due to the broad commercial availability and high flexibility in terms of operations. In general, a wide range of European manufacturers offer state-of-the art electrolysis technology in various sizes from 100 kW_{el} up to 10 MW_{el} and more.

4.2.1. McPhy

McPhy is one of the European leading manufacturers of alkaline electrolysers based in France, Italy and Germany. Their “McLyzer” is available in different power classes, ranging from 0,5 MW up to 4 MW (100 – 800 Nm^3/h hydrogen output) as well as a customable solution where 20, 100 MW and more are possible. The McLyzers have an output pressure of 30 bar and a specific energy demand of 4.5 kWh/Nm^3 hydrogen. The manufacturer as well claims that its products have a very fast dynamic response making them suitable for grid services such as primary reserve. (McPhy, 2022)

4.2.2. Nel Hydrogen

Nel Hydrogen is a Norwegian based and worldwide active manufacturer of AEL and PEMEL systems. Their atmospheric alkaline electrolyser is scaleable up to 3,880 Nm^3/h with a maximum power rating of 2.2 MW per stack. They claim to have the world’s most efficient electrolyser with an electrical consumption of about 3.8 kWh/Nm^3. (Nel Hydrogen, 2022)

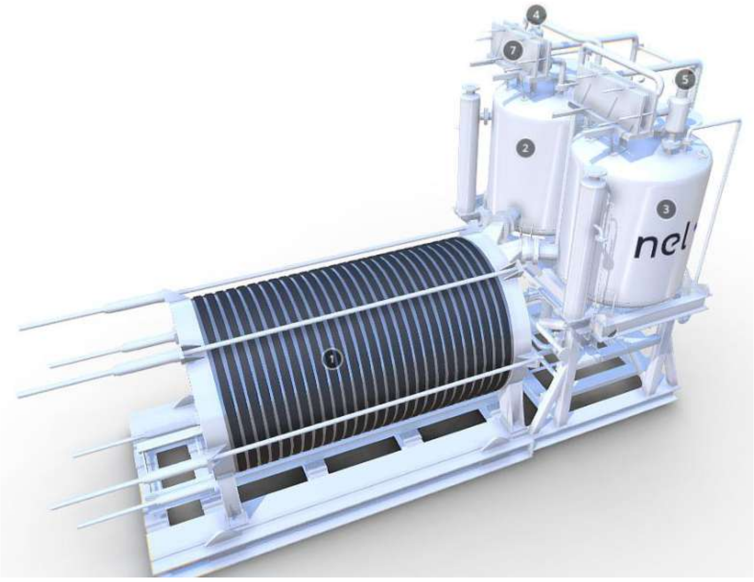

Figure 20: Nel Hydrogen atmospheric AEL. (Nel Hydrogen, 2022)

Nel Hydrogen also offers a scaleable PEM electrolyser with 2,000 – 5,000 Nm³/h hydrogen as well as a smaller containerized solution of its PEM electrolyser with an output capacity of 246 – 492 Nm³/h hydrogen. (Nel Hydrogen, 2022)

4.2.3. Siemens Energy

Siemens Energy offers with its Silyzer 300 also large scale and scaleable state-of-the-art PEM electrolyser made in Germany. The Silyzer 300 consists of up to 24 modules which sum up to a 17.5 MW array and has a system efficiency of 75% (HHV). Their product can produce 100 – 2.000 kg/h of hydrogen with a very high and flexible load range of 10%/s in 0-100%. The minimal load is 20% per single module, plant availability is 95% and module lifetime is around 10 years. They claim to have a water consumption of about 10 l/kg hydrogen and the delivered pressure is customable. The Silyzer 300 also is suitable for primary frequency response service (primary balance energy) due to its fast start up time of less than 1 min. (Siemens Energy, 2022)

One application of a 6 MW Siemens Silyzer 300 is the project H_2Future by voest alpine in Linz, Austria. (Verbund Energy4Business, 2020)

Figure 21: 6 MW array of Siemens Silyzer 300 in Linz, Austria. (Verbund Energy4Business, 2020)

4.2.4. H-Tec Systems

The German based manufacturer H-Tec Systems, which is part of MAN Energy Solutions, has two container PEM electrolysers made in Germany on the market. The small ME100/350 with 225 kW_{el} and the large ME450/1400 with 1 MW_{el} nominal power rating. The ME450/1400 can produce up to 210 Nm³/h hydrogen with a nominal energy consumption of 4.8 kWh/Nm^3 hydrogen. The output pressure is between 15 and 30 bar and the load flexibility from minimum (20%) to nominal load can be achieved in 30 seconds. Furthermore, H-Tec Systems also offers customable stacks for bigger plants as well. (H-Tec Systems GmbH, 2021)

Figure 22: H-TEC Systems 1 MW ME450/1400. (H-Tec Systems GmbH, 2021)

4.2.5. Sunfire

Sunfire is also a German based manufacturer of alkaline as well as high temperature electrolysers. The Sunfire-Hylink alkaline system can produce up to 2,230 Nm^3/h of hydrogen per day and has a maximum power rating of 10 MW_{el}. The specific power consumption at system level is 4.7 kWh/Nm^3 with a stack lifetime of over 90,000 hours. The delivered output pressure is 30 bar and the operation temperature is 85°C. (sunfire, 2022)

One application in Austria is the currently world’s biggest pressurized alkaline electrolyser in Völs, Tirol with 3.2 MW, which was started operation in March 2022 for the Demo4Grid project. (Demo4Grid, 2022)

Figure 23: 3.2 MW pressurized alkaline electrolyser Hylink by Sunfire in Völs, Austria. (Demo4Grid, 2022)

4.2.6. ITM POWER

ITM Power is a British manufacturer of PEM electrolysers from 600 kW up to 100 MW. The HGAS3SP is a medium-sized containerized plug & play PEMEL system of 2 MW, consists of 3 stacks and can deliver 30 bar hydrogen generation pressure. The manufacturer claims that its rapid response enables the participation in primary and secondary balance energy market. They also offer a two-sack module with 5 MW capacity called “2 GEP Skid”, which is modular up to 250 MW and a 3-stack cube solution of 2 MW capacity called “3MEP Cube” which is modular up to 50MW. (ITM Power, 2022)

Figure 24: 2 MW HGA3SP PEMEL by ITM Power.

4.3. *Biological methanation market research*

When it comes to biological methanation, the major reactor supplier and therefore also the first pilot projects are situated in Germany and Switzerland, but also Austria plays a relevant role especially in research and innovation.

4.3.1. microbEnergy by Hitachi Zosen INNOVA

The German company microbEnergy was recently integrated into the Swiss company Hitachi Zosen INOVA. Their biological methanation reactor “BiON 400” can convert 400 Nm³/h of hydrogen and 100 Nm³/h of CO_2, uses the slurry from biogas plants as substrate and operates at 10 bar and 65°C. It is a classic continuously stirred tank reactor (CSTR) with a footprint of 1000- 1200 m². In case of heat integration, up to 350 kW of heat can be used and therefore the efficiency can reach up to 95%. Their BiON reactor is individually scaleable and the first industrial application was put in operation combination with a 2.5 MW_{el} electrolyser (2x Siemens Silyzer 200) in 2021 in Dietikon, Switzerland within the Limeco project. (microbEnergy, 2020) (Limeco, 2021)

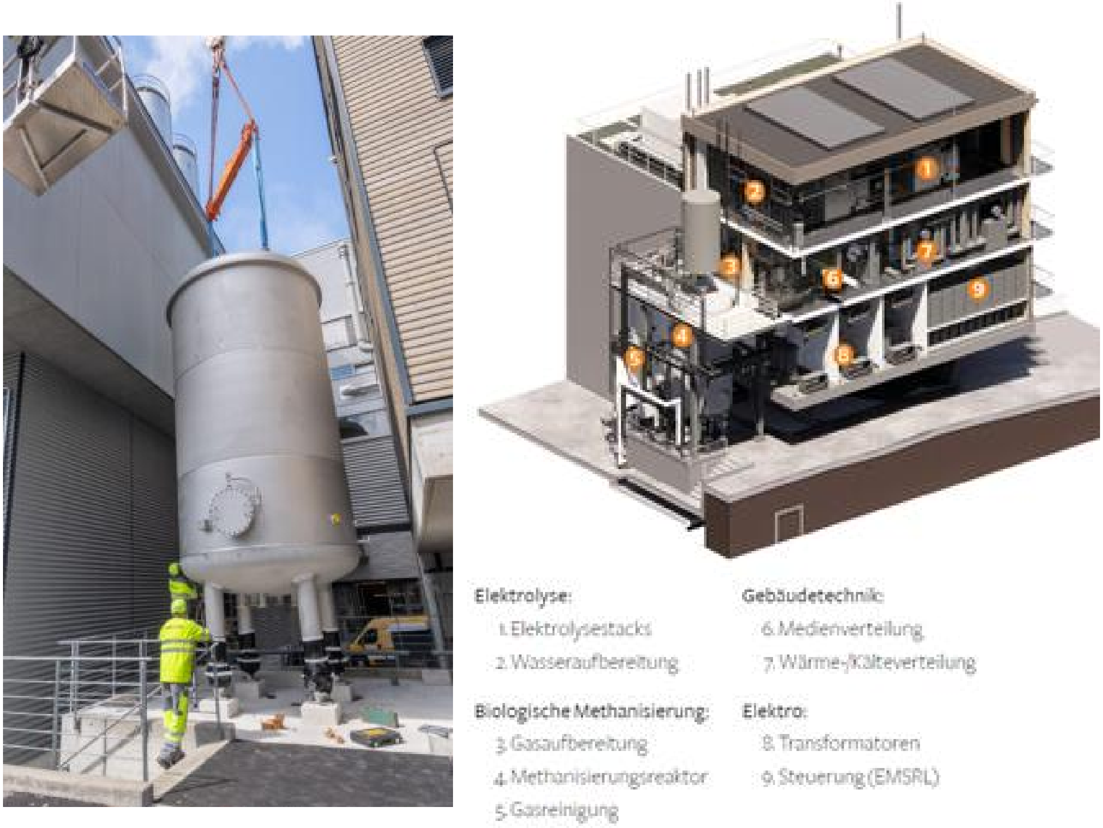

Figure 25: BiON Reactor at the Limeco facility in Dietikon, Switzerland. (Limeco, 2021)

4.3.2. Electrochaea

The German plant designer Electrochaea has a small scale and large scale industrial biological methanation system in place with the specifications shown in Figure 26. Electrochaea offer their special biological catalyst ECH 0100 under a user-specific license. The BioCat pilot plant was tested in the commercial scale project Store&Go in Solothurn, Switzerland and in the commercial scale Biocat project in Avendore, Denmark. (Electrochaea GmbH, 2021)

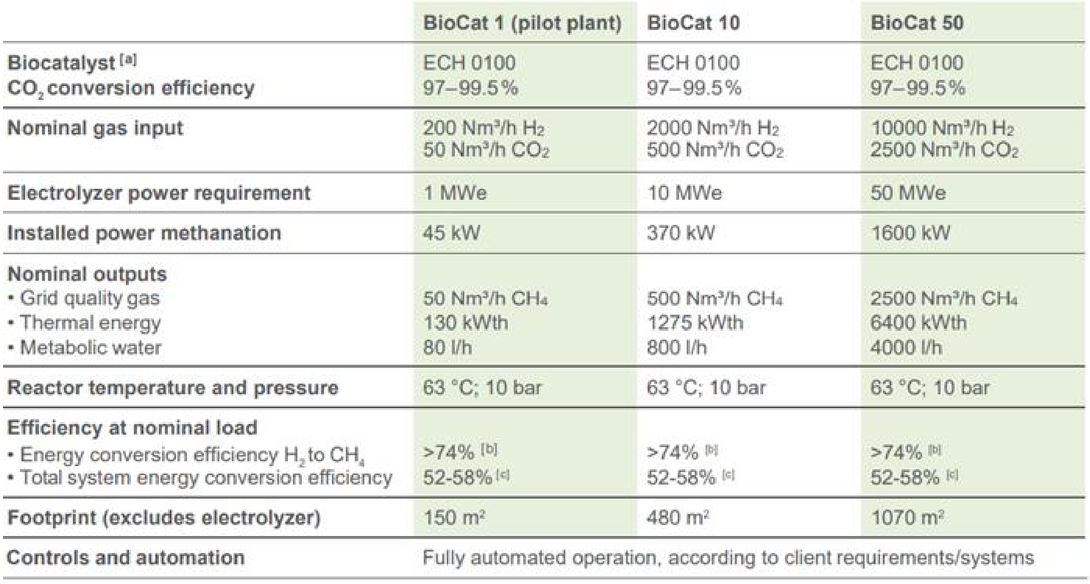

	BioCat 1 (pilot plant)	BioCat 10	BioCat 50
Biocatalyst [a] **CO_2 conversion efficiency**	ECH 0100 97–99.5%	ECH 0100 97–99.5%	ECH 0100 97–99.5%
Nominal gas input	200 Nm^3/h H_2 50 Nm^3/h CO_2	2000 Nm^3/h H_2 500 Nm^3/h CO_2	10000 Nm^3/h H_2 2500 Nm^3/h CO_2
Electrolyzer power requirement	1 MWe	10 MWe	50 MWe
Installed power methanation	45 kW	370 kW	1600 kW
Nominal outputs • Grid quality gas • Thermal energy • Metabolic water	 50 Nm^3/h CH_4 130 kWth 80 l/h	 500 Nm^3/h CH_4 1275 kWth 800 l/h	 2500 Nm^3/h CH_4 6400 kWth 4000 l/h
Reactor temperature and pressure	63 °C; 10 bar	63 °C; 10 bar	63 °C; 10 bar
Efficiency at nominal load • Energy conversion efficiency H_2 to CH_4 • Total system energy conversion efficiency	 >74% [b] 52-58% [c]	 >74% [b] 52-58% [c]	 >74% [b] 52-58% [c]
Footprint (excludes electrolyzer)	150 m^2	480 m^2	1070 m^2
Controls and automation	Fully automated operation, according to client requirements/systems		

Figure 26: Electrochaea BioCat specifications. (Electrochaea GmbH, 2021)

4.3.3. Krajete

Krajete GmbH is an Austrian based company who developed and patented a biological methanation process called “Krajete® Process”. This process takes place in a continuously stirred tank reactor (CSTR) at 15 bar where the monoculture microbes are suspended in an aqueous solution. The reactants enter the reactor at the bottom and are then dispersed by an agitator into the liquid phase. Krajete claims its reactor is suitable for intermittent production patterns and can go from 0 to 100% load within a couple of seconds as well as stand-by periods of more than 500 hours are possible. This highly flexible process is specially made for a dynamic production profile in power-to-gas applications (see Figure 27). Krajete GmbH holds 4 patents for its process and a first pilot plant was set up in 2020. (Krajete GmbH, 2021)

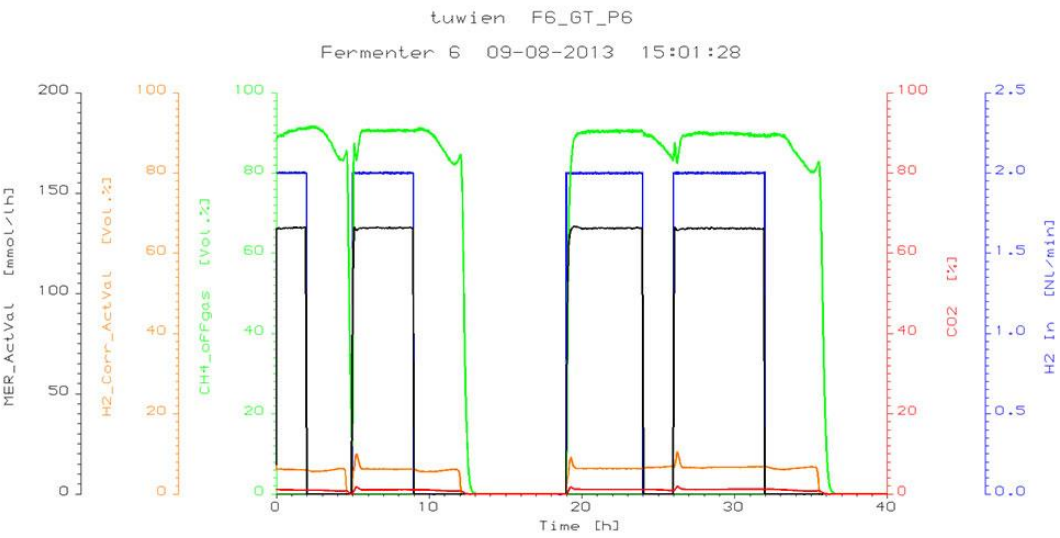

Figure 27: "Intermittency of Krajete® Process with instant methane production and no energy consumption during transition periods in stand-by (follow the blue curve, H2, which symbolizes electrolytic H_2 and therefore stored electricity and compare to black curve)". (Krajete GmbH, 2021)

4.4. Catalytic methanation market research

When it comes to catalytic methanation, the major reactor supplier and therefore also the first pilot projects are situated in Germany and Denmark, but also Austrian companies and universities play a relevant role especially in research and innovation.

4.4.1. Christof Industries

Christof Industries is an Austrian based but worldwide active company which is specialized in plant engineering. Together with Montanuniversity Leoben, they developed and patented a special honeycomb catalyst (Figure 13) which showed promising laboratory tests results concerning load-flexible methanation operation in combination with electrolysis, which made it suitable for the power-to-gas application. (Friedacher, 2021)

This honeycomb catalyst will be field-tested in Austria's first Power-to-Gas pilot plant within the "Renewable Gasfield" project in Gabersdorf, Styria. The aim of this project is to demonstrate the feasibility of the power-to-gas process (1 MW_{el} electrolyser) with catalytic methanation) in combination with a biogas plant. Within that project, the honeycomb catalyst will be tested in a water-cooled tube in tube reactor in terms of performance, long-time stability, and flexibility. (Salbrechter, 2022)

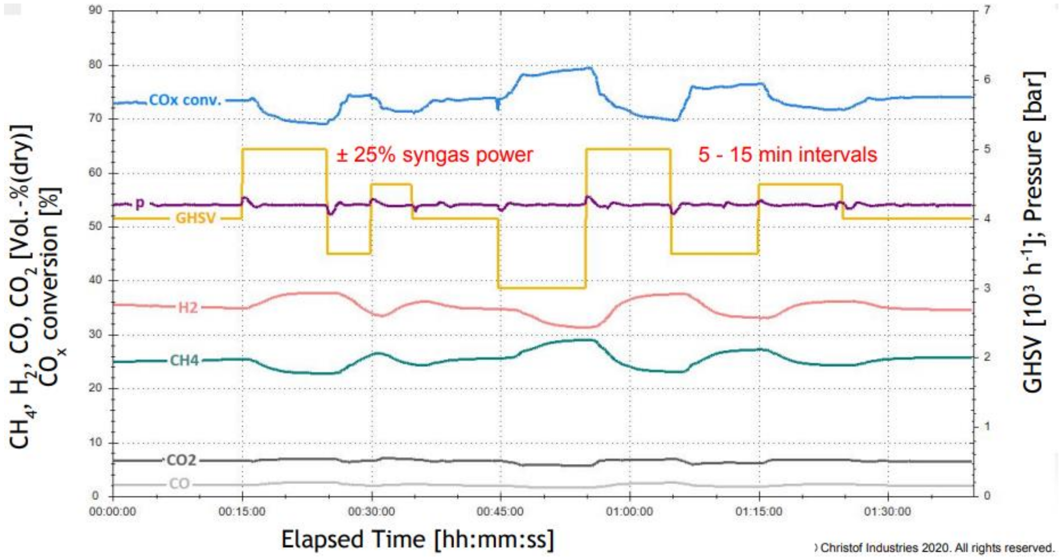

© Christof Industries 2020. All rights reserved.

Figure 28: Laboratory tests results of a honeycomb catalyst under dynamic load operation. (Friedacher, 2021)

4.4.2. Hitachi Zosen INOVA

The Swiss plant engineering company Hitachi Zosen INOVA offers with its EtoGas technology a cooled fixed bed catalytic methanation system in combination with a 2 MW$_{el}$ per module scaleable pressurized alkaline electrolyser. The plant sizes can vary between 8 – 500 Nm³/h of synthetic biomethane. One example for an industrial application would be the Power-to-Gas Plant in Werlte, Germany which is in operation since 2013. This plant has an electrolyser of 6 MW$_{el}$ to produce hydrogen and in combination with the off-gas CO$_2$ of the nearby biogas plant it can produce up to 3 MW synthetic biomethane. (Hitachi Zosen INOVA, 2020)

Figure 29: EtoGas Power-to-Gas plant in Werlte, Germany. (Hitachi Zosen INOVA, 2020)

4.4.3. TOPSOE

The Danish company TOPSOE, specialized in carbon reducing technologies offers a TREMP™ (Topsøe Recycle Energy-efficient Methanation Process) process with their own medium to high temperature catalysts. The methanation reaction takes place in adiabatic fixed bed reactors. The advantage of this process is the usage of the waste process heat of the methanation to produce superheated steam (100 bar, 540°C) of about 3-3.5 kg/Nm³ SNG. Therefore, the process can achieve very high efficiencies, when superheated steam is required in other processes. (HALDOR TOPSOE, 2009)

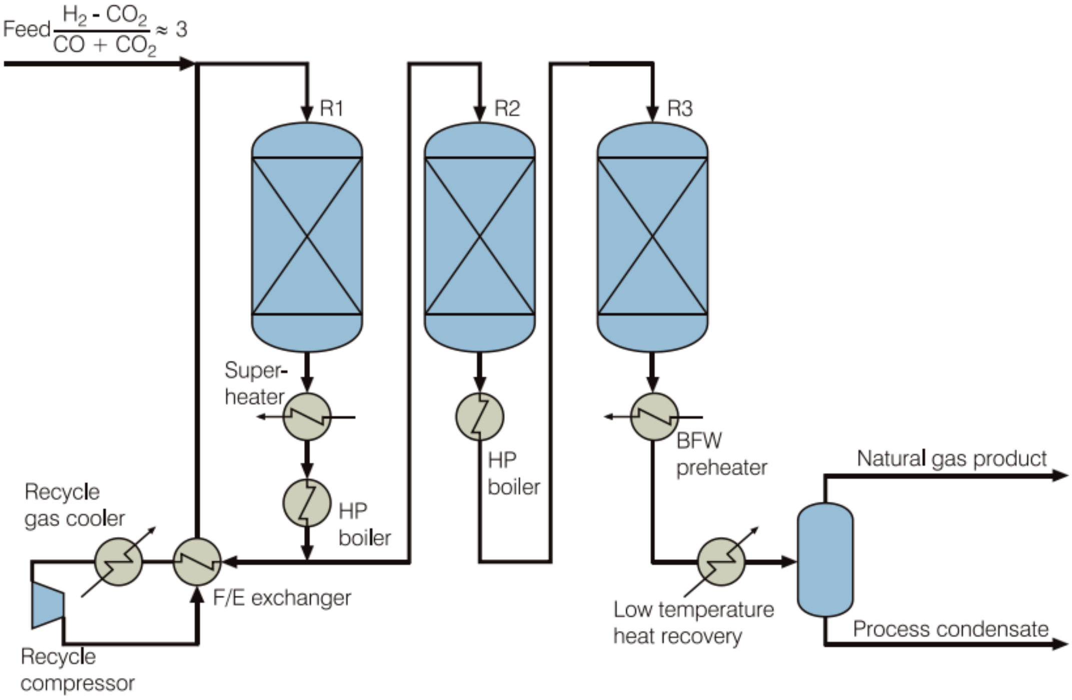

Figure 30: TREMP process. (HALDOR TOPSOE, 2009)

4.5. CO_2 Storage

Due to the fact, that a biogas plant has a variable production of CO_2 (Figure 18) which is determined by the availability of feedstock and gas processing and utilisation equipment (upgrading and grid injection), a storage tank for a smoother methanation input stream could make sense. When comparing the density of hydrogen of at 20 bar and -25°C, which is approx. 20 kg/m³ (Figure 31) to the density of liquid CO_2 at the same conditions, which is around 1000 kg/m³, it is obvious to store CO_2 rather than hydrogen.

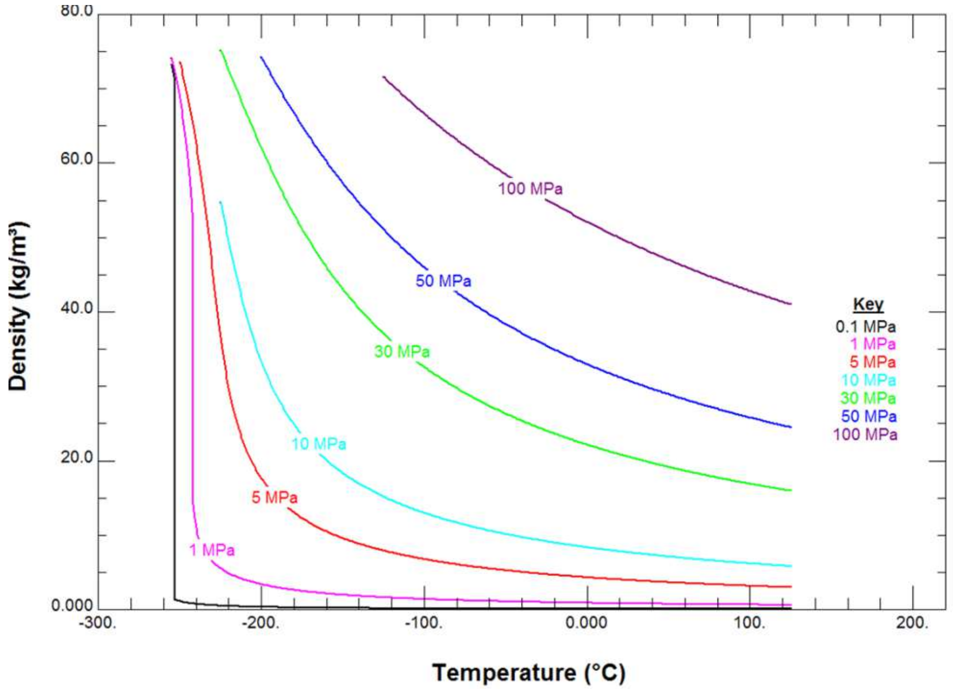

Figure 31: Temperature-Density diagram of hydrogen. (Hydrogen Tools, 2020)

The most efficient way to store large amounts of CO_2 is in its liquid form. According to its phase diagram (Figure 32) CO_2 is liquid at 20 bar and -20 °C and usually stored at these conditions.

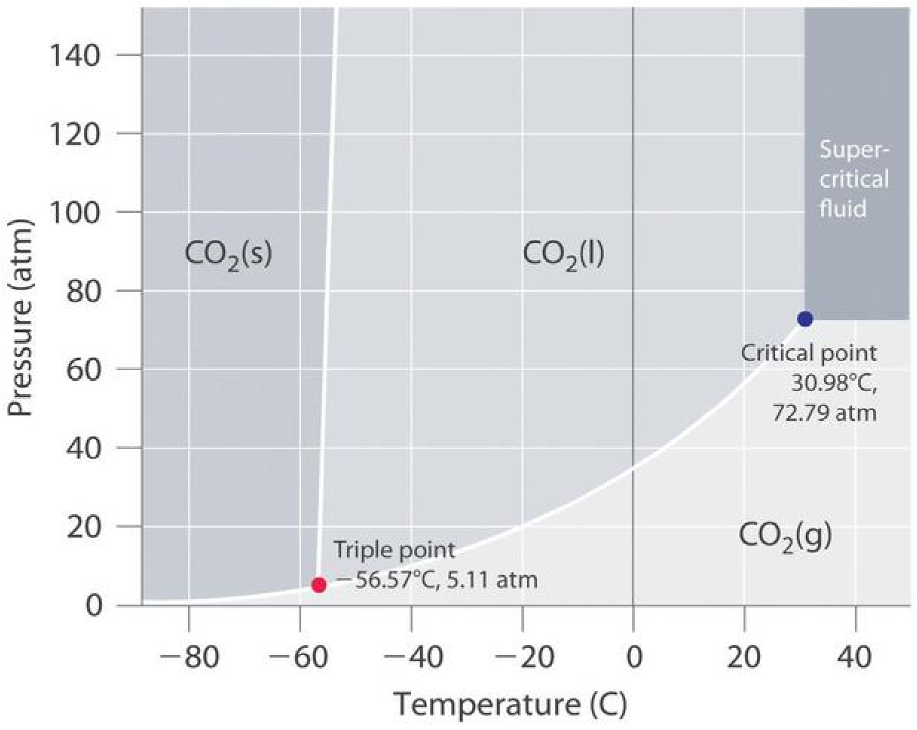

Figure 32: Phase diagram of CO2. (LibreTexts, 2020)

Common CO_2 liquification units compress the off-gas stream to approx. 20 bar and cool it down afterwards in a CO_2 condenser to approx. -24 °C until it turns liquid and the remaining methane in the off-gas is fed back to the upgrading unit. This also removes the methane emissions in the off-gas stream. CO_2 liquification plants are common in the food and beverage industry and therefore widely available by plant manufacturers specialized in CO_2 technology such as Pentair for example. Pentair offers a CO2 liquification unit called CO_2BOLT-ON, which is especially designed to add to biogas upgrading plants. This liquification unit by Pentair requires approx. 30 kW for 250 Nm³/h of CO_2. (Pentair, 2021)

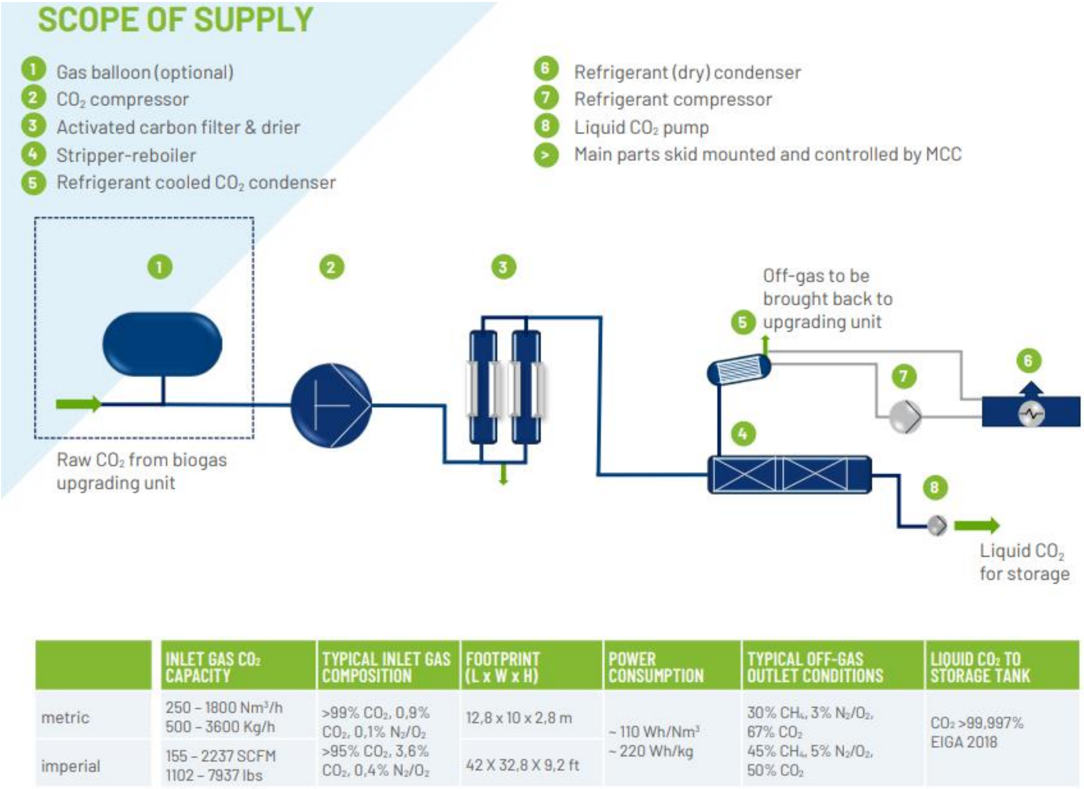
SCOPE OF SUPPLY

① Gas balloon (optional)
② CO_2 compressor
③ Activated carbon filter & drier
④ Stripper-reboiler
⑤ Refrigerant cooled CO_2 condenser
⑥ Refrigerant (dry) condenser
⑦ Refrigerant compressor
⑧ Liquid CO_2 pump
\> Main parts skid mounted and controlled by MCC

	INLET GAS CO_2 CAPACITY	TYPICAL INLET GAS COMPOSITION	FOOTPRINT (L x W x H)	POWER CONSUMPTION	TYPICAL OFF-GAS OUTLET CONDITIONS	LIQUID CO_2 TO STORAGE TANK
metric	250 – 1800 Nm³/h 500 – 3600 Kg/h	>99% CO_2, 0,9% CO_2, 0,1% N_2/O_2	12,8 x 10 x 2,8 m	~ 110 Wh/Nm³ ~ 220 Wh/kg	30% CH_4, 3% N_2/O_2, 67% CO_2 45% CH_4, 5% N_2/O_2, 50% CO_2	CO_2 >99,997% EIGA 2018
imperial	155 – 2237 SCFM 1102 – 7937 lbs	>95% CO_2, 3,6% CO_2, 0,4% N_2/O_2	42 X 32,8 X 9,2 ft			

Figure 33: CO2BOLT-ON process of Pentair. (Pentair, 2021)

The liquid CO_2 can then be stored in 6.4 to 100 t vertical or horizontal vacuum isolated steel tanks. For the use in a methanation reactor, the CO_2 must be regasified using a so-called atmospheric vaporizer with the use of ambient air. The vaporizer requires for the same flow approx. 2.4 kW of electrical energy. (ASCO KOHLENSÄURE AG, 2021) (ASCO KOHLENSÄURE AG, 2021)

4.6. Agricultural PV plant "Sonnenfeld"

Directly next to the biogas plant Bruck/Leitha, Energiepark Bruck/Leitha is installing on an agricultural area of 5.5 ha a free-space photovoltaic plant as a research project. The plant is supposed to produce approx. 4,000,000 kWh per year and therefore could have a capacity of 3.6 MW_{peak}. (EWS Sonnenfeld, 2021)

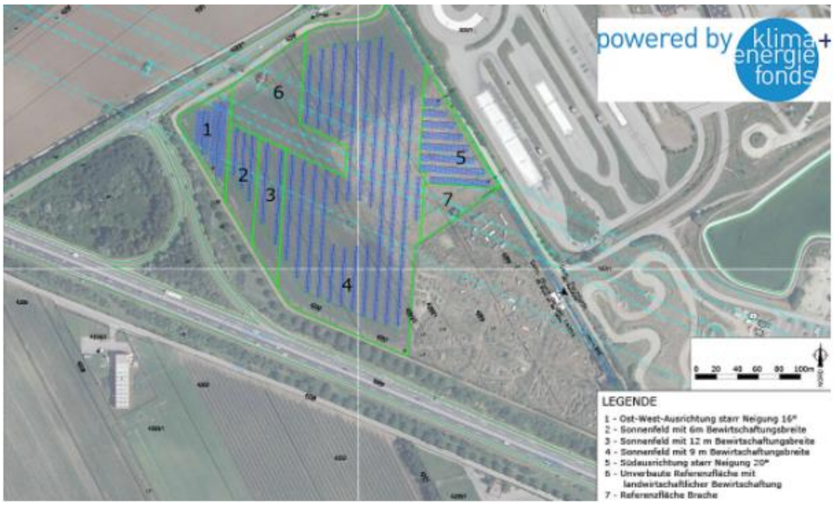

Figure 34: Plan of the Sonnenfeld Bruck/Leitha. (EWS Sonnenfeld, 2021)

An assumption of the hourly production profile of the 3.6 MW_{peak} Sonnenfeld according to global solar atlas is shown in Figure 35.

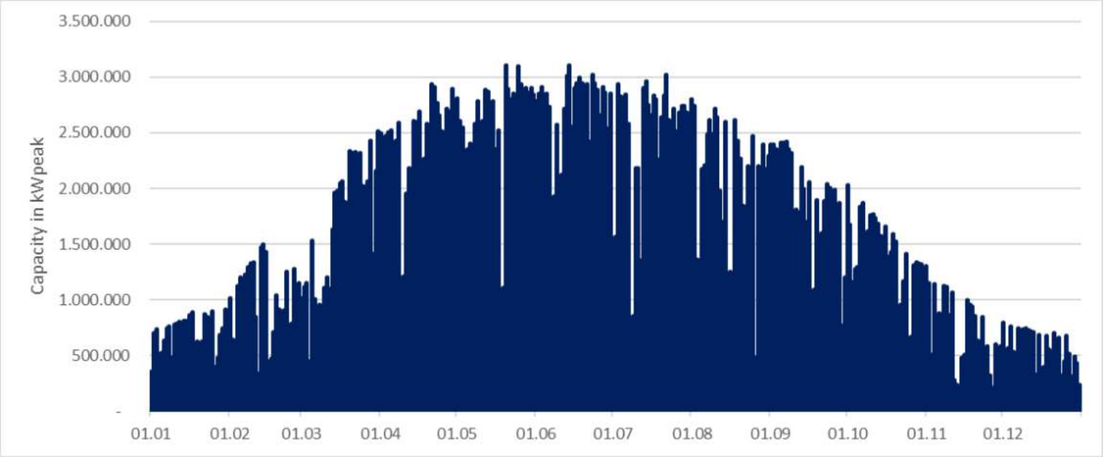

Figure 35: Assumption of the hourly production profile of Sonnenfeld. (Leaflet, 2022)

The grid connection will be at the transformer station of the biogas plant and therefore this electricity could be directly used for powering the electrolyser without feeding it into the local public power grid.

4.7. Electricity market in Austria

Electricity prices is a major regarding the economics of a power-to-gas plant in the scale of several MW of electrolysis input power. Therefore, a special focus lies on energy procurement and a proper procurement strategy must be implemented by the plant operator. The are several prices models possible:

Fixed price model

Within the fixed price model, the energy supplier guarantees a fixed energy price for a period of one or two years. The advantage of this model on the one hand is that is a plannable and secure price can be agreed upon, which limits the risk of short-term price increases. On the other hand, periods of low price, especially in summer, cannot be used effectively and total costs may be higher than necessary.

Day/Night price model

Like the fixed price model, prices differ only between daytime (06:00-22:00) and night-time (22:00-06:00) but day and night-time prices are also fixed over a longer period. This price model makes sense when continuous consumption (e.g., at a biogas plant), also during night-time, takes place.

Monthly floating price model

This model has a monthly adapted energy price calculated by the monthly average of the EPEX SPOT base price of the previous monthly multiplied by a load factor plus a handling fee. This flexible model profits from seasonal and monthly price differences but is less predictable.

Realtime spot price model

The most flexible energy price model is a real-time spot price model, where the consumer receives directly the EPEX spot prices per hour or 15 min including a handling fee of around 0.6 EUR/MWh. Figure 36 and Figure 37 show the Austrian wholesale market prices for 2020 and 2021 in EUR/MWh. These figures show that negative prices are possible and the spread between day/night and weekday/weekend is significant. Furthermore, especially end of 2021, the electricity prices showed a very strong increase.

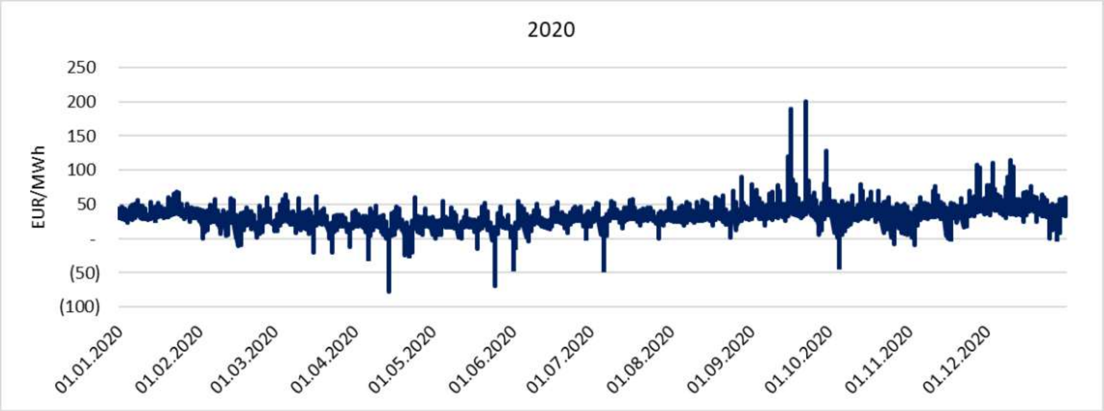

Figure 36: Hourly Day-Ahead Spot prices in Austria 2020. Own figure based on (Austrian Power Grid AG, 2020)

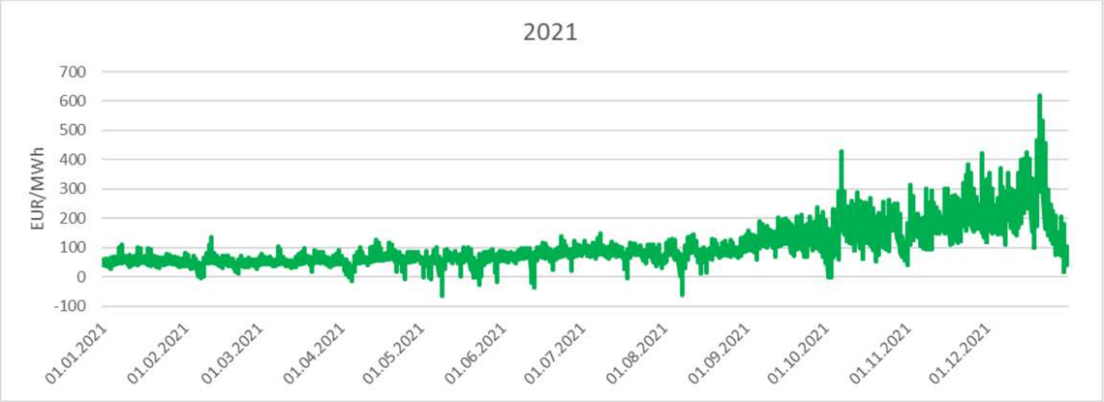

Figure 37: Hourly Day-Ahead Spot prices in Austria 2021. Own figure based on (Austrian Power Grid AG, 2021)

4.7.1. Control reserve market in Austria

For a stable grid frequency, a balance between generation and consumption is always necessary. Deviations from this balance, which may be caused by power plant outages or unexpected changes in consumption for example, must be permanently compensated for by activating reserve power from generation or consumption units. As the control area manager, Austrian Power Grid (APG) is responsible for procuring and activating the required reserve power in the APG control area. Since 2012, the procurement of the required control reserve in the APG control area has been carried out uniformly by APG by means of regular tenders. Any market participant that fulfils the technical prequalification conditions and has signed a corresponding framework agreement can participate in these tenders. (Austrian Power Grid AG, 2022)

Therefore, apart from the wholesale electricity market, the control reserve market is a possible market to participate as an operator of an electrolyser larger than 1 MW which meets the requirements to participate in the control reserve market.

For technical and economic reasons, three types of control reserve are distinguished:

Primary reserve: FCR (Frequency containment reserve)

The primary control reserve is a solidarity reserve in continental Europe. It is needed to automatically compensate for an occurring imbalance between generation and consumption within a few seconds through appropriate activation (regulation). The primary control reserve will be automatically activated and must deliver the maximum power within 30 seconds after frequency deviation and must last at least 30 minutes. (Austrian Power Grid AG, 2020)

FCR is procured daily in six 4-hour products and the minimum bid is +/-1 MW. Any further bids may be submitted in whole MW increments, up to a maximum of the prequalified capacity. For indivisible bids applies a maximum bid size of +/- 25 MW. The bidding period for tenders usually starts 14 days before delivery and ends at 08:00 on the day before delivery. At the end of the bidding period, bids are ranked by price - cheapest bids first - until the required sum of +/-73 MW in 2022 is reached. Each supplier receives the determined marginal price ("pay as cleared") for its bids that were accepted and thus at least the power price. There is no work price since, since the actual grid frequency oscillates around the mean value of 50 Hz, the primary control energy should be about zero on average. (Austrian Power Grid AG, 2020)

Figure 38 and Figure 39 show that the allocated capacity prices of the FCR auctions are usually between 5 and 20 EUR/MWh.

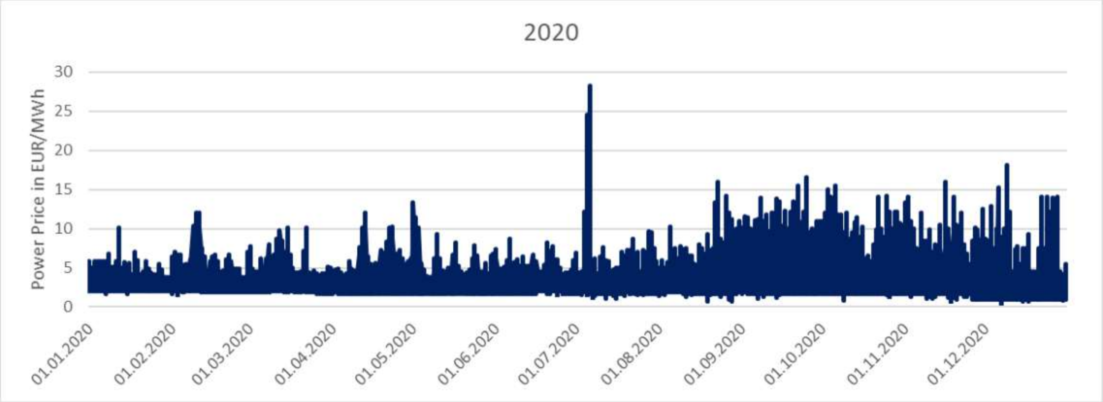

Figure 38: Capacity prices of the FCR tender in Austria, 2020. Own figure based on (Austrian Power Grid AG, 2020)

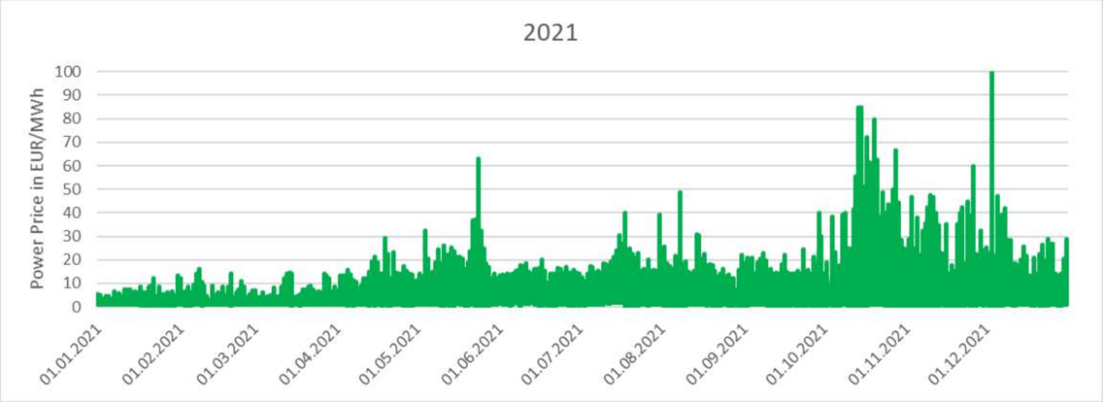

Figure 39: Capacity prices of the FCR tender in Austria, 2021. Own figure based on (Austrian Power Grid AG, 2021)

Secondary reserve: aFRR (Automatic frequency restoration reserve)

The secondary control reserve is an individual, automatically acting reserve that each control area must keep ready for itself. In the event of an imbalance, it follows the deployment of the joint primary control reserve, but it is only activated in the control area in which the imbalance occurred. While the primary control reserve must be activated within a few seconds, the secondary control reserve is activated within a maximum of 5 minutes in Austria. Currently the needed secondary reserve is +/- 200 MW. The minimum bid size for a supplier's first bid per product is 1 MW. The minimum bid for each additional one is 5 MW. Bids more than this may be submitted in whole 1 MW increments, up to a maximum of the prequalified capacity. (Austrian Power Grid AG, 2022)

The secondary reserve market is consisting of two separate stages: the balancing capacity and the balancing energy tender. Within the framework of the balancing capacity, market participants offer pre-qualified capacities, which they must also offer on the balancing energy market if they are awarded the contract. In addition to the capacity offered, a bid for secondary control reserve is characterized by the capacity price. The bids submitted are ranked in ascending order according to this price (merit order list for power). The bids that are most favourable for APG are finally accepted. The second stage of the market is made up of energy tenders conducted within the day. Here, suppliers can adjust their energy prices already submitted in the power bidding process or offer other prequalified capacities, independently of the power bidding process. The bids submitted are in turn ranked in a merit order list according to their energy price. Tenders take place on the electronic tender platform provided by APG. (Austrian Power Grid AG, 2022)

The required aFRR capacity is tendered in Austria on a calendar day basis (from Monday to Sunday) and at the end of the bidding period, the offers are ranked according to the lowest capacity price. The selected bids receive the quoted capacity price (“pay as bid”). The required secondary control energy is tendered then during the day (from Monday to Sunday). Bids for a delivery period of 4 hours can be submitted and adjusted until one hour before the delivery period of the respective product time slice. After the end of the bidding period of the energy tender, the bids are ranked, and awards are made according to the lowest energy price in case of positive secondary control reserve or highest energy price in case of negative secondary control reserve. Positive control energy means, electrical energy is fed into the grid or load is decreased to counter a decreasing frequency, whereas negative control energy referees to electrical energy pulled from the grid (by increasing the load for example) to counter an increase in frequency. One unit can only take part in either positive or negative auction at the same time. (Austrian Power Grid AG, 2022)

Figure 40 till Figure 43 show that the capacity price for aFRR is usually below 10 EUR/MWh with short periods and peaks of up to 200 EUR/MWh.

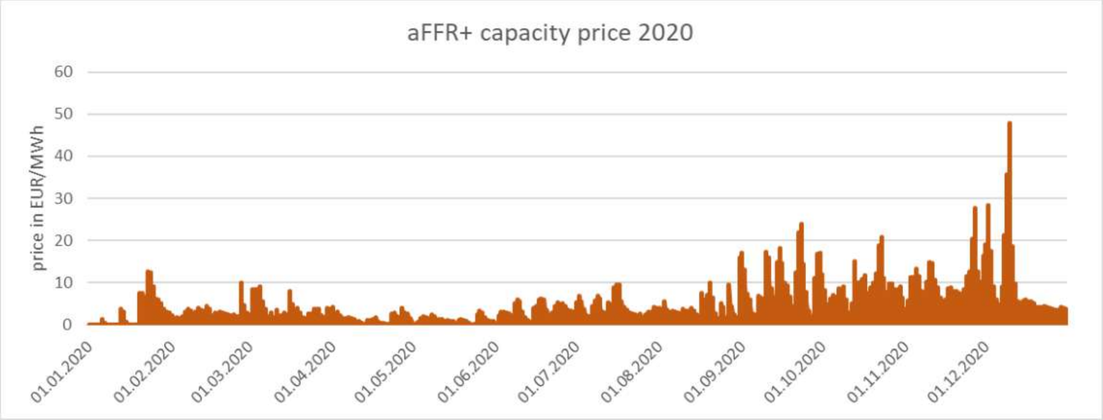

Figure 40: Capacity price for positive aFRR in Austria, 2020. Own figure based on (Austrian Power Grid AG, 2020)

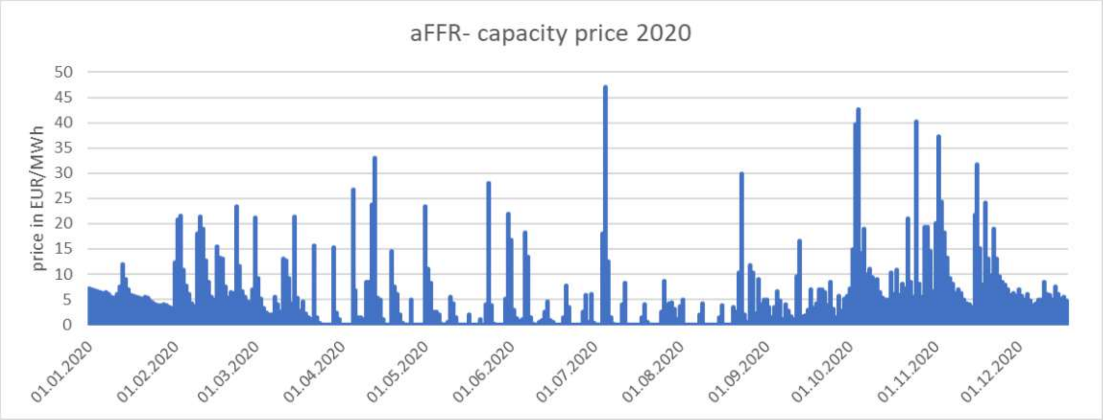

Figure 41: Capacity price for negative aFRR in Austria, 2020. Own figure based on (Austrian Power Grid AG, 2020)

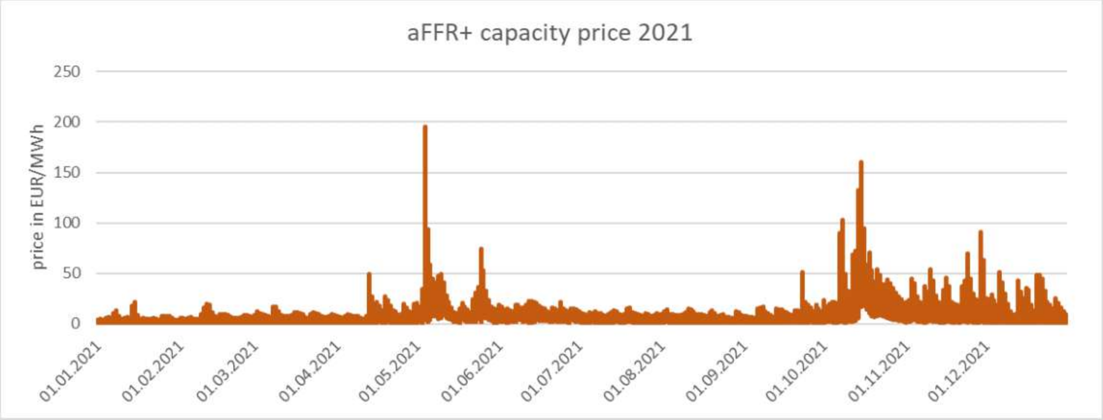

Figure 42: Capacity price for positive aFRR in Austria, 2021. Own figure based on (Austrian Power Grid AG, 2021)

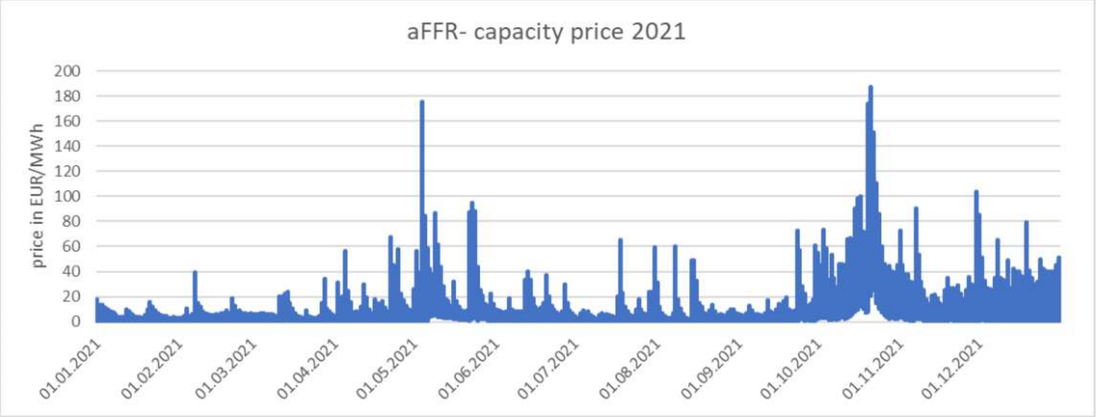

Figure 43: Capacity price for negative aFRR in Austria, 2021. Own figure based on (Austrian Power Grid AG, 2021)

Figure 44 till Figure 47 show the activated positive and negative automatic frequency restoration reserve in Austria for 2020 and 2021 and its weighted energy price. The positive aFRR is around 100 EUR/MWh for 2020 and the first half of 2021. This means, that for delivering positive aFRR to the grid (the electrolyser decreases the load) a compensation of approx. 100 EUR/MWh will be paid by APG. When the electricity spot price increases, also the energy price for positive increases respectively (compare Figure 37).

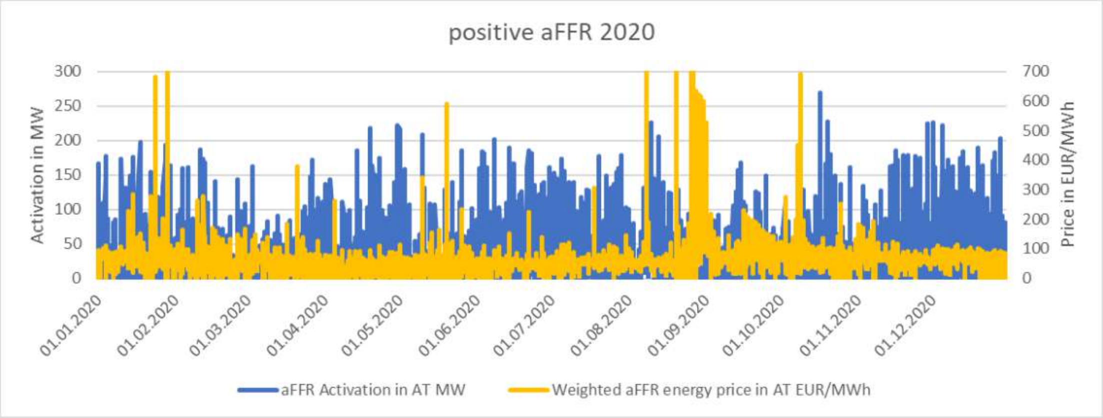

Figure 44: Weighted energy price and activated positive aFRR in Austria, 2020. Own figure based on (Austrian Power Grid AG, 2020)

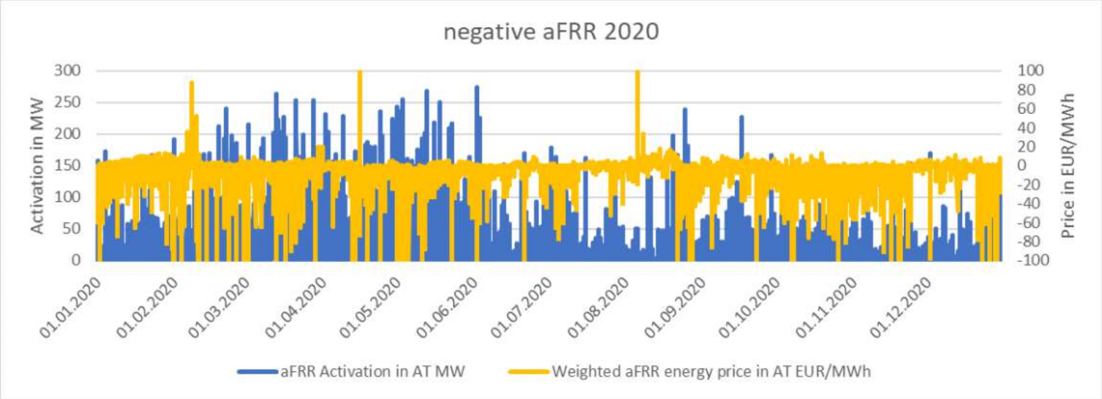

Figure 45: Weighted energy price and activated negative aFRR in Austria, 2020. Own figure based on (Austrian Power Grid AG, 2020)

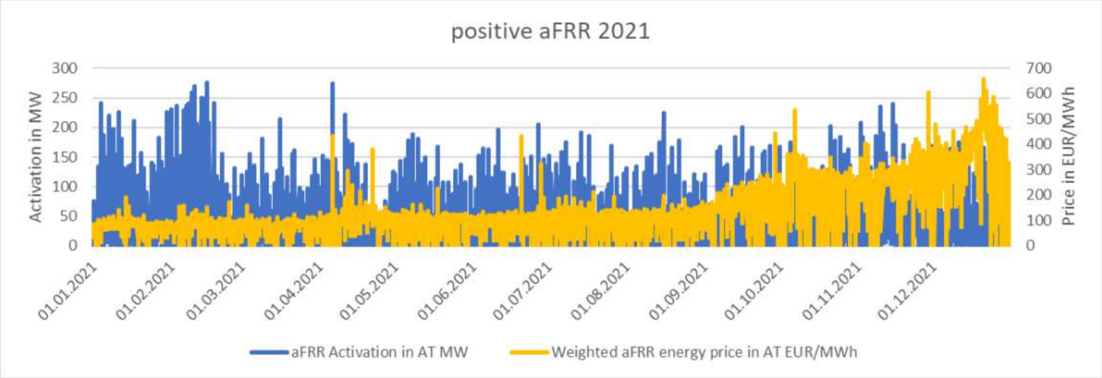

Figure 46: Weighted energy price and activated positive aFRR in Austria, 2021. Own figure based on (Austrian Power Grid AG, 2021)

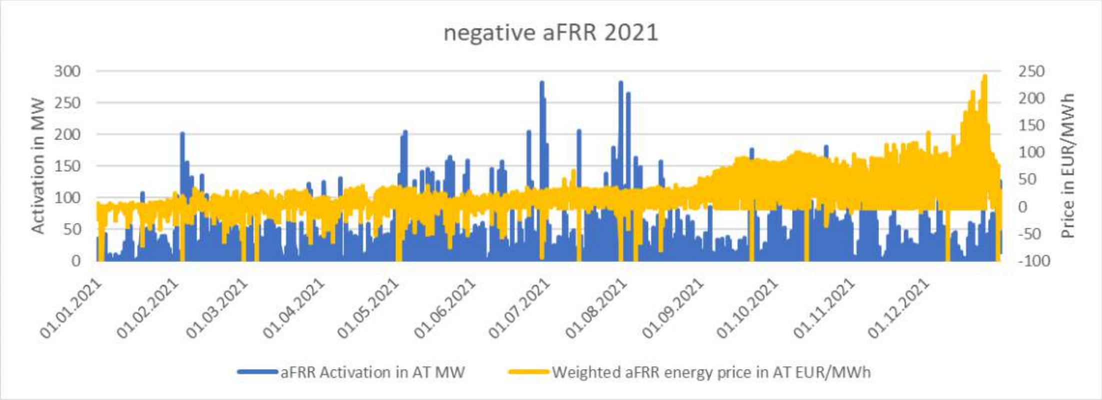

Figure 47: Weighted energy price and activated negative aFRR in Austria, 2021. Own figure based on (Austrian Power Grid AG, 2021)

The negative aFRR is slightly positive, which mean the provider for negative aFRR (electrolyser increases the load and pulls energy from the grid), must pay for the energy. In case of negative prices, the provider receives compensation according to the activated control reserve energy. In the end of 2021, even with very high spot market prices, the provider would have to pay more than 100 EUR/MWh for negative aFRR. This is still less than the actual spot price for energy.

When the automatic secondary control reserve is not enough to compensate for the failure of the largest power plant unit, a supplementary manual reserve is needed - the tertiary control reserve. (Austrian Power Grid AG, 2022)

Tertiary reserve: mFRR (Manual frequency restoration reserve)

The tertiary control reserve basically serves to avoid a prolonged activation of the secondary control. In Austria, it must also supplement the secondary control reserve in the event of major imbalances such as major power plant outages, as the latter would otherwise be too small to compensate for the imbalance on its own. The manual frequency restoration reserve must be activated within 15 minutes. The tender process is basically the same as for secondary reserve and the currently tendered volume in Austria is 280 MW positive mFFR and -195 MW negative mFFR. (Austrian Power Grid AG, 2022)

Figure 48 till Figure 51 show the capacity price for tertiary reserve in Austria. Similar to the secondary reserve, capacity prices are most of the time below 10 EUR/MWh for 2020 and are increasing at the end of 2021, when spot prices also increased tremendously.

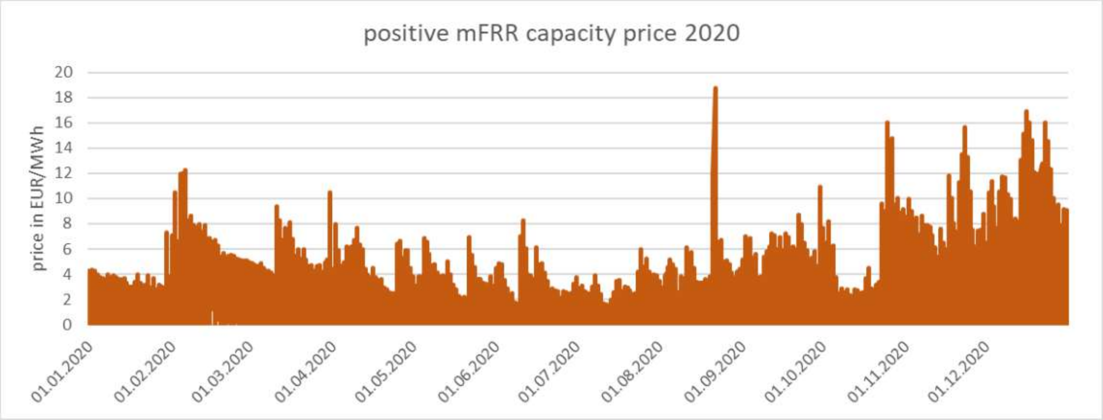

Figure 48: Capacity price for positive mFRR in Austria, 2020. Own figure based on (Austrian Power Grid AG, 2020)

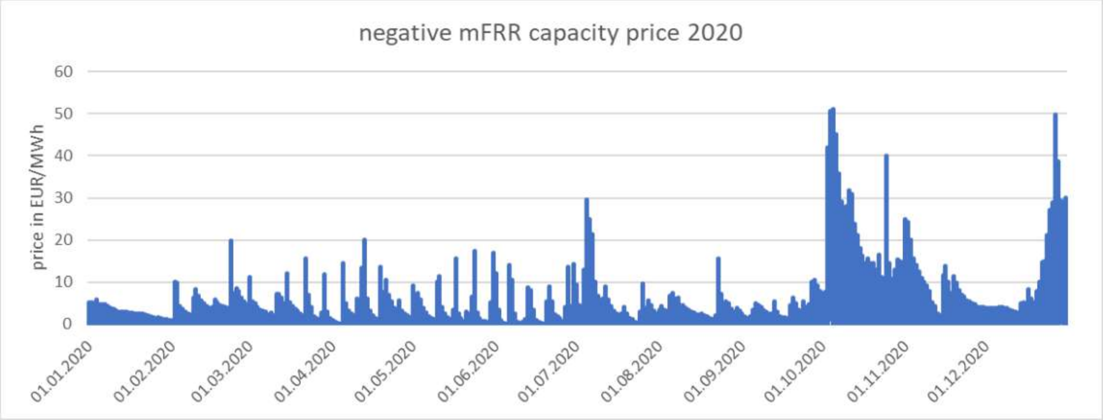

Figure 49: Capacity price for negative mFRR in Austria, 2020. Own figure based on (Austrian Power Grid AG, 2020)

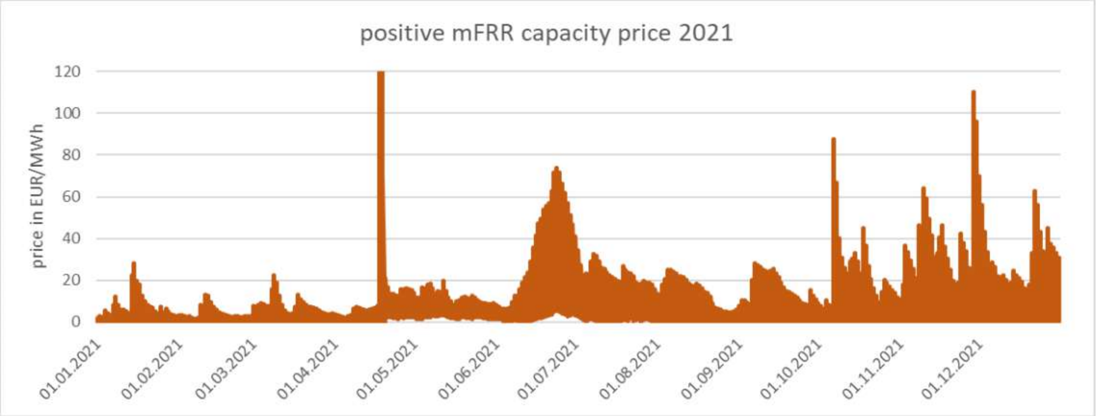

Figure 50: Capacity price for positive aFRR in Austria, 2021. Own figure based on (Austrian Power Grid AG, 2021)

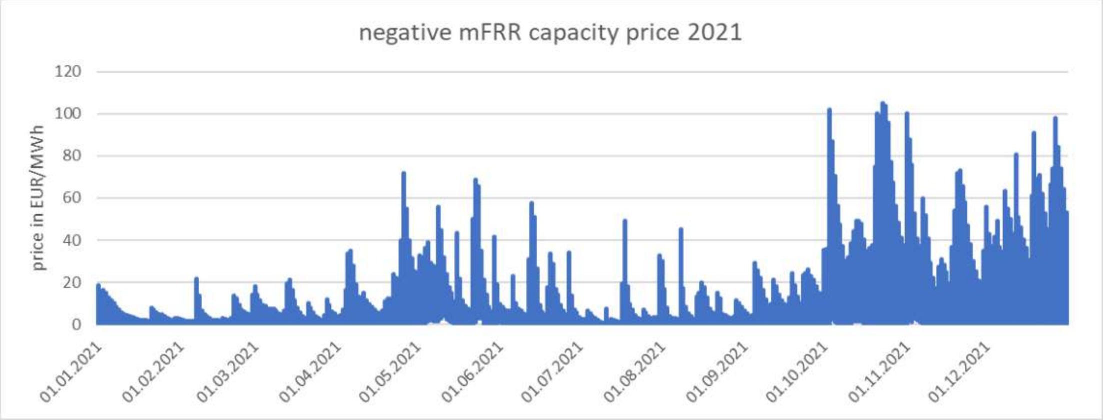

Figure 51: Capacity price for negative mFRR in Austria, 2021. Own figure based on (Austrian Power Grid AG, 2021)

Figure 52 till Figure 55 show the energy prices and the activated tertiary reserve for 2020 and 2021 in Austria. Compared to secondary reserve it is activated much less but with higher energy prices.

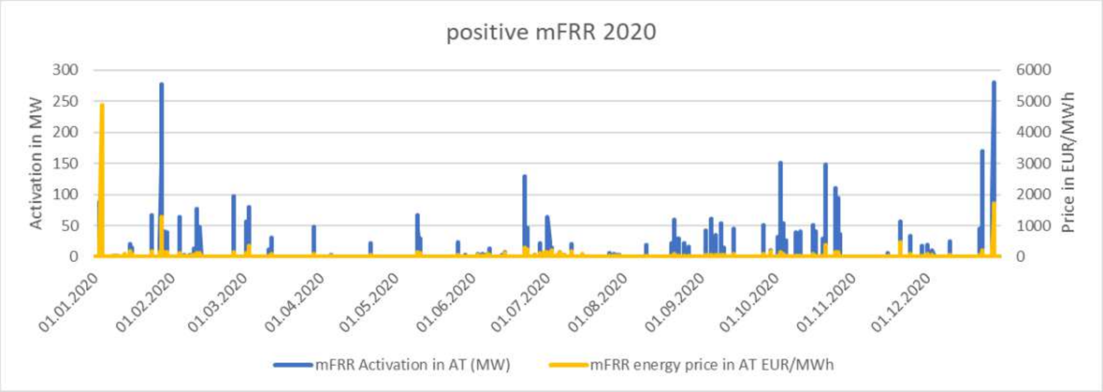

Figure 52: Weighted energy price and activated positive mFRR in Austria, 2020. Own figure based on (Austrian Power Grid AG, 2020)

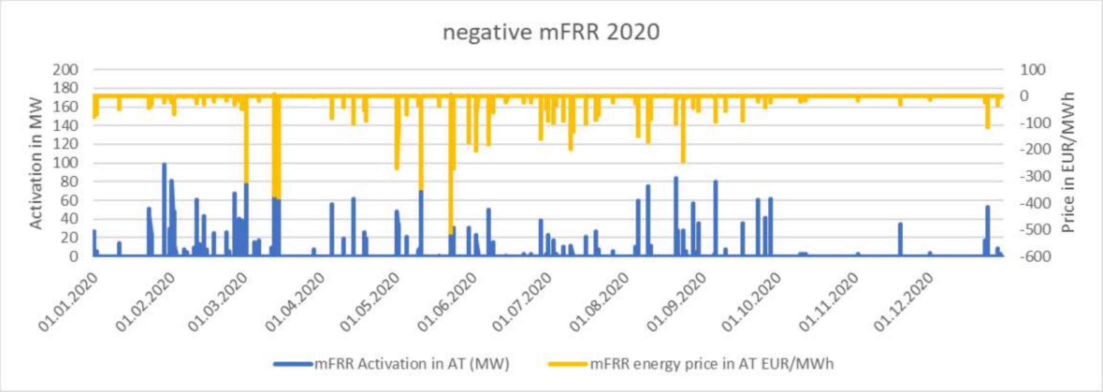

Figure 53: Weighted energy price and activated negative mFRR in Austria, 2020. Own figure based on (Austrian Power Grid AG, 2020)

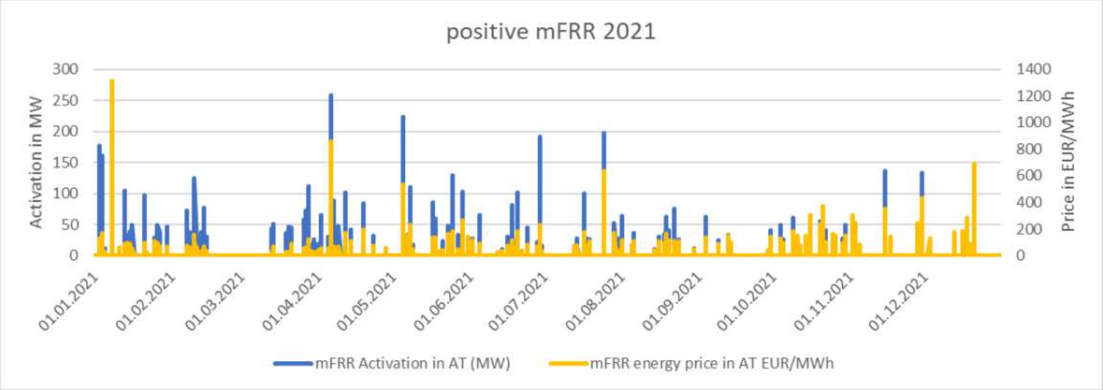

Figure 54: Weighted energy price and activated positive mFRR in Austria, 2021. Own figure based on (Austrian Power Grid AG, 2021)

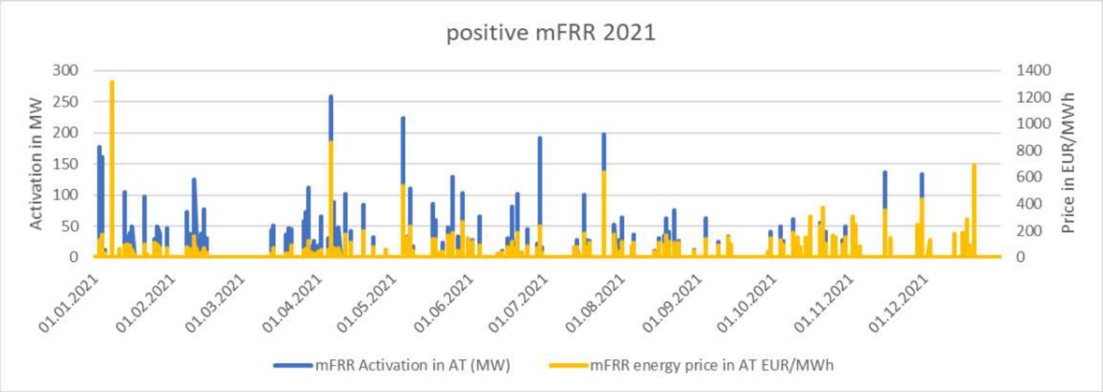

Figure 55: Weighted energy price and activated negative mFRR in Austria, 2021. Own figure based on (Austrian Power Grid AG, 2021)

5. Scenarios of the techno-economic analysis

In this chapter, the input parameters for the economic calculation are presented as well as the different scenarios, concerning plant size, technology, costs, electricity price and balance energy price.

5.1. Considered technologies

Since the biogas plant Bruck/Leitha already has an existing biogas upgrading unit in place, the ex-situ methanation with a pure CO_2 stream after upgrading is selected as the base concept (see Figure 56).

Regarding the electrolyser technology, only the alkaline and the PEM technology are considered in the analysis, due to the higher technology readiness level, lower costs, more flexibility, and bigger market compared to a high temperature electrolysis.

For the methanation technology, the biological methanation was selected for this evaluation, since several synergies with the existing biogas plant, for example using the digestate from the fermenter as biomass input for the methanation reactor, can be achieved. Moreover, the higher flexibility for the biological reactor to load changes and on-off operation compared to the catalytic reactor is especially important and beneficial when taking part in the control reserve energy market, where high flexibility is a prerequisite. Also, for the post-treatment of the synthetic biomethane, the existing gas cleaning units could be used as well.

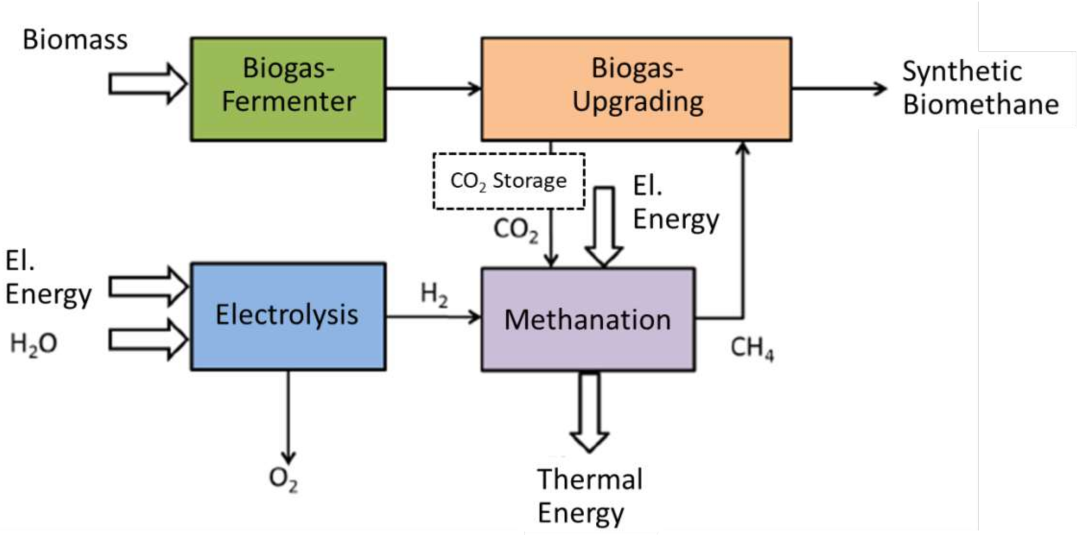

Figure 56: Considered methanation concept. Own figure

5.2. Input Parameter

Table 5 and Table 6 show the summary of the techno-economic parameter of different electrolysis and methanation technologies. Because of the broad range of CAPEX, three price scenarios are used, reflecting a low, base and high case of CAPEX. For sake of simplicity and comparability, operating and maintenance costs as percentage of CAPEX per year, lifetime and efficiency were kept constant in the low, base and high case. Another variation were the electricity costs, where 6 different cases of electricity costs were assumed: five fixed day/night energy prices and 2 floating price cases using the 2020 and 2021 spot market prices (including taxes and grid fees).

According to §62 EAG 2021 Renewable Energy Expansion Act (Erneuerbaren-Ausbau-Gesetz), facilities converting renewable electricity into hydrogen and synthetic methane can receive an investment grant of up to 45%. This 45% investment grant was considered in the CAPEX of electrolyser, methanation unit and for CO_2 storage.

Table 5: Review of literature data on electrolysers. Own table based on (Milanzi, et al., 2018) & (Graf, et al., 2021)

	Unit	**AEL**	**PEMEL**	**HTEL**
Electrolyte		KOH-Solution	Water (liquid)	Water (steam)
TRL		8	6	4
Power Rating	MW	0.005 - 5.3	0.005 – 17.5	0.0018 – 0.15
Efficiency	% H_2	68 – 85	67 – 75	73 – 82
Min.-Max. Load	%	10 – 110	0 – 200	5 - 100
Cold Standby	min	10 – 60	1 - 40	
Lifetime	h	75,000	60,000	20,000
CAPEX	EUR/kW	500 – 1,500	1,000 – 2,300	2,000 – 5,600
CAPEX 2030	EUR/kW	500 – 1,400	650 – 1,500	460 – 2,800
CAPEX 2050	EUR/kW	200 – 700	200 – 900	153 – 1,000

Table 6: Review of literature data on methanation. Own table based on (Bär, et al., 2015) & (Graf, et al., 2014)

	Unit	Biological Methanation	Catalytic Methanation
TRL		6	7
Catalyst		Microorganisms	mostly Ni-based
Pressure	bar	4 – 10	> 10
Temperature	°C	40 -70	300 - 700
Tolerance		high	low
Flexibility		high	moderate
Electricity Demand	kWh/m$^3_{SNG}$	0.4 – 1.8	< 0.4
Heat integration		moderate	high
CAPEX	EUR/kW$_{SNG}$	110 – 1,500	100 – 1,500

Table 7 show the used techno-economic input parameters such as CAPEX, OPEX, electrical energy consumption, grid connection fee and usable waste heat.

Table 7: Techno-economic input parameter of the technology. (Own table)

	AEL	PEMEL	Methanation	Storage
Low CAPEX	500 EUR/kW$_{el}$	1000 EUR/kW$_{el}$	600 EUR/kW$_{SNG}$	100 EUR/kW$_{el}$
Base CAPEX	1000 EUR/kW$_{el}$	1650 EUR/kW$_{el}$	800 EUR/kW$_{SNG}$	100 EUR/kW$_{el}$
High CAPEX	1500 EUR/kW$_{el}$	2300 EUR/kW$_{el}$	100 EUR/kW$_{SNG}$	100 EUR/kW$_{el}$
OPEX [% CAPEX]	3%	2%	4%	6%
Electrical energy consumption	5 kWh/Nm^3 H_2	5 kWh/Nm^3 H_2	1 kWh/Nm^3 SNG	0.12 kWh/Nm^3

Grid connection (Level 5)	101.48 EUR/kW_{el}	101.48 EUR/kW_{el}	-	-
Usable Waste Heat (at 50°C)	0.2 kWh_{th}/kWh_{el}	0.2 kWh_{th}/kWh_{el}	0.34 kWh_{th}/kWh_{SNG}	-

Table 8 show the used basic economic parameter. Table 9 and Figure 57 show the used day and night electricity prices (all-in) including electricity duty, handling fee and renewable fee. According to §111 (3) ElWOG, facilities converting renewable electricity into hydrogen and synthetic methane are exempt from grid utilisation and grid losses fees for a period of 15 years.

Table 8: Basic economic input parameter. (Own table)

Discount rate	2%
WACC	2.5%
Discount period	10 years

Table 9: Electricity input prices. (Own table)

		Day	**Night**
Very Low	EUR/MWh	50	30
Low	EUR/MWh	90	50
Mid	EUR/MWh	135	75
High	EUR/MWh	180	100
Float 2020	Figure 57 (light blue)		
Float 2021	Figure 57 (green)		

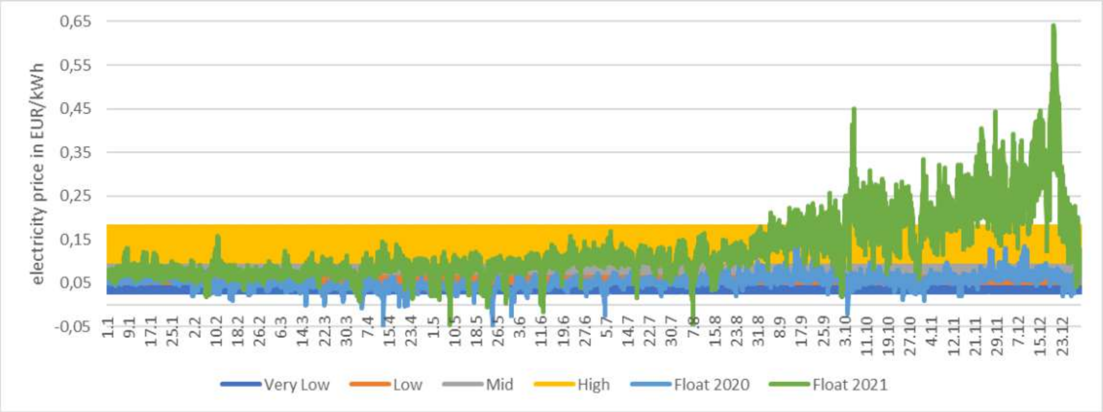

Figure 57: Electricity prices for all considered cases. Own figure based partly on (Austrian Power Grid AG, 2020) & (Austrian Power Grid AG, 2021)

5.3. Power-to-Gas Dimensions

In order to find out which power-to-gas size fits best to the existing biogas plant in Bruck/Leitha and its off-gas stream, different electrolyser and methanation sizes ranging from 2 MW_{el} up to 5 MW_{el} are considered in the calculations as well.

Table 10 shows that with a 5 MW_{el} electrolyser and 250 Nm^3/h methanation reactor, 100% of the off-gas CO_2 could be converted to synthetic biomethane. Since the off-gas stream is fluctuating, a smaller electrolyser of 2 MW_{el} in combination with a 100 Nm^3/h methanation reactor would utilise 60% of the off gas (Figure 58).

Table 10: Considered power-to-gas sizes. (Own table)

Off-gas Nm^3/h	**Hydrogen** Nm^3/h	**Electrolyser** MW	**SNG** Nm^3/h	**SNG** GWh	**Utilisation** %
100	400	2	100	9	60
125	500	2.5	125	11	73
150	600	3	150	12.4	82
175	700	3.5	175	13.4	89
200	800	4	200	14.2	94
250	1000	5	250	15	100

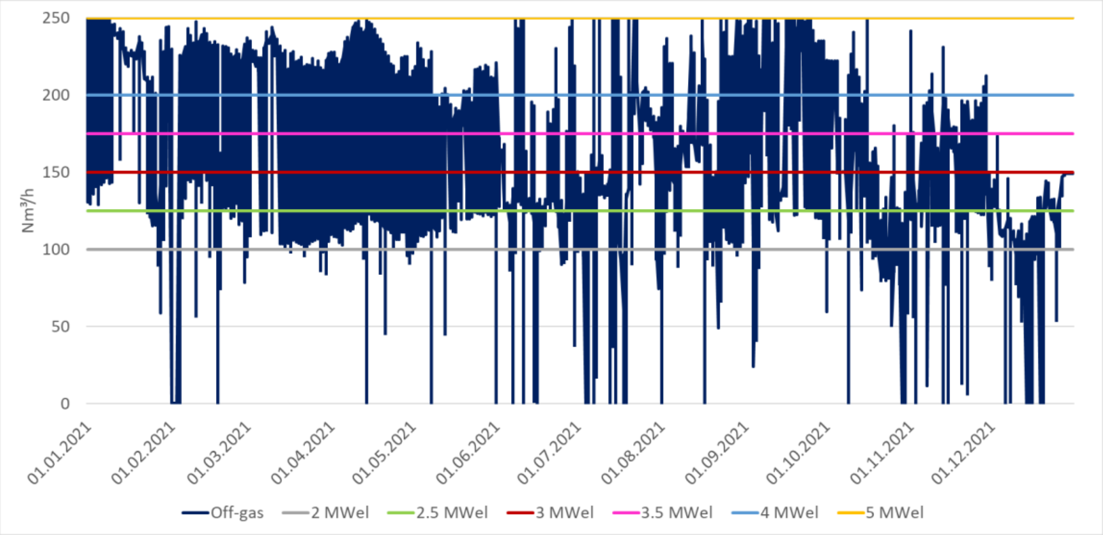

Figure 58: Off-gas and different SNG streams of different power-to-gas sizes. Own figure based partly on (Mauthner, 2021)

5.4. Operational Scenarios

For reflecting different electricity market situations and operating schedules six operational scenarios were examined in the techno-economic assessment. In all scenarios, the same amount waste heat integration for fermenter heating was assumed. Since neither electrolyser nor biological methanation can deliver waste heat with temperatures higher 60°C it can only be used for fermenter heating, which can be up to 200 kW in Winter according to Figure 19. The continuous 200 kW disinfection process requires temperature of more than 70°C and feeding into the nearby district heating grid requires temperatures of approximately 90°C. For these two applications, an additional heat pump would be needed, which was not taken into account in the scenarios. Also, no utilisation or revenues from the produced oxygen were considered in the scenarios.

5.4.1. Scenario 1a: Maximum PtG utilisation without storage

This scenario considers a maximization of the power-to-gas (electrolyser and methanation) full load hours without a CO_2 storage. This means for example a 4 MW electrolyser can produce under nominal full load maximum 800 Nm³/h of hydrogen. The methanation therefore can convert max. 200 Nm³/h of off-gas to synthetic biomethane. In cases of a higher off-gas production by the biogas plant, the surplus of CO_2 is not used in the power-to-gas unit and vented into the environment, thus reducing the utilisation factor. In cases of a lower off-gas stream, due to a reduction in biogas production, the electrolyser and the methanation must adapt as well and decrease the load, accordingly, thus also decreasing the utilisation factor.

5.4.2. Scenario 1b: Maximum PtG utilisation with storage

Similar to scenario 1a, this scenario also aims to maximize the utilisation factor of the power-to-gas unit but in combination of a liquid CO_2 storage tank (see chapter 4.5). The advantage of a storage tank is to buffer fluctuations in the off-gas stream, thus allowing a higher utilisation with less installed power-to-gas capacity.

5.4.3. Scenario 2a: PtG uses only electricity from Sonnenfeld

In this scenario, the power-to-gas plant follows the electricity of the nearby 3 MW agricultural PV plant "Sonnenfeld" (see chapter 4.6). If the PV plant is directly connected to the transformer station of the biogas plant, using its electricity would not cause any grid fees. The only fee would be the electricity duty of 15 EUR/MWh. On the other hand, the low full load hours of approx. 1100 hours of PV causes very low utilisation factors of the power-to-gas plant. The aim of this scenario is to give conclusions if the power-to-gas process is economically feasible in combination with the photovoltaic production profile only. No storage was considered in this scenario.

5.4.4. Scenario 2b: PtG operates only below certain electricity price

This scenario should represent an operational strategy, where the power-to-gas unit is only in operation at times, when the spot market price is below 40 EUR/MWh. Therefore, the plant is supplied with the hourly spot market electricity prices of 2020 including taxes and fees. The year 2021 was excluded since the prices this year were often significantly higher than 40 EUR/MWh. No storage was considered in this scenario.

5.4.5. Scenario 3a: Positive secondary reserve (aFRR+) market

In this scenario, the electrolyser uses its flexibility and takes part in the secondary reserve market, since it has the highest energy prices and requests compared to primary and tertiary reserve market. In the positive secondary reserve market, the electrolyser is running normally on nominal load, while offering its capacity to decrease from nominal load to zero in the capacity tender. Since the capacity prices are usually low, no revenues from the capacity tender were considered. Regarding offered prices for reserve energy in the auction, an optimum price was determined based on the monthly average of the day-ahead spot prices and increased by 30% (Figure 59 and Figure 60). The data also show that the weighted energy price of positive aFRR correlates with the spot market price. The higher the spot price, the higher the aFRR energy price, which compensates the high electricity spot market price.

Figure 59: Offered price of positive aFRR 2020. Own figure based partly on (Austrian Power Grid AG, 2020) & (Austrian Power Grid AG, 2020)

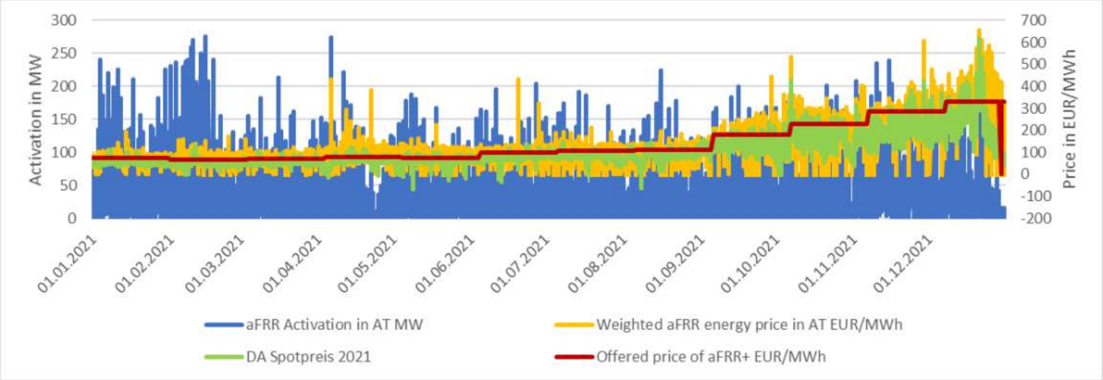

Figure 60: Offered price of positive aFRR- 2021. Own figure based partly on (Austrian Power Grid AG, 2021) & (Austrian Power Grid AG, 2021)

Compared to the other scenarios, also revenue by offering secondary reserve energy can be generated apart from the revenues from the synthetic methane.

In order to take part in the secondary reserve market, a very high availability of the electrolyser has to be met. Therefore, the hydrogen must be processed in the methanation immediately, since no large hydrogen buffer tank is in place. To provide this flexibility, a certain CO_2 stream has to be available at all times when offering reserve capacity. This is achieved with a liquid CO_2 tank large enough to ensure a very high availably of the whole power-to-gas plant throughout the whole year.

5.4.6. Scenario 3b: Negative secondary (aFRR-) reserve market

In this scenario, the electrolyser takes part in the negative secondary reserve market. Here the electrolyser capacity is offered in the capacity auction to increase its load from 0 to nominal load and thus providing negative secondary reserve energy to the grid. Since the offered prices are significantly lower than for positive aFRR, the optimum offered energy price for this calculation equals 10% of the monthly spot market average (Figure 61 and Figure 62). Additionally, a positive energy price means costs for negative reserve energy and therefore, the aim is offering energy with a price as low as possible. Also, no revenues from the capacity tender were considered in this scenario as well. In this scenario also a liquid CO_2 storage tank to increase the availability was included in the calculations.

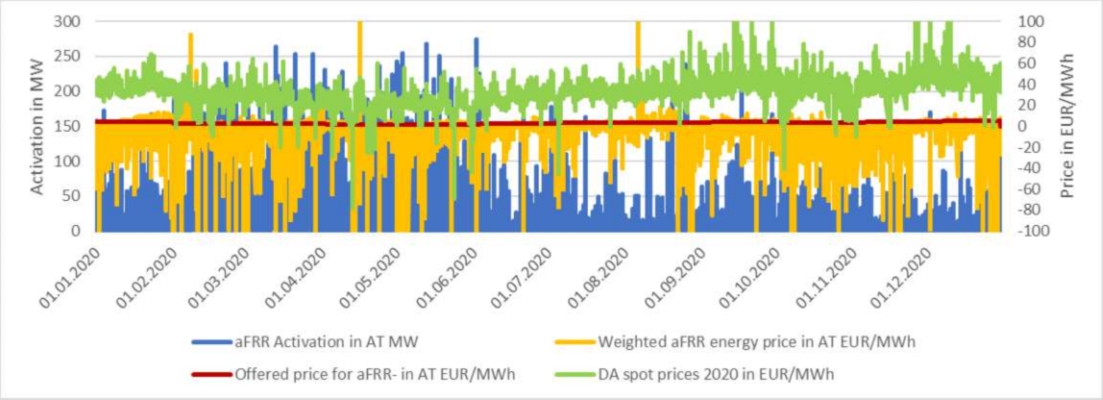

Figure 61: Offered price of negative aFRR 2020. Own figure based partly on (Austrian Power Grid AG, 2020) & (Austrian Power Grid AG, 2020)

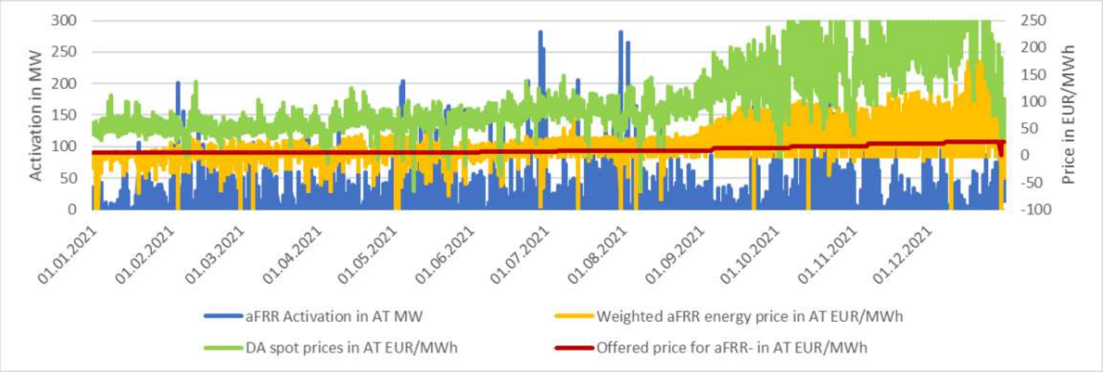

Figure 62: Offered price of negative aFRR 2021. Own figure based partly on (Austrian Power Grid AG, 2021) & (Austrian Power Grid AG, 2021)

6. Results

In this chapter, results of the techno-economic assessment are discussed and the different scenarios and technology options as well as price case are compared to each other in terms of long rang generation costs of synthetic methane (LRGC).

6.1. Mass and Energy balance of a 5 MW$_{el}$ Power-to-Gas plant at Bruck/Leitha

Figure 63 shows the simplified ideal mass balance for the biomethane production of 500 Nm³/h in combination with a 5 MW$_{el}$ electrolyser and 250 Nm³/h$_{SNG}$ biological methanation reactor. It shows that with the power-to-gas unit, the biomethane yield of the biogas plant can be increased by 50% and that the produced gas composition meets the high grid requirements and can therefore be injected into the public gas grid without any concern. Also, the methane losses in the upgrading unit can be mitigated since, the off-gas stream is not vented into the environment anymore.

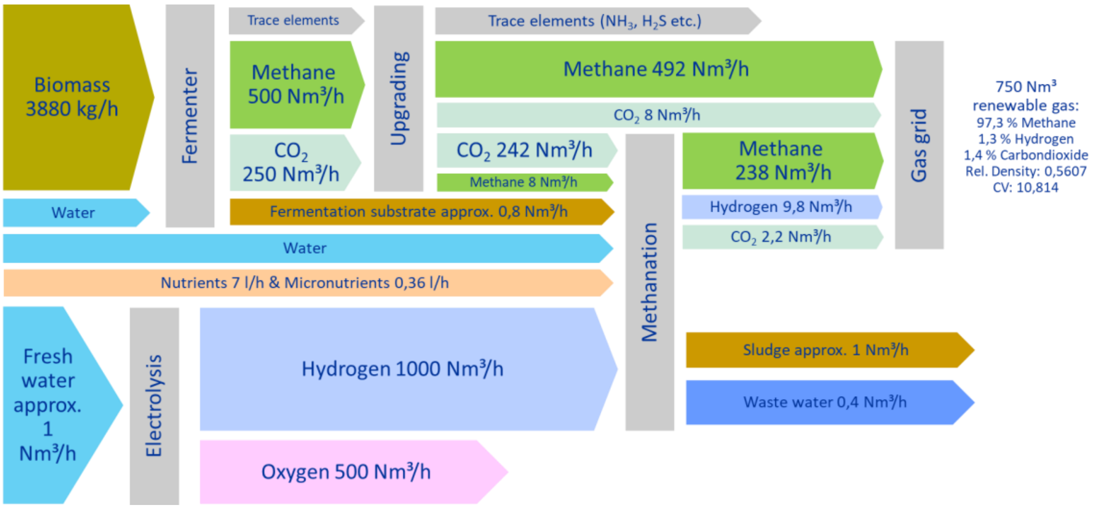

Figure 63: Mass balance of a 5 MW$_{el}$ power-to-gas plant in combination with the biogas plant Bruck/Leitha. (Own Figure)

When looking at the energy balance (Figure 64) of the same plant size and configuration, the whole process is quite efficient with an overall efficiency of almost 75% since a part of the waste heat can be integrated in the current biogas process. In the ideal case, where the whole 1.7 MW of waste heat at 55°C could be used, the efficiency increases up to 90%. When taking the additional 200 kW of heat demand from disinfection as own consumption into account, the residual 1.5 MW could be either used for a low temperature anergy district heating grid, for heating up the back flow of the nearby district heating grid. In combination with an electrical heat pump, which raises the temperature from 55°C to 90 – 100°C, this heat could also be fed into the main flow of the district heating grid as a base load.

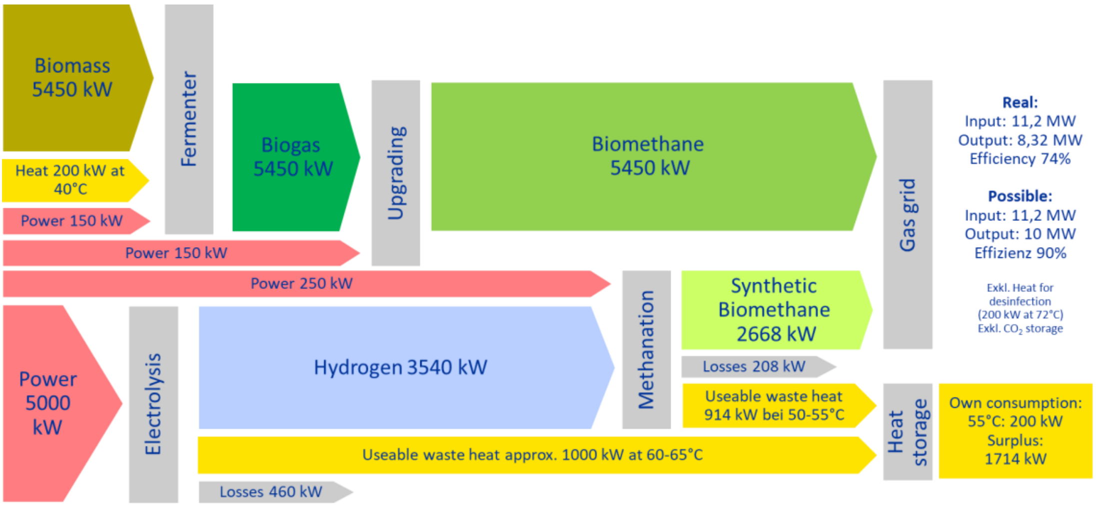

Figure 64: Energy balance of a 5 MW_{el} power-to-gas plant in combination with the biogas plant Bruck/Leitha. (Own Figure)

6.2. Long range generation costs of synthetic biomethane

The Long-range generation costs of synthetic biomethane (LRGC) were based on the annuities of CAPEX, OPEX and energy costs and revenues from the control reserve market.

6.2.1. Results of Scenario 1a

Appendix 1 shows the results of Scenario 1a, where the utilisation of the power-to-gas plant was maximized without a storage. It can be seen, that even with very low electricity prices, the LRGC never reach values less than 100 EUR/MWh. Also, the strong sensitivity and therefore linear relationship between electricity price and LRGC are illustrated. Furthermore, larger power-to-gas capacities do not result in lower LRGC, because the utilisation factor decreases, since the biogas plant delivers a fluctuating CO_2 stream. Therefore, smaller capacities or a storage system for CO_2 can increase the utilisation factor.

6.2.2. Results of Scenario 1b

Appendix 2 illustrates the influence of a CO_2 storage. With a storage capacity of 100 t CO_2, which refers to a vertical tank of 15 m in height and 3.6 m in diameter, and a power-to-gas unit of 3.2 MW_{el} all the produced CO_2 in 2020 could be converted to 15 GWh of synthetic biomethane. With a smaller storage of 78 t and 3 MW_{el} power-to-gas capacity, 14 GWh SNG could be produced. When comparing the LRGC of scenario 1a and 1b, an additional storage would increase the LRGC for 2 MW_{el} and 2.5 MW_{el} plant sizes by 1-2 % and above that it would only decrease the LRGC by 2-4%, which is only a minor impact.

6.2.3. Results of Scenario 2a & 2b

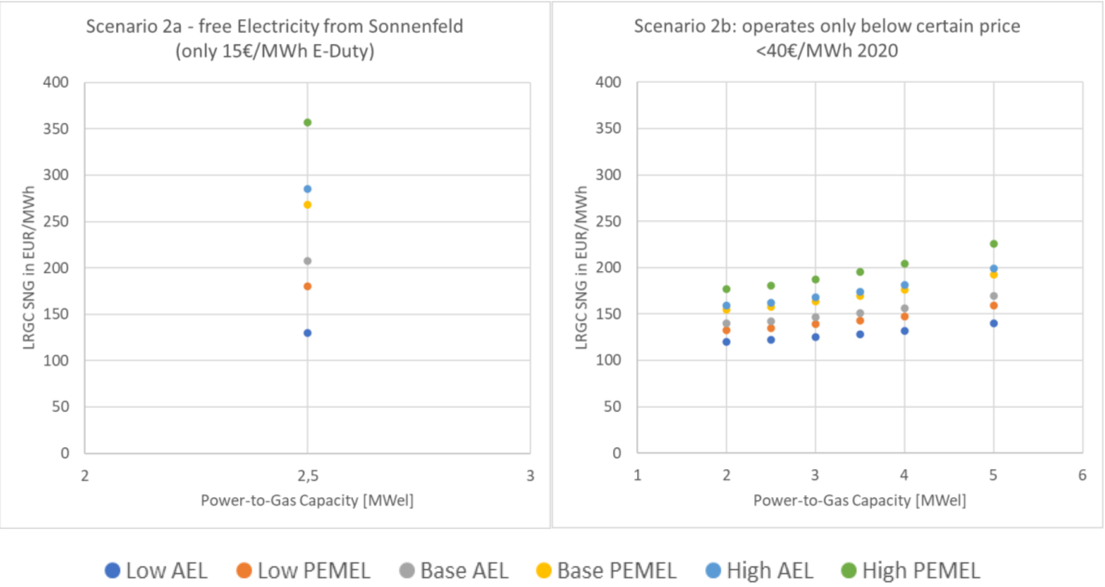

Figure 65: Results of Scenario 2a (left) & 2b (right). (Own figure)

Scenario 2a (Figure 65 left) displays the ideal case of a 2.5 MW_{el} power-to-gas unit with the 3 MW_{peak} agricultural PV plant, where the electricity costs are only assumed to be 15 EUR/MWh according to the electricity duty. Even in this very optimistic and rather unrealistic case of "almost" free energy from the PV plant, the LRGC are between 135 and 360 EUR/MWh, depending on the CAPEX case. This is because with only 1100 full load hours, 1.98 GWh of synthetic biomethane could be produced. Therefore, it does not really make sense to use a power-to-gas plant with such a low utilisation of only 1500 full load hours.

Even in the scenario 2b (Figure 65 right) when the power-to-gas unit is only operating when the spot price (reference year 2020) is below 40 EUR/MWh and a utilisation of 4,000 (5 MW_{el})– 6,000 (5 MW_{el}) full load hours could be reached, the LRGC are still higher than 100 EUR/MWh.

6.2.4. Results of Scenario 3a

A completely different situation occurs when entering the control reserve market with electrolyser and use the flexibility of the whole power-to-gas process in order to generate also revenues from offering positive control reserve energy.

Figure 66: Results of Scenario 3a for positive aFRR with 2020 prices. (Own figure)

Figure 66 shows that the revenues from the positive control energy market (with 2020 prices) compensate the electricity costs. In this operational scenario, where the electrolyser reduces the load, when positive control energy is required in the electricity grid, only 2,200 – 2,935 full load hours could be reached. For example, the 5 MW_{el} power-to-gas unit has around costs for electricity 2,000,000 EUR/a in the floater 2020 case and generates 1,300,000 EUR/a revenue from offering positive control energy. A smaller power-to-gas unit of 2 MW_{el} could even generate in the Low CAPEX case revenues for positive control energy, which are higher than the costs for electricity, depreciation, operating costs, thus having negative LRGC.

The big advantage of the positive control energy is, that the price increases with increasing electricity prices, which generates a dampening effect. This was the case at the end of 2021 when the electricity skyrocketed to more than 300 EUR/MWh. In this case, displayed in Figure 67, the price for positive control energy was so high, that in combination with a floater electricity tariff 2021, the LRGC are in any CAPEX and capacity case negative. The full load hours when taking part in the 2021 positive energy market are between 2955 and 3156 and therefore producing 4 – 8.5 GWh of synthetic biomethane. For a production of 8.5 GWh of SNG with the 5 MW_{el} power-to-gas unit, a CO_2 storage of around 30 t would be needed to provide the necessary operational flexibility and security for the control reserve market. See also Appendix 3 for detailed results.

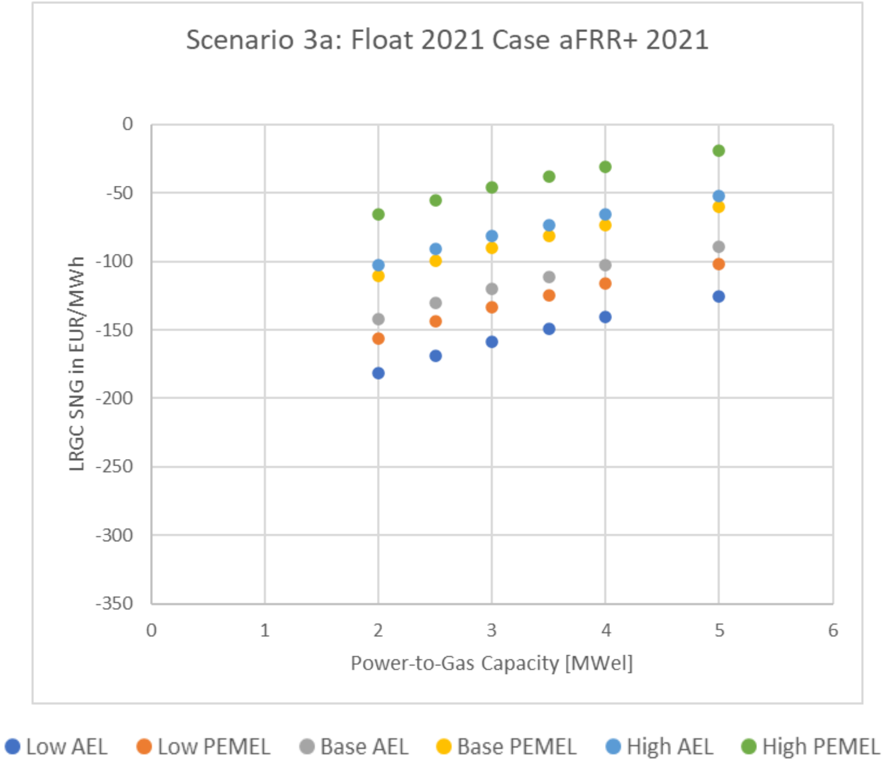

Figure 67: Results of Scenario 3a for positive aFRR with 2021 prices. (Own figure)

6.2.5. Results of Scenario 3b

Figure 68 and Figure 69 show the results of participating in the negative control market, thus operating only with negative control energy.

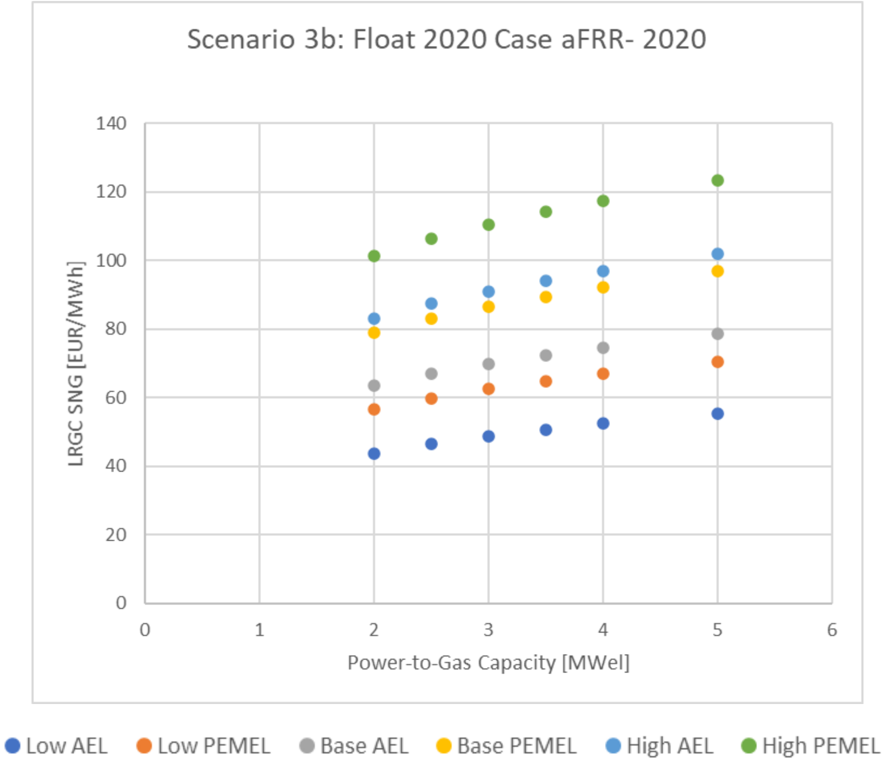

Figure 68: Results for Scenario 3a for negative aFRR with 2020 prices. (Own figure)

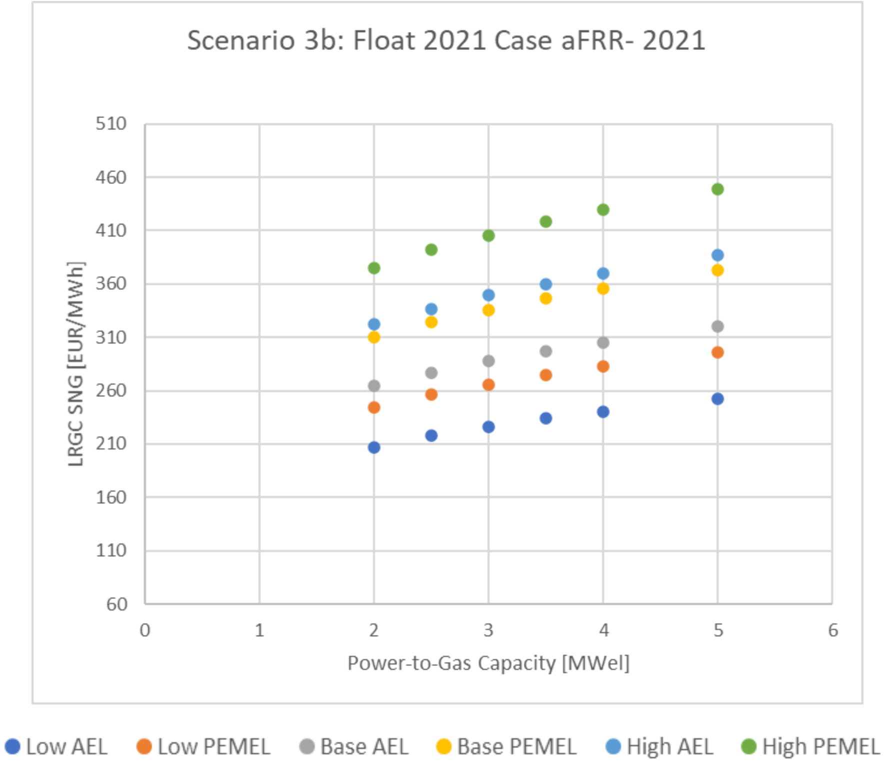

Figure 69: Results of Scenario 3a for negative aFRR with 2021 prices. (Own figure)

Therefore, the electricity price has a rather low to no influence on the LRGC. For low negative control energy prices like 2020, LRGC below 100 EUR/MWh can be achieved in almost every CAPEX and capacity case. But when the electricity prices a rising, which was the case in 2021, also the prices for negative control energy a rising and therefore creating higher costs when the power-to-gas plants operates with this energy. Compared to the positive energy market, using negative control energy generates costs. See also Appendix 4 and Appendix 5 for detailed results.

6.2.6. Economic results for a 5 MW_{el} power-to-gas plant in the positive control reserve market

Table 11, Table 12, Table 13 show the results of a 5 MW_{el} power-to-gas plant, which operates in the positive control reserve market for 2020 and 2021 prices and differentiated between AEL and PEMEL technology.

According to literature data, there is still quite a big difference between alkaline and PEM electrolyser when it comes to investment costs. This is also reflected in the total revenues, since the depreciation and other operating costs as included as well. The revenues generated by the SNG production refer to a price of 100 EUR/MWh.

Due to the fact, that the revenues in the positive control reserve market are quite high, the profits from the power-to-gas plant are positive in a year (2020) with low electricity prices and are even higher in a year (2021) with high electricity prices, because the positive control energy prices correlate almost linear with the electricity spot prices.

Table 11: Summary of economic data of a 5 MW_{el} power to gas plant. (Own table)

	CAPEX [EUR]	**OPEX [EUR/a]**		**CAPEX [EUR]**	**OPEX [EUR/a]**
PEMEL	8,250,000	165,000	**AEL**	5,000,000	150,000
Methanation	2,124,000	85,360	**Methanation**	2,124,000	85,360
Storage	500,000	30,000	**Storage**	500.000	30,000
Grid connection fee	532,770	-	**Grid connection fee**	532,770	-
Sum without funding	11,416,770		Sum without funding	8,116,770	
Sum with 45% funding	**5,986,200**	**280,360**	**Sum with 45% funding**	**4,464,200**	**265,360**

Table 12: Techno-economic results of a 5 MW_{el} power to gas plant in the aFRR+ market. (Own table)

	2020	**2021**
Production SNG [GWh]	7.83	8.42
FLH Electrolyser [h]	2,935	3,156
Electricity costs [EUR/a]	854,321	2,138,760
Revenues aFRR+ [EUR/a]	1,282,031	3,722,727
Revenues SNG [EUR/a]	783,000	842,000
Savings Heat [EUR/a]	28,600	

Table 13: Total revenue per year of a 5 MW_{el} power to gas plant in the aFRR+ market. (Own table)

	AEL 2020	**PEM 2020**	**AEL 2021**	**PEM 2021**
Total Profits [EUR/a]	375,850	135,000	1,822,000	1,533,000

7. Discussion & Conclusion

This techno-economic assessment showed that even today a power-to-gas plant, using the highly concentrated CO_2 off-gas stream of a biogas plant to increase the biomethane yield of the plant by 50% does not only make sense from the technical point of view but also under certain conditions from the economic point of view.

The first and most important conditions is, that with today's CAPEX for the electrolyser and the methanation reactor a substantial funding (more than 40%) is required to operate economically feasible. Without a funding, total investment costs for a 5 MW_{el} power-to-gas plant with a PEM electrolyser and a biological methanation would reach almost 12 Mio. EUR. When investment costs will decrease as forecasted in the literature, a power-to-gas plant can also sustain without funding. Also, the exemption from electricity grid utilisation fees for the first 15 years is very important to achieve profitability.

Even more important for a power-to-gas plant are the operating costs, especially the electricity costs. Therefore, is it crucial to establish a procurement strategy for the input energy. One way could be on the electricity market, with a floating tariff. With this floating tariff according to the electricity spot market, the plant could benefit from times with low or even negative prices. Unfortunately, in the last year, electricity prices increased by over 300%. This tremendous increase is a substantial risk for the whole business, therefore using the electrolyser also as a flexibility provider for the electricity grid in terms of positive or negative control reserve energy can generate additional revenues.

In terms of technology, the cheaper alkaline electrolyser is capable for secondary control reserve according to literature, with the downside, that frequent load changes and on/off operations can reduce the lifetime of the stack, or cause a higher heat demand, so the stack does not cool off, when positive control energy is provided for a longer period (meaning reducing the load to 0). The PEMEL has the advantage of the smaller footprint, no harmful liquids and overload capacity, which could also be used for offering even more secondary control reserve capacity than the nominal load or. This short-term overcapacity, when designed accordingly, could also be used for offering primary reserve energy.

Regarding the methanation reactor, a biological methanation is preferred due to synergies with the existing biogas plant (gas treatment, availability of digestate as input biomass, Know-how) over a catalytic methanation. The biggest advantage of the biological methanation is the flexibility in part load operation as well as on/off operation and the higher technology readiness compared to the catalytic one. The disadvantage would be a higher footprint. The total footprint for a 10 MW_{el} AEL power-to-gas plant with a biological methanation reactor is approx. 1000 m^2 according to the manufacturer's specification. This footprint must be kept in mind.

One main outcome of this assessment was, that providing positive control reserve energy with the flexible electrolyser and using the gas grid via a methanation in combination with a CO_2 as a storage, can counter high electricity prices. Reducing the load of the electrolyser when the prices for positive control reserve are high can generate enough revenues to compensate for very high prices and even generate profits apart from the synthetic biomethane production. This reduction in SNG production sacrifices the utilisation factor on the one hand, but on the other hand the plant would not be sustainable otherwise, with reasonable prices for biomethane.

With the aim to take the next step in implementing such a power-to-gas unit at the biogas plant Bruck/Leitha, further investigation in process design and plant layout must be done in order to identify synergies with the existing infrastructure in terms of heat integration, waste heat utilisation etc. Since the investment costs in the literature showed a broad variance, it is crucial to get an idea about the real investment and operating costs. With these costs, an energy procurement strategy can be implemented. Especially a tendering strategy for the secondary control energy market must be elaborated in order to achieve revenues from providing flexibility to the electricity grid. This could also be another topic of a further master thesis, since it is one of the most import issues.

Another big issue are the high investment costs, even with funding. Therefore, a power purchase agreement with big utilities could be one way of financing the plant upfront, since banks are not likely to finance such a project.

Anyway, first movers should step forward in order to do gain practical experience with new but necessary technologies for achieving a sustainable and climate neutral energy system. This power-to-gas plant could be one of these technologies.

Bibliography

AGGM Austrian Gas Grid Management AG, 2021. Long-term and integrated planning 2021.

ASCO KOHLENSÄURE AG, 2021. Gesamtkatalog CO2 Lagerung.

ASCO KOHLENSÄURE AG, 2021. Gesamtkatalog CO2 Verdampfung.

Austrian Power Grid AG, 2020. Balancing Energy Bids.

Austrian Power Grid AG, 2020. EXAA Spot Market Prices.

Austrian Power Grid AG, 2020. Procured Balancing Capacity.

Austrian Power Grid AG, 2021. Balancing Energy Bids.

Austrian Power Grid AG, 2021. EXAA Spot Market Prices.

Austrian Power Grid AG, 2021. Procured Balancing Capacity.

Austrian Power Grid AG, 2022. *Market Information - Balancing.* [Online] Available at: https://www.apg.at/en/markt/netzregelung [Retrieved on 20 January 2022].

Bär, K., Mörs, F., Götz, M. & Graf, F., 2015. Vergleich der biologischen und katalytischen Methanisierung für den Einsatz bei PtG-Konzepten. *gwf-Gas|Erdgas*, 07.

Biegger, P. et al., 2016. Methanisierung im Umfeld von "Power to Gas". *Kurzfassungsband zum 14. Symposium Energieinnovation*, February, p. 463–464).

Biogas Bruck/Leitha GmbH & Co KG, 2021. Current Folder of Biogas Bruck/Leitha.

Demo4Grid, 2022. *Project info | Demo4Grid.* [Online] Available at: https://www.demo4grid.eu/project/ [Retrieved on 11 March 2022].

Electrochaea GmbH, 2021. Data Sheet BioCat Plant.

Electrochaea GmbH, 2021. *Electrochaea GmbH Power-to-Gas Energy Storage | Technology.* [Online]
Available at: https://www.electrochaea.com/technology/
[Retrieved on 20 December 2021].

Energiepark Bruck an der Leitha, 2022. *Biogas - Energiepark.* [Online]
Available at: https://energiepark.at/biogas/
[Retrieved on 28 Feburary 2022].

EWS Sonnenfeld, 2021. *EWS Sonnenfeld - Bruck/Leitha (NÖ).* [Online]
Available at: https://www.ews-sonnenfeld.com/referenzprojekte/detail/ews-sonnenfeld-bruck-an-der-leitha
[Retrieved on 23 December 2021].

Friedacher, A., 2021. Load flexible methanation in an advanced power-to-gas system.

Götz, M. et al., 2015. Renewable Power-to-Gas: A technological and economic review. *Renewable Energy*, 3 August, p. 1371–1390.

Graf, F., Krajete, A. & Schmack, U., 2014. *Techno-ökonomische Studie zur biologischen Methanisierung bei Power-to-Gas-Konzepten,* Bonn: DVGW Deutscher Verein des Gas- und Wasserfaches e.V..

Graf, F., Schoof, R. & Zdrallek, M., 2021. *Power-to-Gas.* 1 Hrsg. Essen: Vulkan-Verlag GmbH.

HALDOR TOPSOE, 2009. From solid fuels to substitute natural gas (SNG) using TREMP.

Hitachi Zosen INOVA, 2020. *EtoGas Power-to-Gas.* [Online]
Available at: https://www.hz-inova.com/de/renewable-gas/etogas/
[Retrieved on 23 December 2021].

H-Tec Systems GmbH, 2021. *PEM electrolysers and stacks.* [Online]
Available at: https://www.h-tec.com/en/products/detail/h-tec-pem-electrolyser-me450-1400/me450-1400/
[Retrieved on 28 December 2021].

Hydrogen Tools, 2020. *Hydrogen Density at different temperatures and pressures.* [Online]
Available at: https://h2tools.org/hyarc/hydrogen-data/hydrogen-density-different-temperatures-and-pressures
[Retrieved on 11 March 2022].

ITM Power, 2022. *Products | ITM Power.* [Online]
Available at: https://itm-power.com/products
[Retrieved on 02 January 2022].

Koonaphapdeelert, S., Aggarangsi, P. & Moran, J., 2020. *Biomethane.* Singapore: Springer Nature Singapore.

Krajete GmbH, 2021. *FAQ | Krajete GmbH.* [Online]
Available at: https://www.krajete.com/en/technology/faq
[Retrieved on 25 December 2021].

Kranzl, L. & Haas, R., 2008. *Strategien zur optimalen Erschließung der Biomassepotenziale in Österreich bis zum Jahr 2050 mit dem Ziel einer maximalen Reduktion an Treibhausgasemissionen,* Wien: Bundesministerium für Verkehr, Innovation und Technologie.

Leaflet, 2022. *Global Solar Atlas.* [Online]
Available at: https://globalsolaratlas.info/
[Retrieved on 02 January 2022].

LibreTexts, 2020. *Phase Diagrams | Chemistry.* [Online]
Available at: https://chem.libretexts.org/@go/page/24249
[Retrieved on 26 December 2021].

Limeco, 2021. *Baufortschritt, Power-to-Gas-Anlage von Limeco.* [Online]
Available at: https://www.powertogas.ch/anlage/baufortschritt/
[Retrieved on 20 December 2021].

Lindorfer, J., Fazeni, K., Tichler, R. & Steinmüller, H., 2017. *Erhöhung des Einsatzes von erneuerbarem Methan im Wärmebereich,* Linz: JKU Linz.

Mauthner, B., 2021. *Biogasplant Bruck/Leitha* [Interview] (16 October 2021).

McPhy, 2022. McPhy Portfolio ELY McLyzer.

microbEnergy, 2020. Fachinformation BiON®.

Milanzi, S. et al., 2018. *Technischer Stand und Flexiblität des Power-to-Gas Verfahrens,* Berlin: Technische Universität Berlin.

Nel Hydrogen, 2022. *Water electrolysers/hydrogen generations | Nel Hydrogen.* [Online]
Available at: https://nelhydrogen.com/water-electrolysers-hydrogen-generators/
[Retrieved on 02 January 2022].

ÖVGW, 2021. *Richtlinie G B210 Gasbeschaffenheit,* Wien: ÖVGW.

Pentair, 2021. Biogas upgrading plant CO2bolt-on leaflet.

Salbrechter, K., 2022. *Renewable Gasfield.* Energieforschungsgespräche Disentis 2022, Alpenforce.

Schmidt, M. et al., 2018. *Technologiebericht 4.2a Power-to-gas (Methanisierung chemisch-katalytisch),* Wuppertal: Institut für ZukunftsEnergie- und Stoffstromsysteme (IZES).

Siemens Energy, 2022. Datasheet Silyzer 300.

Statistik Austria, 2021. Gesamtenergiebilanz Österreich 1970 bis 2020.

Sunfire, 2022. Sunfire Factsheet HyLink Alkaline.

Thema, M. et al., 2019. Biological CO2-Methanation: An Approach to Standardization. *Energies,* 12(9).

Tjarks, G., 2017. PEM-Elektrolyse-Systeme zur Anwendung. *Energy & Environment*.

Verbund Energy4Business, 2020. *H2Future Project.* [Online]
Available at: https://www.h2future-project.eu/
[Retrieved on 11 January 2022].

Watter, H., 2019. *Regenerative Energiesysteme.* Wiesbaden: Springer Vieweg.

List of Abbreviations

AEL	Alkaline electrolyser
aFRR	Automatic frequency restoration reserve
APG	Austrian Power Grid
BCR	Bubble column reactor
CAPEX	Capital expenditures
CSTR	Continuously stirred tank reactor
EUR	Euro
FCR	Frequency containment reserve
GHSV	Gas hourly space velocity
GWh	Gigawatthours
HHV	Higher heating value
HTEL	High temperature electrolyser
kWel	Kilowatt electric
LRGC	Long rang generation costs
MFR	Methane formation rate
mFRR	Manuel frequency restoration reserve
MR	Membrane reactor
MW	Megawatt
MWel	Megawatt electric
MWh	Megawatthours
Nm^3/h	Normkubicmeter per hour
OPEX	Operating expenditures
PEM	Proton exchange membrane
PEMEL	Proton exchange membrane electrolyser
PtG	Power-to-Gas
PV	Photovoltaic
SNG	Synthetic Biomethane
TBR	Trickle-bed reactor
TRL	Technology readiness level

List of Figures

List of Tables

List of Appendices

Appendix 1: Results of Scenario 1a.
Appendix 2: Results of Scenario 1b.
Appendix 3: Results of Scenario 3a for positive aFRR with 2020 prices.
Appendix 4: Results of Scenario 3a for positive aFRR with 2021 prices
Appendix 5: Results of Scenario 3a for negative aFRR with 2020 prices.
Appendix 6: Results of Scenario 3a for negative aFRR with 2021 prices.

Appendix 1: Results of Scenario 1a.

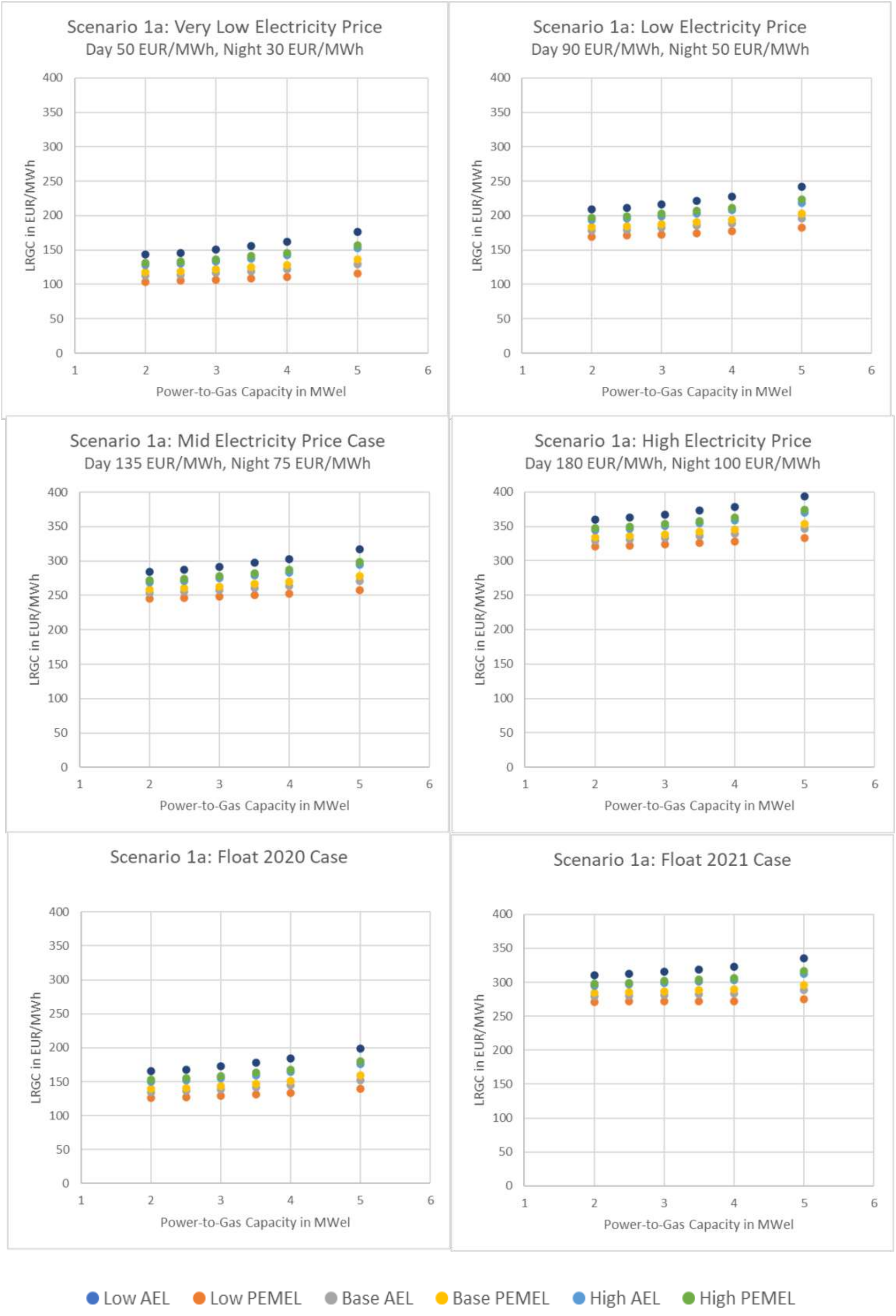

Source: Own figure

Appendix 2: Results of Scenario 1b.

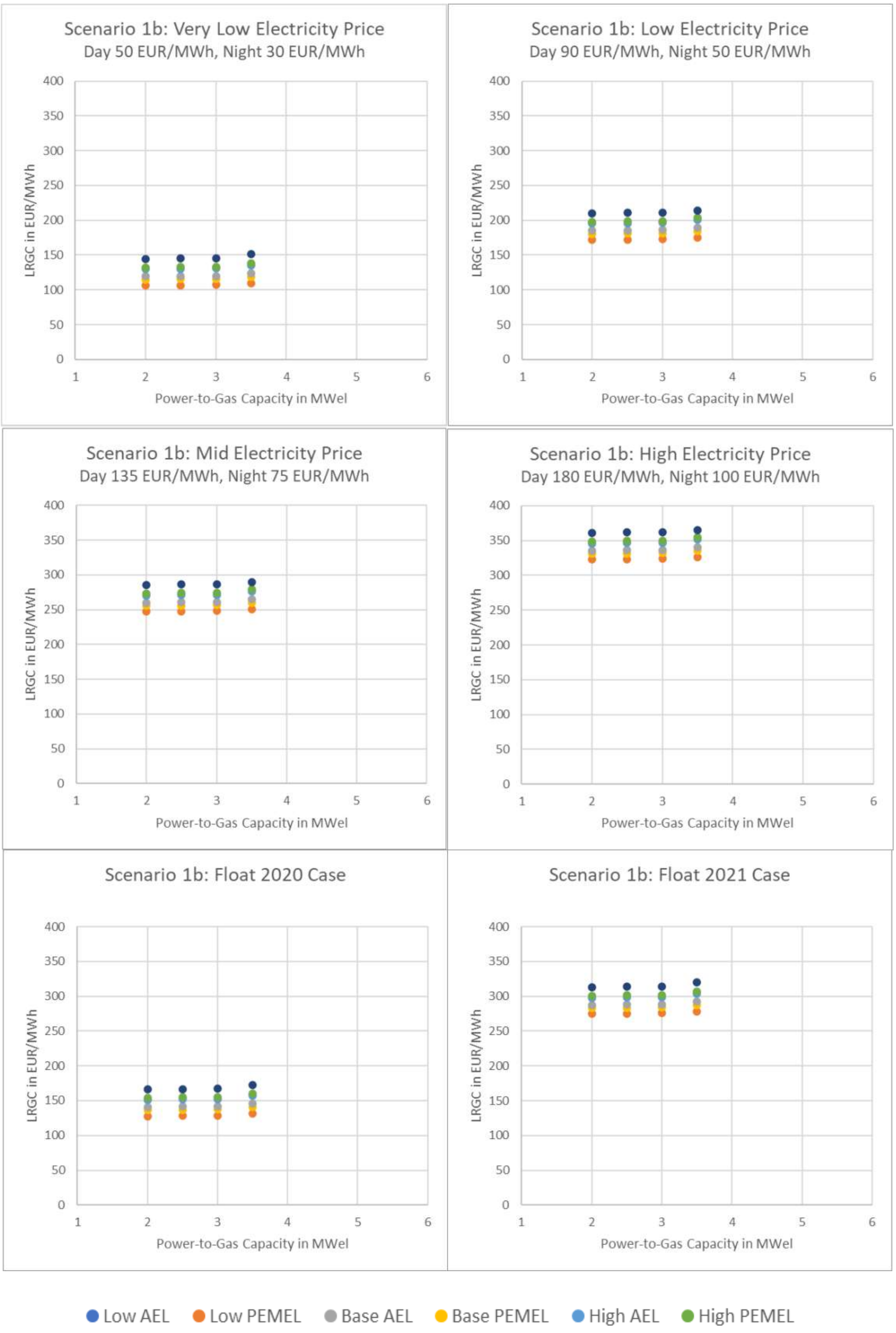

Source: Own figure

Appendix 3: Results of Scenario 3a for positive aFRR with 2020 prices.

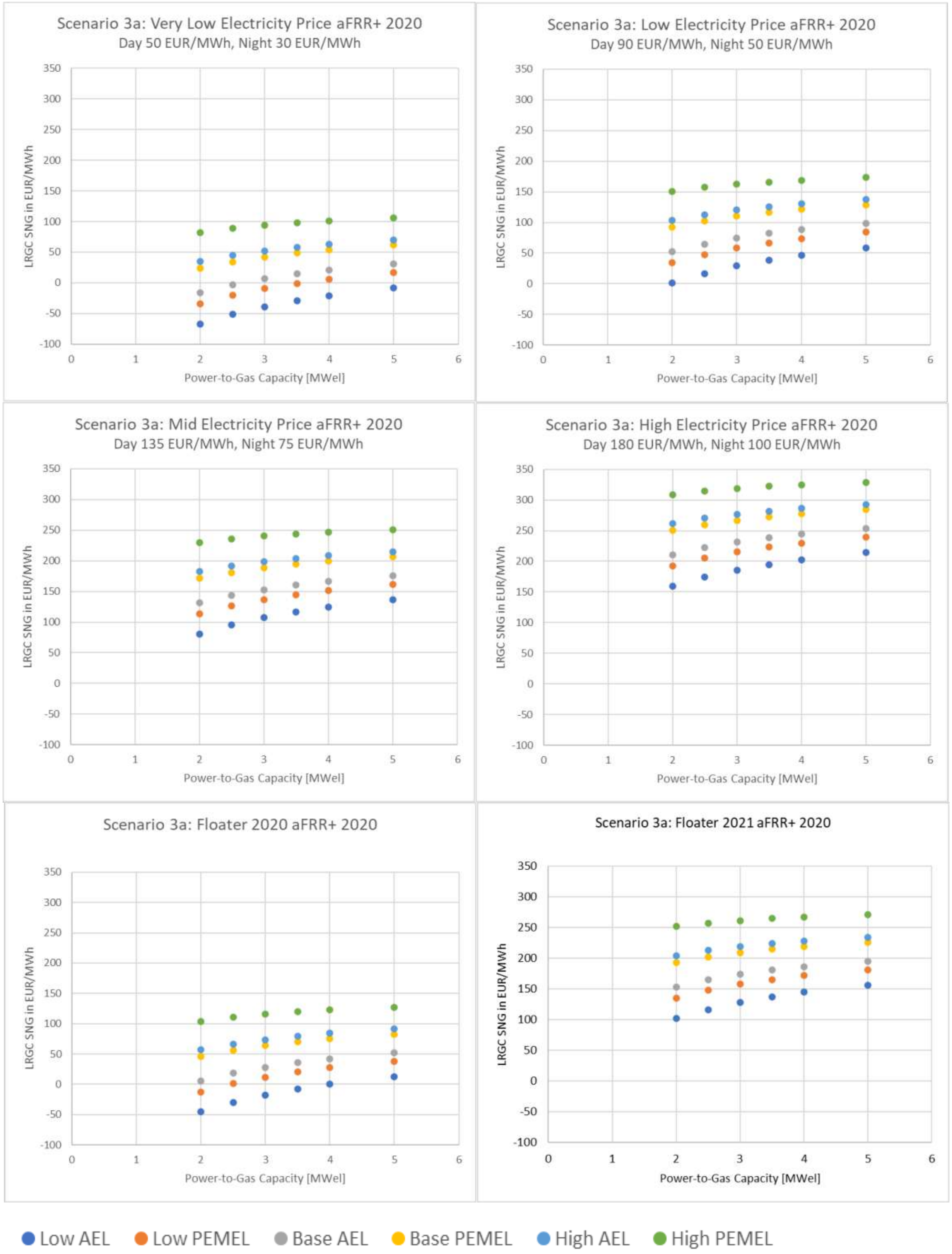

Source: Own figure

Appendix 4: Results of Scenario 3a for positive aFRR with 2021 prices.

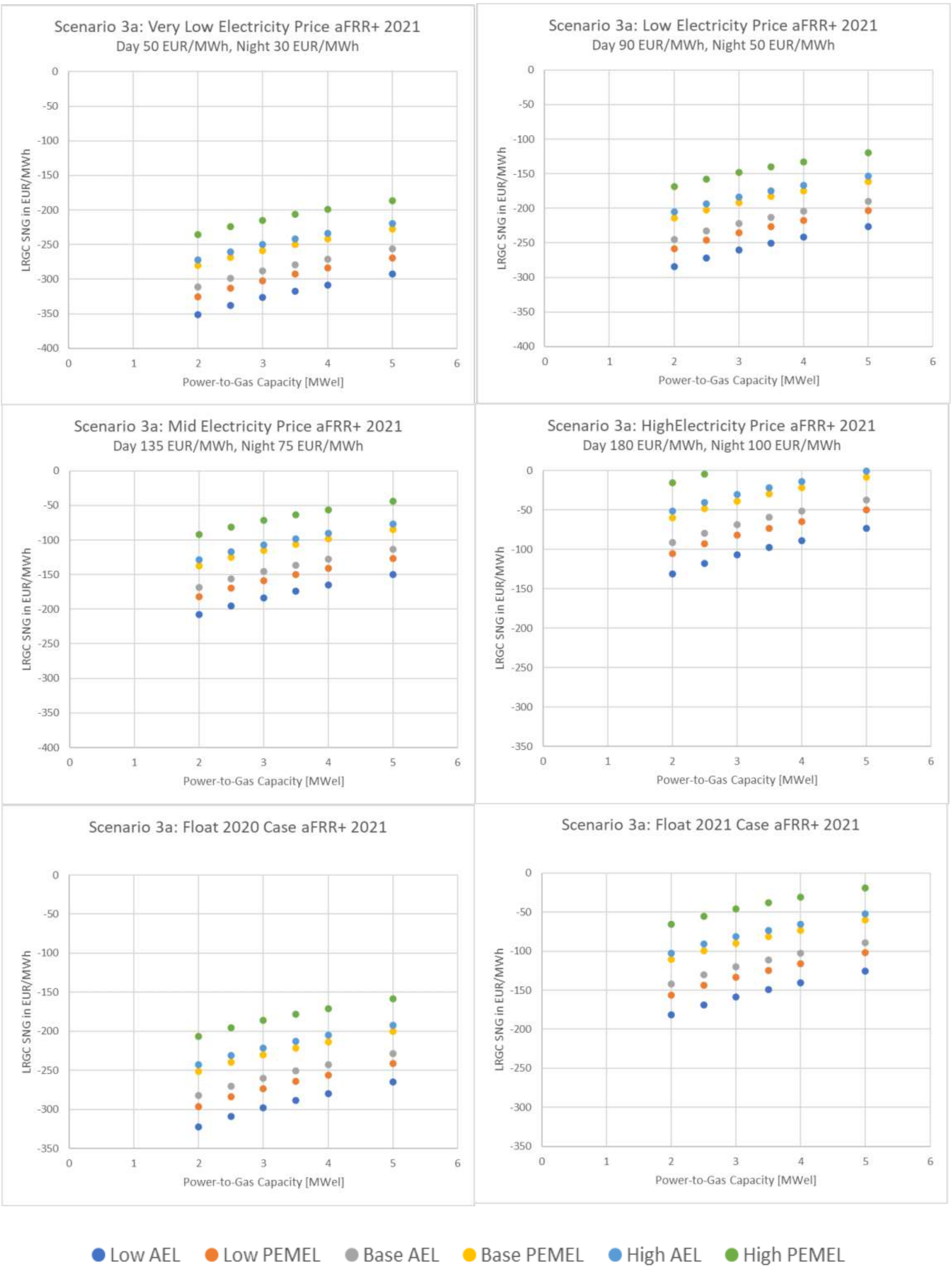

Scenario 3a: Very Low Electricity Price aFRR+ 2021
Day 50 EUR/MWh, Night 30 EUR/MWh

Scenario 3a: Low Electricity Price aFRR+ 2021
Day 90 EUR/MWh, Night 50 EUR/MWh

Scenario 3a: Mid Electricity Price aFRR+ 2021
Day 135 EUR/MWh, Night 75 EUR/MWh

Scenario 3a: HighElectricity Price aFRR+ 2021
Day 180 EUR/MWh, Night 100 EUR/MWh

Scenario 3a: Float 2020 Case aFRR+ 2021

Scenario 3a: Float 2021 Case aFRR+ 2021

Source: Own figure

Appendix 5: Results of Scenario 3a for negative aFRR with 2020 prices.

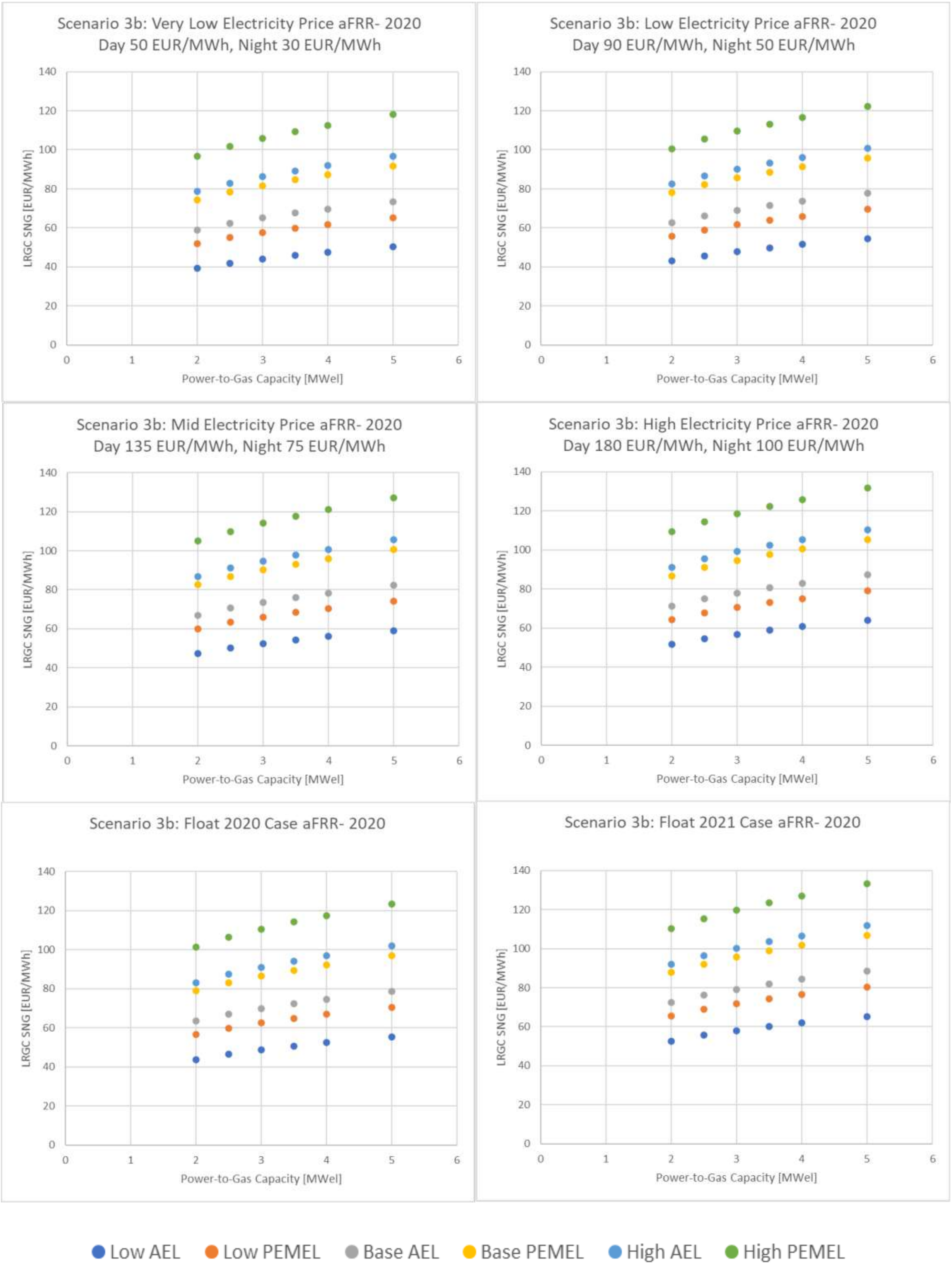

Source: Own figure

Appendix 6: Results of Scenario 3a for negative aFRR with 2021 prices.

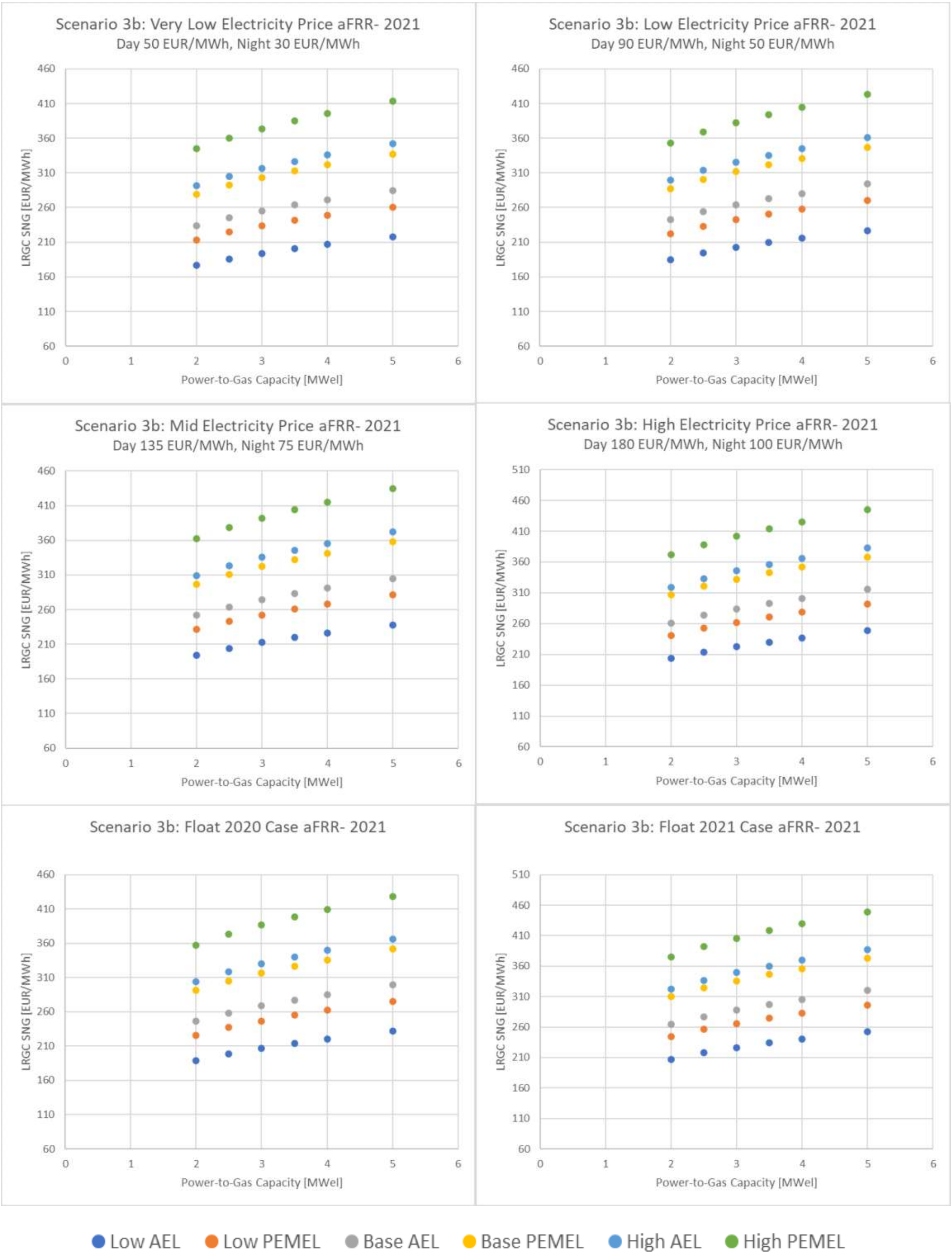

Scenario 3b: Very Low Electricity Price aFRR- 2021
Day 50 EUR/MWh, Night 30 EUR/MWh

Scenario 3b: Low Electricity Price aFRR- 2021
Day 90 EUR/MWh, Night 50 EUR/MWh

Scenario 3b: Mid Electricity Price aFRR- 2021
Day 135 EUR/MWh, Night 75 EUR/MWh

Scenario 3b: High Electricity Price aFRR- 2021
Day 180 EUR/MWh, Night 100 EUR/MWh

Scenario 3b: Float 2020 Case aFRR- 2021

Scenario 3b: Float 2021 Case aFRR- 2021

Source: Own figure